



## **Three-Dimensional Activation Analysis for the ITER Divertor Cassette**

**H.Y. Khater and M.E. Sawan**

**November 1997**

**UWFDM-1058**

**FUSION TECHNOLOGY INSTITUTE**

**UNIVERSITY OF WISCONSIN**

**MADISON WISCONSIN**

**Three-Dimensional Activation Analysis for the  
ITER Divertor Cassette**

Hesham Y. Khater and Mohamed E. Sawan

Fusion Technology Institute  
University of Wisconsin-Madison  
1500 Engineering Drive  
Madison, WI 53706

November 1997

**UWFDM-1058**

## **DISCLAIMER**

This report is an account of work undertaken within the framework of the ITER EDA Agreement. Neither the ITER Director, the Parties to the ITER Agreement, the U.S. DOE, the U.S. Home Team Leader, the U.S. Home Team, the IAEA or any agency thereof, or any of their employees, makes any warranty, express or implied, or assumes any legal liability or responsibility for the accuracy, completeness, or usefulness of any information, apparatus, product, or process disclosed, or represents that its use would not infringe privately owned rights. Reference herein to any specific commercial product, process, or service by trade name, trademark, manufacturer, or otherwise, does not necessarily constitute or imply its endorsement, recommendation, or favoring by the parties to the ITER EDA Agreement, the IAEA or any agency thereof.

The views and opinions of authors expressed herein do not necessarily state or reflect those of the ITER Director, the Parties to the ITER Agreement, the U.S. DOE, the U.S. Home Team Leader, the U.S. Home Team, the IAEA or any agency thereof.

## **Abstract**

A detailed three-dimensional model has been developed for the divertor cassette in the ITER detailed design. Each divertor cassette in the model was divided into 103 regions to provide detailed spatial distribution of the neutron flux. The layered configurations of the dome PFC and vertical targets were modeled accurately with the front tungsten layer modeled separately. 3-D neutronics calculations have been performed using the continuous energy MCNP-4A code with cross section data from FENDL-1 to determine the detailed spatial distribution of the neutron flux in the divertor cassette. A detailed activation analysis has been performed for zones representing the different critical components of the divertor cassette. The activation calculations have been performed using the latest version of the activation code DKR-PULSAR2.0 and the FENDL/A-2.0 and FENDL/D-2.0 data libraries. The calculations have been performed for two operational scenarios. Special attention has been given to the top 1 cm tungsten layer of the divertor dome. The radioactivity generated in the tungsten layers of the divertor is mostly dominated by  $^{187}\text{W}$  during the first day after shutdown. Accurate calculation of the  $^{187}\text{W}$  inventory that takes into account the self-shielding effect, also yielded accurate results for other radioisotopes produced by multi-step reactions with  $^{187}\text{W}$ . The GlidCop copper and 316 SS-LN parts of the divertor also generated considerable level of activity and decay heat. Nevertheless, the analysis showed that the tungsten PFC is clearly the most critical part of the divertor from the decay heat generation point of view.

## 1. INTRODUCTION

The divertor cassette design went through several changes to improve its performance. The latest ITER design is the Detailed Design [1]. The design utilizes 60 divertor cassettes with vertical targets and a central dome. These cassettes are exposed to direct source neutrons coming from the plasma as well as secondary lower energy neutrons resulting from neutron interactions in the cassettes themselves and other in-vessel components. Knowledge of the amount of radioactivity and decay heat produced by these neutrons in the different components of the divertor cassette is essential for proper safety and environmental analysis. As a first step in the activation calculation, neutron transport calculations are performed to determine the neutron spectra in the different regions. These spectra, along with the material composition and the operating scenario, are utilized in the activation calculation to determine the radioactive inventory and decay heat in each region as a function of time following shutdown. Due to the geometrical complexity of the divertor region, three-dimensional (3-D) analyses are required to account for the effects of the geometrical details on the neutron flux. 3-D neutronics and shielding calculations were performed for the divertor region in the Detailed Design to determine the nuclear parameters in the divertor cassette and surrounding vacuum vessel and TF coils [2]. In these calculations, the neutron spectra in the divertor zones are calculated and used in the activation calculations. The activation calculations are performed for two operational scenarios to determine the level of activity and decay heat generated in the different zones of the divertor. The results are given at different times up to 1000 years following shutdown.

## 2. THREE-DIMENSIONAL CALCULATIONAL MODEL

Due to the geometrical complexity of the divertor region, 3-D models are required to properly determine the neutron flux. The continuous energy, coupled neutron-gamma ray Monte Carlo code MCNP-4A [3] has been used in the 3-D neutron transport calculations. The nuclear data used is based on the FENDL-1 evaluation [4]. The detailed geometrical configuration of the divertor cassette has been modeled for 3-D neutronics calculations. The drawings provided by the Joint Central Team (JCT) at Garching for the Detailed ITER Design are the basis for the 3-D modeling. The model represents a nine degree toroidal sector of ITER. Hence, it includes one and a half cassettes with the associated nominal 1 cm gaps between adjacent cassettes. The model includes in detail the high heat flux plasma facing components (PFC), the vertical targets, the wings with

associated plates, and the gas boxes, as well as the central dome and cassette bodies. The 37.5 cm wide and 17.5 cm thick divertor pumping duct at the bottom of each cassette is included in the model. The rails upon which the cassettes move toroidally during maintenance are also included. Each divertor cassette in the model was divided into 103 regions to provide detailed spatial distribution of the neutron flux. The layered configurations of the dome PFC and vertical targets were modeled accurately with the front tungsten layer modeled separately. This was essential to properly account for self-shielding effects of the giant resonance for  $^{186}\text{W}$  at 20 eV that produces  $^{187}\text{W}$  which dominates decay heat in the W PFC. Separate regions are included in the model to represent the mechanical attachments and coolant pipe connections for the dome, vertical targets, and wings. Figure 1 shows a vertical cross section of the cassette model at a toroidal location at the center of the cassette through the pumping ducts. Figures 2, 3 and 4 give the numbers used to identify the cells used in the MCNP calculations for determining the spatial distribution of the neutron flux.

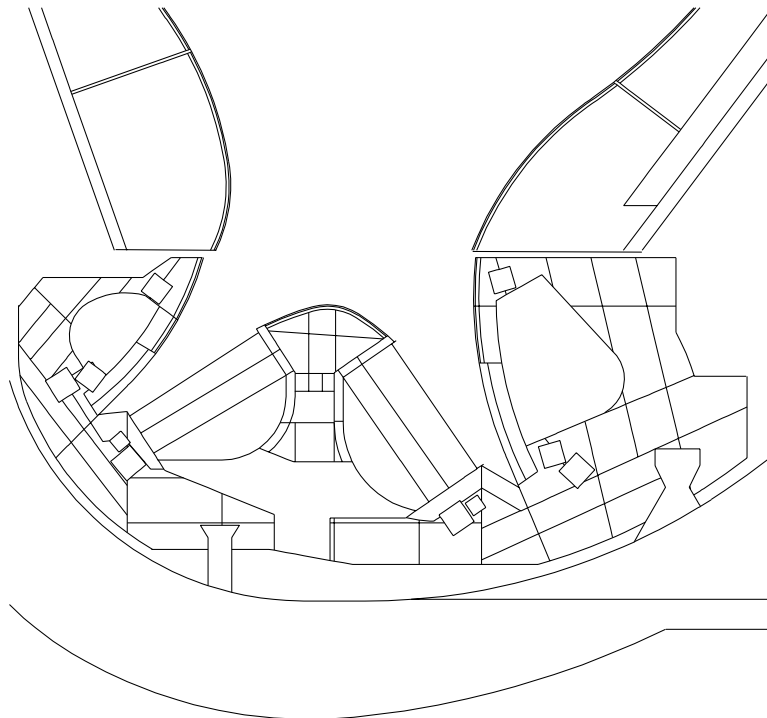


Fig. 1. Vertical cross section at the middle of the cassette model.

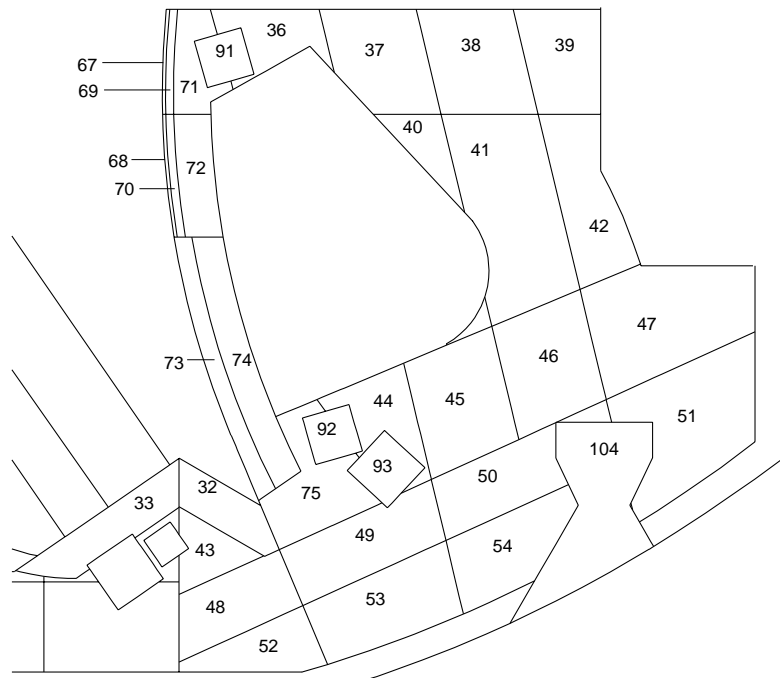


Fig. 2. Vertical cross section in the outer part of cassette showing the cells used to determine the spatial variation of nuclear parameters.

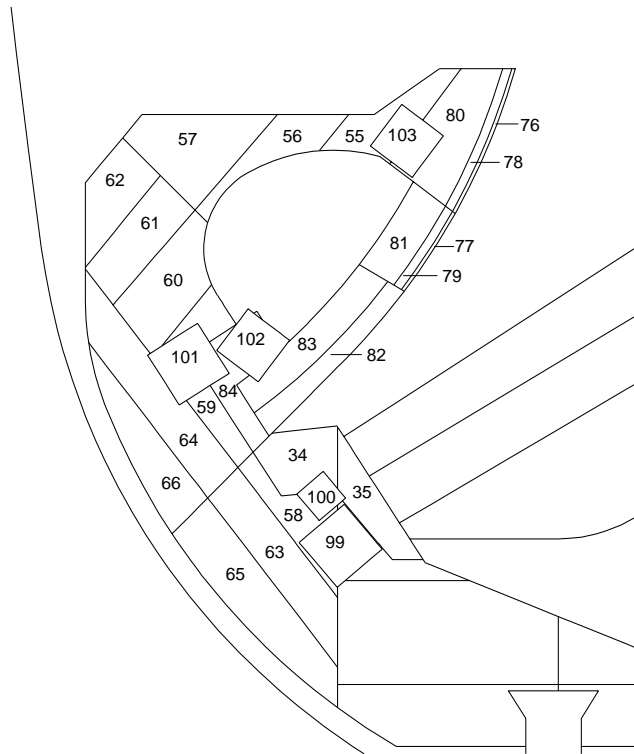


Fig. 3. Vertical cross section in the inner part of cassette showing the cells used to determine the spatial variation of nuclear parameters.

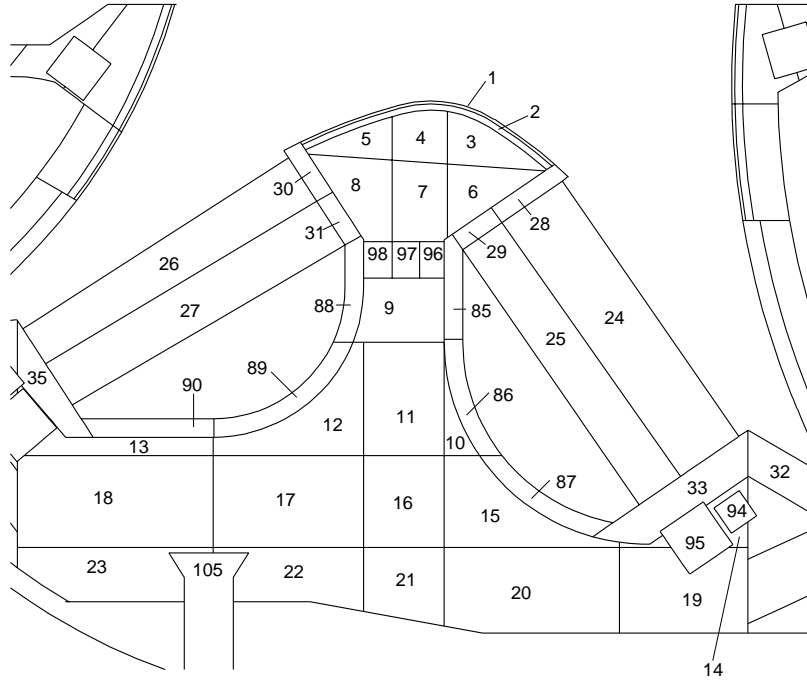


Fig. 4. Vertical cross section in the central part of cassette showing the cells used to determine the spatial variation of nuclear parameters.

The divertor cassette model has been integrated with the general ITER model based on the Interim ITER Design [5]. The integrated model includes detailed modeling of the first wall, blanket with associated coolant manifolds and back plates, VV, TF coils, central solenoid, and PF coils. While Be is used as the plasma facing material at the first walls of the blanket modules, tungsten is used for the inboard and outboard baffle modules above the divertor cassette. All toroidal and poloidal gaps between adjacent blanket modules are included. The major vacuum vessel penetrations are included in the model. This includes the divertor port at the bottom of the reactor. Due to symmetry, only 1/40 of the reactor is modeled with surrounding reflecting boundaries. The blanket design in the ITER Interim Design was used since the blanket design was not fully developed in the Detailed Design. Since most of the design changes in the blanket are expected to be in the back plate, module attachment and manifolds, the impact will be mainly on shielding and streaming through the large ports and the impact on the neutron flux in the divertor cassette will be minimal.

The output of the MCNP geometry plotting routine given in Fig. 5 shows a vertical cross section through the middle of the vacuum vessel ports. Figure 6 is a horizontal cross section at  $z=-6$  m in the middle of the divertor port. The divertor pumping ducts in the divertor cassettes are

shown in this figure. Several splitting surfaces have been added in the divertor region to allow for utilizing the geometry splitting with Russian Roulette variance reduction techniques employed in MCNP which are needed to improve the accuracy of the calculated neutron flux particularly at the back of the cassette.

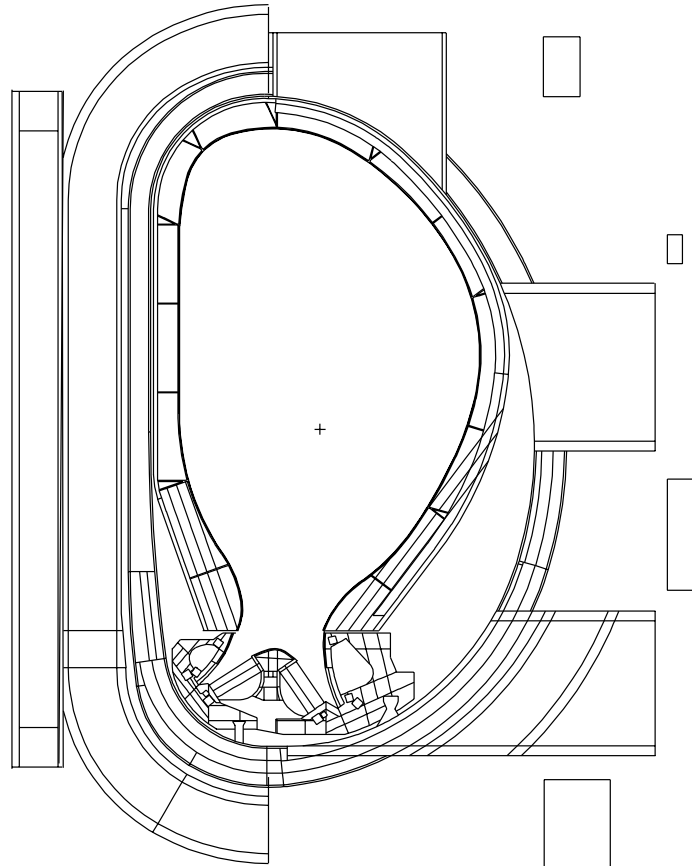


Fig. 5. Vertical cross section through the VV ports of the ITER 3-D model for MCNP calculations.

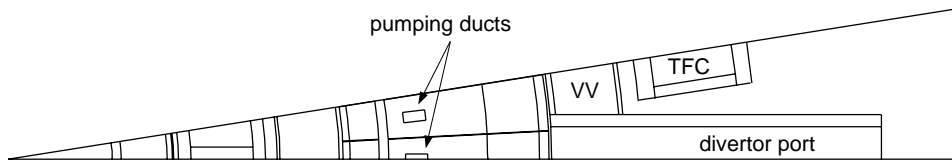


Fig. 6. Horizontal cross section of the 3D model at  $Z = -6$  m.

A combination of cones, tori, cylinders, and planes was utilized for accurate modeling of the geometry. A total of 543 surfaces has been used in the model, of which 175 are fourth degree tori. The model employs 593 geometrical cells. The volumes of the different cells have been determined stochastically by ray tracing. A source subroutine has been written to modify MCNP to sample source neutrons from the source distribution in the ITER plasma provided numerically by the San Diego JCT at 1600 mesh points. Cell flux tallies are used to determine the volume averaged flux in the components of the divertor. Energy bins were also utilized to determine the neutron spectra in the multi-group structures used in the activation calculations. The appropriate material compositions are used for the different cells of the model. The material composition used for the divertor cassette is given in Table 1. The calculation has been performed using 50,000 source particles. The results are normalized to the nominal fusion power of 1500 MW.

Table 1. Material Composition

Dome PFC	1 cm W 2 cm 75% Cu, 25% water Cu dome body 85% Cu, 15% water SS dome body 75% SS, 25% water
Wings	16% W, 79% Cu, 5% water packing fraction: 21% outer, 26% inner
Gas Box Liners and Wing Plates	8% W, 74% Cu, 18% water
Vertical Targets	top section: 1 cm W 2.5 cm 82% Cu, 18% water back region 97% SS, 3% water lower section: 5.5 cm 89% C, 4% Cu, 7% water back region 97% SS, 3% water
Cassette Body	80% SS, 20% water
Mechanical Attachments	100% SS
Coolant Pipe Connections	70% SS, 30% water
Rails	100% SS

### 3. NEUTRON FLUX AND ENERGY SPECTRUM IN THE DIVERTOR CASSETTE

The neutron flux has been calculated in the different components of the divertor cassette. The energy integrated values as well as the energy spectra were evaluated for use in the activation calculations. The energy spectra were determined for the VITAMIN-J fine group structure of 175 energy groups used to represent the FENDL data and a coarse group structure of 46 energy groups. The volume averaged results were determined for 103 segments of the cassette using cell flux tallies. The values of the energy integrated neutron flux are given along with the one-sigma standard deviation in Table 2. The zone numbers correspond to the numbers given in Figs. 2-4. The largest flux occurs in the dome PFC which has a full view of the plasma and has the largest neutron wall loading. In response to a request by the safety group of the JCT at San Diego, we performed activation calculations for the front 2 mm of the W PFC of the dome. The 3-D model was modified to segment the 10 mm thick W zone (cell 1) to two segments; a front 2 mm thick segment and an 8 mm thick back segment. The flux values in these segments are  $2.23 \times 10^{14}$  and  $2.14 \times 10^{14}$  n/cm<sup>2</sup>s, respectively, compared to an average flux of  $2.16 \times 10^{14}$  n/cm<sup>2</sup>s for the 10 mm thick W PFC (cell 1).

The W PFC at the top of the vertical targets experiences relatively high levels of neutron flux. The rest of the vertical targets and wings experience moderate levels of neutron flux with values dropping rapidly as one moves deeper in the cassette body. Notice that the statistical uncertainty is larger at the back cells of the cassette. However, the flux is relatively low at these cells and contribution to divertor activation and decay heat is small. In other words, the statistical uncertainty in the calculated flux is reasonable (<5%) in the cells which have major contribution to the activation and decay heat. These are the front cells with the highest flux values. In general, the neutron flux in the inboard side of the cassette is lower than in the outboard side which has a larger view of the plasma.

Figure 7 gives the neutron spectra in the W PFC of the dome (cell 1) and cell 7 in the dome body. The effect of attenuation of the high energy neutrons in the dome body is clearly illustrated. This results in a much softer neutron energy spectrum inside the dome body. The large depression in the spectrum in the W PFC around 20 eV is a result of the giant resonance in the (n, $\gamma$ ) cross section for <sup>186</sup>W at 20 eV. The dip in the spectrum in the energy range 3-6 eV represents the effect of the resonance in cross sections for <sup>182</sup>W. The shallow dip at ~8 eV results from the resonance in the <sup>183</sup>W cross sections. No such structure occurs in the spectrum in the steel dome body.

Figure 8 shows the neutron energy spectra in the front of the outer wings (cell 24) and the front 55 mm thick zone of the lower section of the outboard vertical target (cell 73). These two cells surround the outer channel of the divertor. As given in Table 1, the wings include both copper and tungsten. In addition to the structure in the energy spectrum resulting from the tungsten resonances, a dip resulting from the 2 keV resonances is also visible. Since the front of the lower section of the vertical target consists mostly of carbon which is a good slowing down material, the energy spectrum is much softer. This is also a result of the lower neutron wall loading at the vertical target compared to the wings [6] which implies less high energy source neutrons incident on the vertical target compared to lower energy secondary neutrons. In addition, one notices that the spectrum in the wings is slightly softer than that in the dome PFC which has a full view of the plasma. Figure 9 compares the neutron energy spectra in two cells in the inner and outer legs of the divertor cassette. The dip at  $\sim$ 25 keV corresponds to the 25 keV iron resonances. It is clear that the spectra are much softer than those in the dome, wings, and vertical targets shown in Figs. 7 and 8. This is a direct result of the neutron attenuation and slowing down in the cassette body. The flux is lower and softer in the inner leg compared to the outer leg which has a larger view of the plasma. The average neutron wall loading at the outer vertical target is  $0.134 \text{ MW/m}^2$  compared to only  $0.007 \text{ MW/m}^2$  at the inner vertical target [6].

Table 2. Spatial Distribution of the Energy Integrated Neutron Flux in the Divertor Cassette

<b>Zone Number</b>	<b>Neutron Flux (n/cm<sup>2</sup>s)</b>	<b>Standard Deviation (%)</b>
<b>Dome PFC</b>		
1	2.16E+14	2.2
2	2.02E+14	2.2
<b>Dome Body</b>		
3	1.33E+14	3.3
4	1.23E+14	3.8
5	1.44E+14	3.7
6	4.19E+13	3.6
7	1.77E+13	3.8
8	4.03E+13	3.9
9	8.69E+12	3.3
<b>Central Body</b>		
10	1.59E+13	3.9
11	5.48E+12	3.3
12	9.53E+12	4.2
13	1.20E+13	4.5
14	1.19E+13	5.5
15	1.13E+13	3.6
16	2.45E+12	4.4
17	3.46E+12	4.5
18	3.21E+12	4.9
19	1.26E+12	6.2
20	2.75E+12	4.7
21	9.05E+11	5.3
22	8.29E+11	6.2
23	1.72E+11	8.8
<b>Wings</b>		
24	1.03E+14	2.4
25	5.36E+13	2.7
26	9.42E+13	2.9
27	5.07E+13	3.3
<b>Wing Plates</b>		
28	8.97E+13	4.1
29	2.87E+13	4.9
30	1.02E+14	4.7
31	2.85E+13	4.9
32	4.59E+13	4.6
33	3.67E+13	3.9
34	2.68E+13	6.5
35	2.47E+13	5.7

Table 2. Spatial Distribution of Nuclear Responses in the Divertor Cassette  
 (Continued)

<b>Zone Number</b>	<b>Neutron Flux (n/cm<sup>2</sup>s)</b>	<b>Standard Deviation (%)</b>
<b>Outer Leg</b>		
36	2.10E+13	3.5
37	5.68E+12	3.5
38	3.79E+11	8.7
39	1.64E+11	16.3
40	1.23E+13	3.0
41	3.89E+12	3.1
42	1.83E+11	5.5
43	1.03E+13	5.8
44	6.28E+12	3.2
45	2.86E+12	3.3
46	5.86E+11	4.4
47	8.80E+10	7.3
48	1.66E+12	8.7
49	1.32E+12	9.5
50	2.48E+10	10.9
51	3.56E+10	8.4
52	1.85E+11	10.6
53	9.67E+10	12.6
54	4.44E+09	16.8
<b>Inner Leg</b>		
55	1.32E+13	4.7
56	8.31E+12	4.5
57	2.51E+12	5.3
58	4.39E+12	9.9
59	5.08E+12	6.9
60	3.55E+12	5.7
61	1.04E+12	6.9
62	5.19E+11	8.8
63	9.48E+11	10.1
64	5.64E+11	11.4
65	1.69E+11	11.6
66	1.81E+11	13.7

Table 2. Spatial Distribution of Nuclear Responses in the Divertor Cassette  
 (Continued)

<b>Zone Number</b>	<b>Neutron Flux (n/cm<sup>2</sup>s)</b>	<b>Standard Deviation (%)</b>
<b>Outer Vertical Target</b>		
67	1.81E+14	3.7
68	1.46E+14	3.7
69	1.49E+14	3.6
70	1.21E+14	3.8
71	9.25E+13	3.5
72	5.93E+13	3.7
73	8.91E+13	2.7
74	4.03E+13	3.1
75	1.38E+13	5.9
<b>Inner Vertical Target</b>		
76	1.16E+14	4.5
77	9.70E+13	5.5
78	9.96E+13	4.4
79	7.50E+13	5.5
80	5.34E+13	4.4
81	4.06E+13	5.2
82	5.62E+13	4.4
83	2.83E+13	4.9
84	9.75E+12	9.6
<b>Gas Box Liner</b>		
85	2.45E+13	3.6
86	3.04E+13	3.2
87	2.91E+13	3.4
88	2.26E+13	3.9
89	2.62E+13	3.8
90	2.59E+13	4.0

Table 2. Spatial Distribution of Nuclear Responses in the Divertor Cassette  
 (Continued)

<b>Zone Number</b>	<b>Neutron Flux (n/cm<sup>2</sup>s)</b>	<b>Standard Deviation (%)</b>
<b>Attachments and Coolant Pipe Connections</b>		
Outer Vertical Target		
91	4.45E+13	3.9
92	9.13E+12	4.9
93	1.15E+12	7.4
Outer Wings		
94	1.22E+13	6.3
95	5.69E+12	6.6
Dome		
96	9.55E+12	5.3
97	5.20E+12	5.9
98	9.01E+12	5.2
Inner Wings		
99	4.63E+12	9.3
100	1.21E+13	9.9
Inner Vertical Target		
101	1.51E+12	15.2
102	9.93E+12	6.9
103	2.07E+13	5.4
<b>Rails</b>		
104	5.89E+09	11.6
105	3.93E+11	6.2

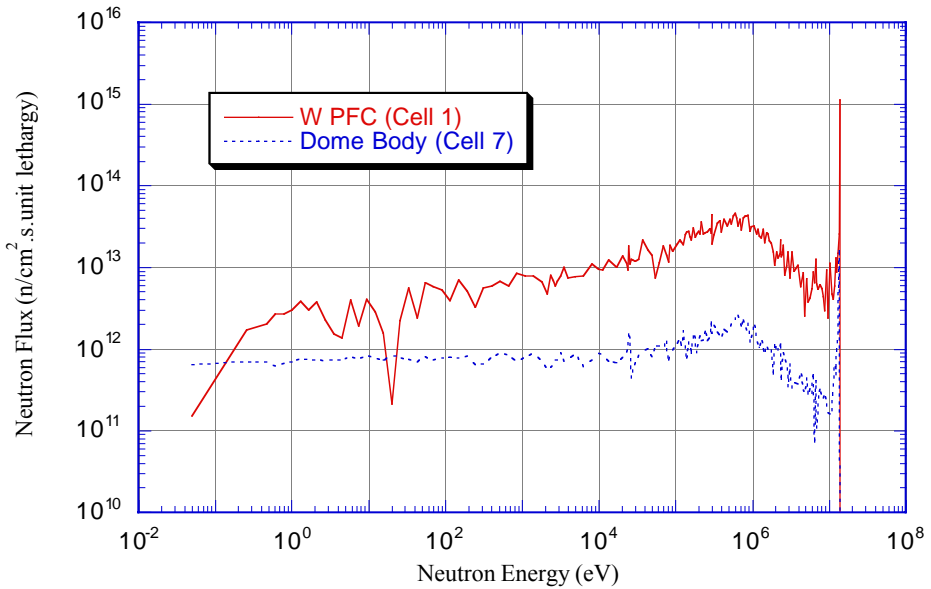


Fig. 7. Neutron spectra in the W PFC of the dome and cell 7 in the dome body.

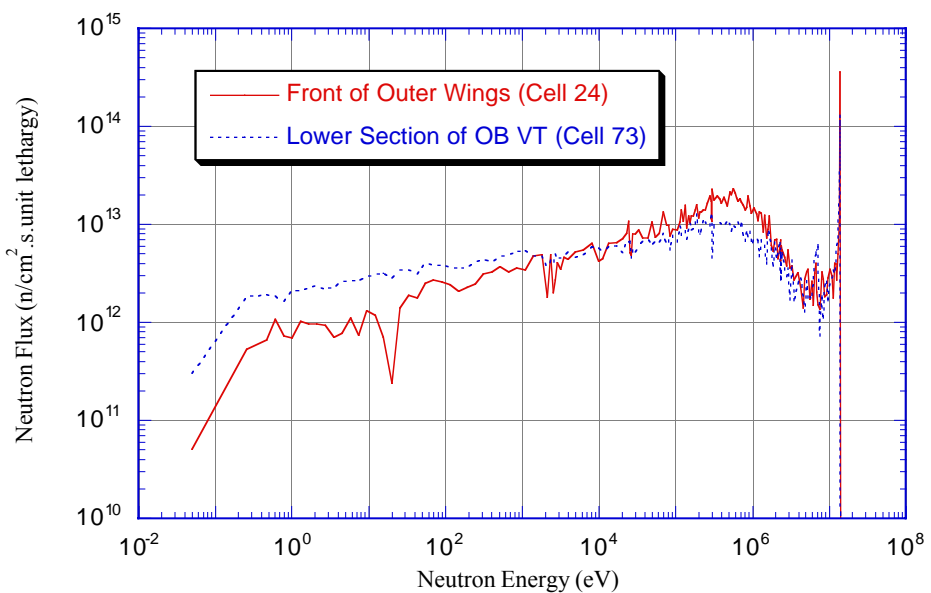


Fig. 8. Neutron spectra in the front of the outer wings (cell 24) and the front of the lower section of the outboard vertical target.

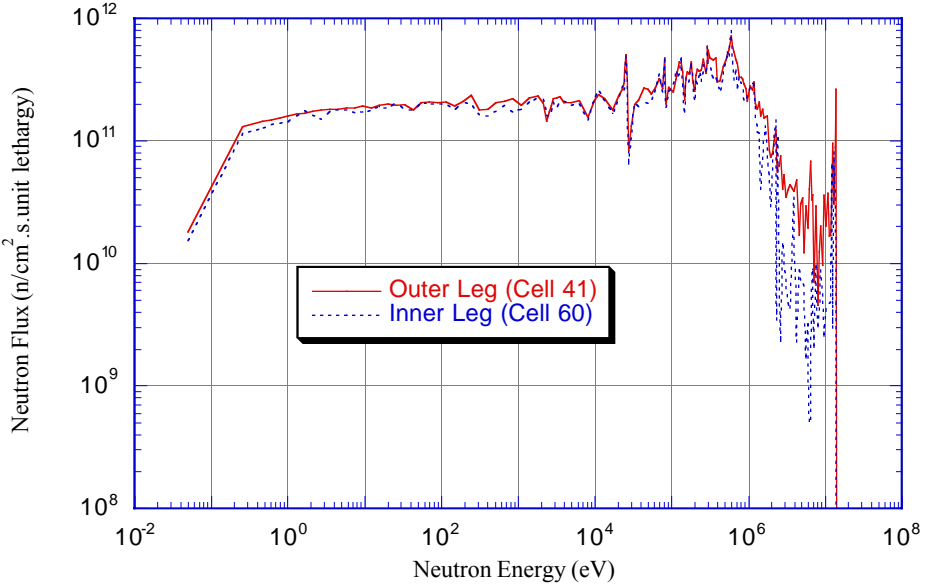


Fig. 9. Neutron spectra in two cells in the inner and outer legs.

#### 4. SELF-SHIELDING EFFECTS IN TUNGSTEN

Short term decay heat is important from the safety point of view regarding the thermal response of the divertor cassette to a loss of coolant accident (LOCA). The amount of decay heat generated in the tungsten plasma facing material at short times after shutdown has important safety consequences and should be determined accurately.  $^{187}\text{W}$  ( $T_{1/2} = 23.85$  h) is the dominant contributor to tungsten decay heat for several days following shutdown.  $^{187}\text{W}$  is produced from the  $^{186}\text{W}(n,\gamma)$  reaction which has a giant resonance at 20 eV as shown in Fig. 10. Precise representation of the geometry and energy variable is essential to properly account for self-shielding effects. In the previous 3-D models for the divertor cassette [6,7], the 1 cm thick tungsten PFC was homogenized with the heat sink material. A 6 cm thick zone was used with a homogeneous mixture of W, Cu, SS and  $\text{H}_2\text{O}$ . It was pointed out by H. Iida et al. [8] that the improper homogenization of the tungsten with other components can lead to results that are incorrect. The effects of the homogenization of the tungsten armor and substrates on the calculated production rate of  $^{187}\text{W}$  were determined using the Monte Carlo code MCNP with a simple cylindrical geometry model. When the W armor and the underlying substrate are homogenized, the  $^{187}\text{W}$  production rate is significantly overestimated since the hydrogen in the homogenized zone helps slow down neutrons to the energy of the  $^{186}\text{W}(n,\gamma)$  giant resonance. The overestimate

increases as the water content increases. The  $^{187}\text{W}$  production rate can be overestimated by up to a factor of two depending on the thickness of the homogenized zone and the water content. This clearly demonstrates that the layered configuration must be modeled correctly to properly account for self-shielding.

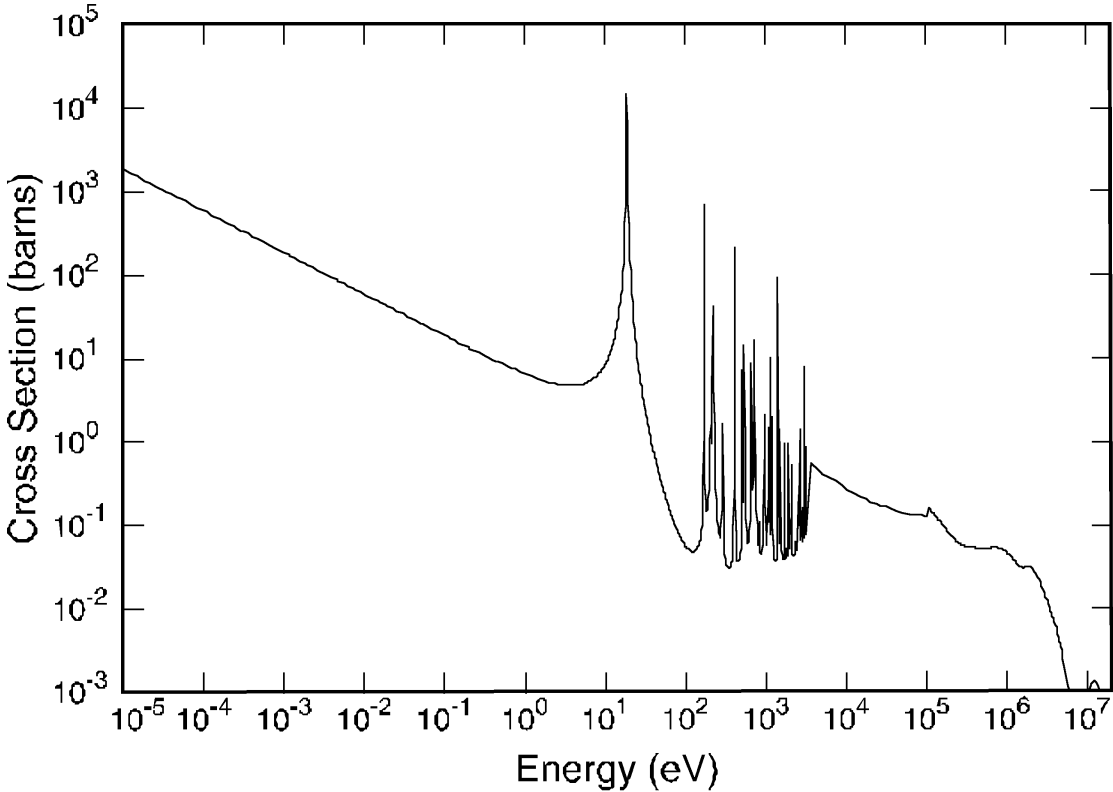


Fig. 10.  $^{186}\text{W}(n,\gamma)$  cross section.

In order to illustrate the effect of homogenization, we performed two calculations using the detailed 3-D model developed here. In the first one, the 1 cm thick W in the dome PFC is modeled separately followed by a 2 cm thick heat sink layer consisting of 75% Cu and 25%  $\text{H}_2\text{O}$ . The calculation is aimed at investigating the homogenization effect. In the second calculation, a homogeneous composition of 34% W, 49.5% Cu and 16.5%  $\text{H}_2\text{O}$  is used in the front 3 cm of the dome. The  $^{187}\text{W}$  production rate is given in Table 3 for both cases. The homogenization effect is clear from these results. The value over the front 1 cm is overestimated by a factor of 1.63. Figure 11 compares the neutron spectra in the front 1 cm of the dome PFC when W is modeled or homogenized with the heat sink back zone. The results are given for 46 neutron energy bins. The softening of the spectrum in the homogenized case is clearly demonstrated.

The effect of homogenization was investigated also by E. Cheng using one-dimensional discrete ordinates calculations [9]. These results indicated that homogenization results in a factor of 1.33 overestimate in the calculated W decay heat. This is in good agreement with the effect found from the 3-D results taking into account the lower water content (18%) used for the heat sink in the 1-D calculation. In addition, J-Ch. Sublet modified his previous 3-D model to include a layered configuration for the dome PFC [10]. The TRIPOLI results are in good agreement with the MCNP results presented here. The flux and  $^{187}\text{W}$  production rate are  $2.26 \times 10^{14} \text{ n/cm}^2\text{s}$  and  $3.28 \times 10^{12} \text{ nuclides/cm}^3\text{s}$  compared to  $2.16 \times 10^{14} \text{ n/cm}^2\text{s}$  and  $3.82 \times 10^{12} \text{ nuclides/cm}^3\text{s}$  from the MCNP calculation presented here. This is an excellent agreement taking into account the differences in codes and modeling. The  $^{187}\text{W}$  production rate from the recent TRIPOLI calculation is about a factor of 4 lower than that obtained previously using the model in which the W PFC is included in a single 6 cm thick homogenized zone [10].

Table 3. Effect of W Homogenization on  $^{187}\text{W}$  Production Rate (nuclides/cm<sup>3</sup>s)

Separate 1 cm W Layer	$3.8 \times 10^{12}$
Homogeneous 3 cm Zone	
Average Over Front 1 cm	$6.2 \times 10^{12}$
Average Over Back 2 cm	$4.4 \times 10^{12}$
Average Over Whole 3 cm Zone	$5.0 \times 10^{12}$

Since the Monte Carlo calculations use pointwise cross section data (continuous energy), the resonance self-shielding effects are treated correctly. Therefore, the neutron energy spectra and reaction rates calculated directly from MCNP take into account the self-shielding effects. This is contrary to the multi-group calculations where the cross sections in each energy group are calculated from the pointwise data using standard weighting spectra. Although some self-shielded multi-group data can be used in the neutron transport calculations to partially account for self-shielding, the multi-group activation libraries do not include self-shielded cross sections. For example, the FENDL activation libraries [11,12] used here include multi-group cross sections generated from the pointwise data using the VITAMIN-E weighting spectrum. In the energy region from 1 to 100 eV, a smooth 1/E spectrum is used. Since the actual spectrum has a big dip at 20 eV, the multi-group activation data overestimate the  $^{186}\text{W}(n,\gamma)$  cross section at the giant 20 eV resonance. Hence, using the correct neutron energy spectrum that accounts for self-shielding as obtained from the MCNP calculations with the multi-group activation data that does not include self-shielding effects in the activation code will result in overestimating the reaction rates and decay heat.

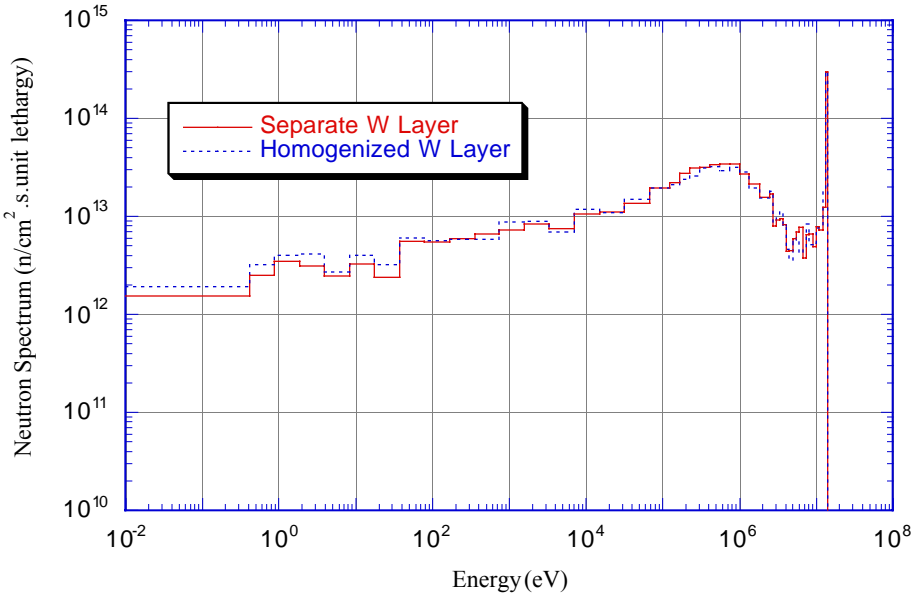


Fig. 11. Effect of homogenization on the neutron spectrum at the W PFC of the dome.

To illustrate this effect, we initially used the neutron flux calculated by MCNP in the activation code DKR-PULSAR2.0 [13] to calculate the decay heat for W. As predicted the value obtained is different from what we get using the exact  $^{187}\text{W}$  production rate calculated by MCNP. Although the flux calculated by MCNP and used by DKR-PULSAR2.0 is correct with the proper self-shielding due to the continuous energy treatment, DKR-PULSAR2.0 couples this with the multi-group activation cross section which does include self-shielding. Hence, the cross section used in DKR-PULSAR2.0 at the group including the 20 eV resonance is higher than it should be if we use the correct flux distribution inside the group for cross section weighting. As a result we are multiplying the exact energy integrated group flux by an overestimated group cross section leading to overestimating the production rate and decay heat.

Based on the MCNP calculation,  $^{187}\text{W}$  production rate is  $3.8 \times 10^{12}$  nuclides/cm $^3$ s. Assuming that the  $^{187}\text{W}$  concentration reaches equilibrium and using a conversion factor of  $1.16 \times 10^{-13}$  W/Bq for  $^{187}\text{W}$  and for the pulse scenario of 1 hour on-1 hour off over a month (360 pulses) we get decay heat of 0.22 W/cm $^3$  at shutdown which drops by 4% in 1 hour to 0.214 W/cm $^3$ . The DKR-PULSAR2.0 calculation gave 1.53 W/ cm $^3$  which is higher by a factor of ~7. The  $^{187}\text{W}$  production rate calculated by DKR-PULSAR2.0 is  $2.7 \times 10^{13}$  nuclides/cm $^3$ s which is higher than

that calculated by MCNP by about the same factor. In this initial DKR-PULSAR2.0 calculation, FENDL/A-1.0 [11] data in 46 energy groups were used. The effect is expected to be lower when a finer group structure is used. E. Cheng used the neutron energy spectrum in the W PFC of the dome as calculated by MCNP to perform activation calculations using the REAC code with the FENDL/A-2.0 [12] activation data in 175 energy groups without self-shielding [9]. The resulting  $^{187}\text{W}$  production rate is  $6.98 \times 10^{12}$  nuclides/cm<sup>3</sup>s, which is a factor of 1.83 higher than that calculated directly by MCNP with self-shielding taken into account [14]. These results clearly demonstrate the overestimation of activation resulting from using an accurately calculated spectrum from MCNP in activation codes with non-self-shielded activation data. It is interesting to note that some cancellation of error might result if non-self-shielded multi-group data are used in the transport calculation instead of the accurate continuous energy MCNP calculation. The error cancellation is not quite full because the flux is not determined only by the cross section of interest with the giant resonance. This effect was demonstrated by comparing the  $^{187}\text{W}$  production rate for a simple 1-D geometry from MCNP to that from ANISN that showed a factor of 1.2 increase [15].

In order to fix this problem one can bypass the reaction rate calculation in the activation code and use the correct reaction rate calculated from MCNP for reactions with big resonances and which produce dominant radionuclides. Alternatively, one can calculate from MCNP the effective multi-group cross sections for the reactions of interest and modify the activation library to include these self-shielded cross sections. This approach was used in the final activation calculations which were performed using the FENDL/A-2 activation data in the 175 group structure. A detailed discussion of the activation calculation is given in the following sections. Unfortunately, this modification is problem dependent and will be different for each cell depending on the material composition.

We repeated the MCNP calculation for the divertor to calculate the  $^{186}\text{W}(\text{n},\gamma)$  reaction rate in the W PFC of the dome in 175 energy bins. The reaction rates were used along with the calculated neutron spectra to determine the effective reaction cross sections in each energy group. These group cross sections take into account the effect of self-shielding since MCNP uses pointwise data and the calculated effective cross section is weighted by the actual pointwise flux from MCNP. The calculations were performed for both the front 2 mm and the whole 10 mm W to investigate the spectrum dependence. The calculated effective cross sections were then compared to the 175 group cross sections in FENDL/A-1.0 [11] and FENDL/A-2.0 [12] which are not self-shielded. Figure 12 gives the neutron spectra in the 2 and 10 mm W regions which are similar but the 2 mm case has higher values because of the lower flux attenuation.

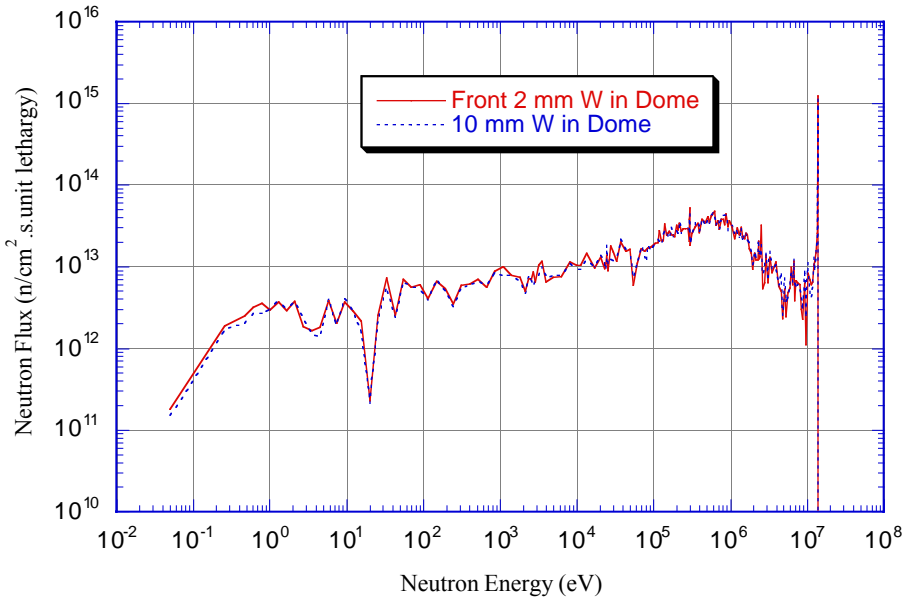


Fig. 12. Neutron spectra in the W PFC of the dome.

We calculated the effective self-shielded  $^{186}\text{W}(n,\gamma)$  cross section for the 175 energy bins (groups). Figure 13 gives the effective cross section for both cases. It is clear that a smaller self-shielding effect takes place in the front 2 mm compared to the thicker 10 mm case. These differences clearly demonstrate that the effective cross section is problem dependent and varies from region to region and different effective cross sections should be generated for the different regions of interest to replace the non-self-shielded cross sections in the activation library. Figure 14 compares the effective self-shielded cross section to the non-self-shielded cross section in FENDL/A-1.0. This demonstrates the large self-shielding effect particularly at the resonances as expected. About an order of magnitude self-shielding is observed at the 20 eV resonance. Despite the possible difference in evaluated data, the self-shielding effect is clearly demonstrated. Figure 15 compares the non-self-shielded FENDL/A-1.0 and -2.0 cross sections for  $^{186}\text{W}(n,\gamma)$  which are nearly identical.

The results indicate that it is essential to modify the production rate of  $^{187}\text{W}$  in the activation calculation by replacing it with the value obtained directly from MCNP to properly account for self-shielding. It was pointed out by J-Ch. Sublet [10] that similar treatment should be applied to other low energy resonances in all W isotopes to account for self-shielding. The 5 eV resonance in the  $^{182}\text{W}(n,\gamma)^{183}\text{W}$  reaction was identified to be of concern regarding the self-shielding effect. However, the  $^{183m}\text{W}$  radionuclide produced is short lived ( $T_{1/2} = 5.2$  s) and does not have a significant contribution to decay heat. In the activation calculations performed here, we modified

the  $^{186}\text{W}(n,\gamma)^{187}\text{W}$  reaction rates only. The reaction rates in the front 1 cm W PFC of the dome and vertical targets as calculated by MCNP are given in Table 4. These values were used in the activation calculations. The  $^{187}\text{W}$  production rates in the W covering the baffle modules were calculated also. The values are  $3.11 \times 10^{12}$  and  $4.43 \times 10^{12}$  nuclides/cm<sup>3</sup>s for the inboard and outboard baffles, respectively.

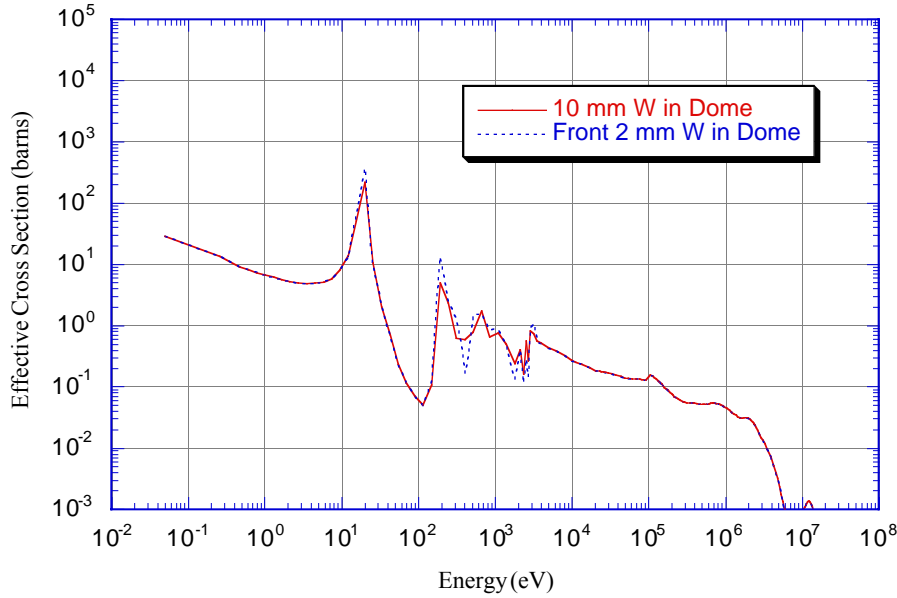


Fig. 13. Effective  $^{186}\text{W}(n,\gamma)$  cross section from MCNP for 175 groups.

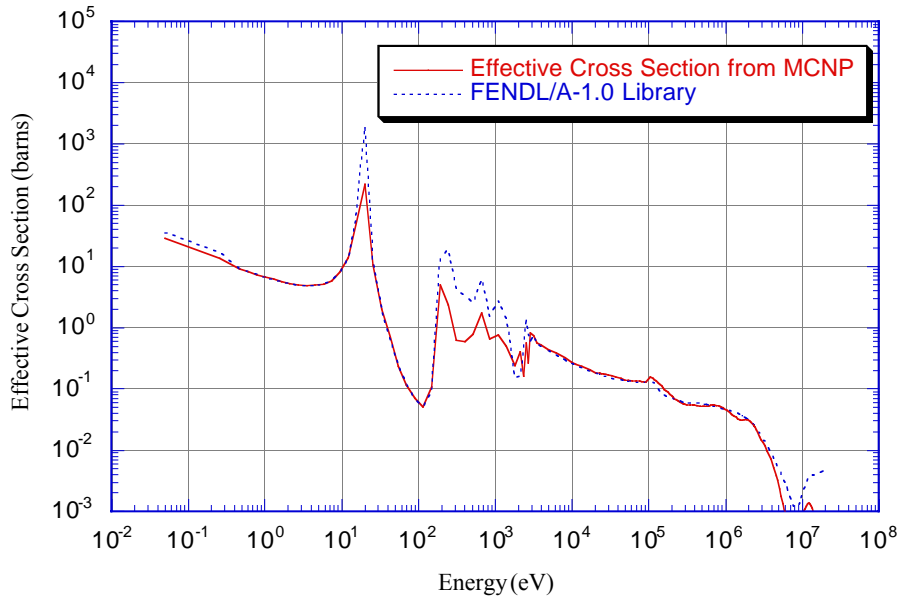


Fig. 14. Comparison between  $^{186}\text{W}(n,\gamma)$  cross section from MCNP with self-shielding and from FENDL/A-1.0.

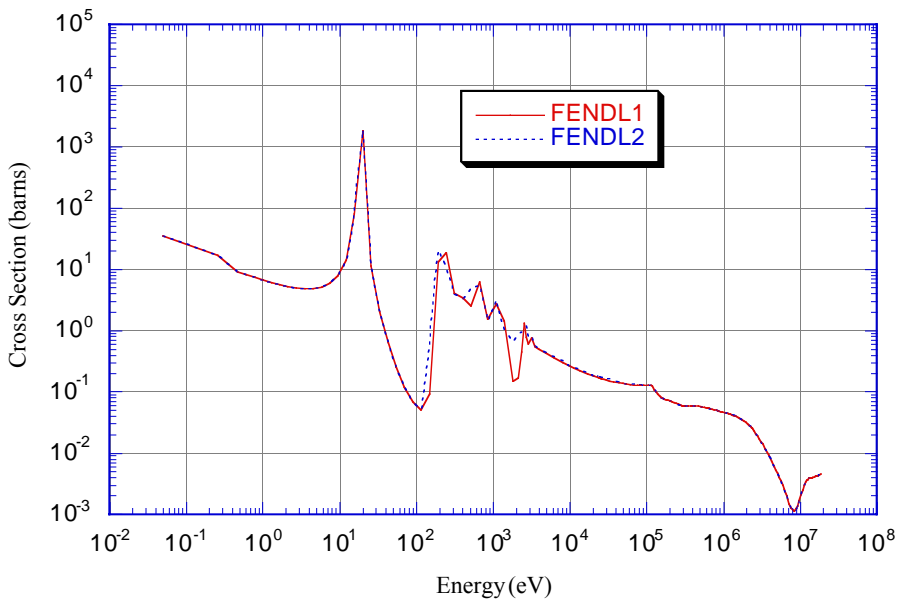


Fig. 15.  $^{186}\text{W}(n,\gamma)$  cross sections from FENDL/A-1.0 and FENDL/A-2.0.

Table 4.  $^{187}\text{W}$  Production Rate (nuclides/cm<sup>3</sup>s) Calculated by MCNP in the W PFC of Dome and Vertical Targets

Dome PFC (Cell 1)	$3.82 \times 10^{12}$
Outer Vertical Target	
Top (Cell 67)	$2.43 \times 10^{12}$
Middle (Cell 68)	$1.89 \times 10^{12}$
Inner Vertical Target	
Top (Cell 76)	$2.03 \times 10^{12}$
Middle (Cell 77)	$1.53 \times 10^{12}$

It is concluded from the analysis presented in this section that the reasons for large discrepancies obtained before in results for W decay heat at 1 hr following shutdown are homogenization with the heat sink that includes water and using non-self-shielded cross sections in the activation calculations. Hence for correct analysis one should rely on the continuous energy 3-D Monte Carlo results with proper layered heterogeneous modeling to calculate the spectra and reaction rates or effective self-shielded cross sections to be used in the activation calculations.

## 5. ACTIVATION CALCULATION

A detailed activation analysis is performed using the latest version of the activation code DKR-PULSAR2.0 [13]. The code combined the 175-group neutron flux calculated by the MCNP-4A code with the FENDL/A-2.0 and FENDL/D-2.0 data libraries [12] to calculate the activity and decay heat generated in the different zones of the divertor. Special attention was given to the top 1 cm tungsten layer of the divertor dome. The FENDL/A-2.0 library contains data for 739 target nuclides. These target nuclides extend from  $^1\text{H}$  up to  $^{248}\text{Cm}$  with the total number of reactions being 13006. On the other hand, the decay library includes data for 1626 nuclides. The FENDL/A-2.0 library follows the 175 Vitamin-J group format which is compatible with the DKR-PULSAR2.0 code.

As mentioned in the previous section, a correct treatment of the tungsten self-shielding problem was taken into account by replacing the  $^{186}\text{W}(\text{n},\gamma)$  cross section in the FENDL/A-2.0 library with the effective cross section calculated from the MCNP-4A calculations. Even though the neutron capture cross sections of  $^{182}\text{W}$  and  $^{183}\text{W}$  also have significant resonances in the thermal energy range, results presented in this report are focused only on correcting for the  $^{186}\text{W}(\text{n},\gamma)$  self-shielding effect. That is due to the fact that the daughters of  $^{182}\text{W}$  and  $^{183}\text{W}$  are mostly short lived with minor impact on the total decay heat generation in the tungsten layer.

The level of activation induced in the divertor is dependent on operation time as well as the corresponding fluence. The current planning for ITER envisions two operational phases. The first phase is the Basic Performance Phase (BPP), which is supposed to last for ten years and involves a few thousand hours of D-T operation. The radioactivity induced in the divertor structure will depend on the pulsing scenarios that are being implemented during the BPP as well as the resulting fluence. A total fluence of  $0.3 \text{ MW}\cdot\text{a}/\text{m}^2$  is envisioned for this phase. The BPP could be followed by an Enhanced Performance Phase (EPP) that lasts for another ten years and would emphasize improved performance and testing. The EPP envisions utilizing a tritium breeding blanket and is expected to reach a total fluence on the order of  $3 \text{ MW}\cdot\text{a}/\text{m}^2$ . The results presented in this report only deal with the BPP phase.

The choice of pulsing sequences, including dwell times, used in activation analysis are of great importance to safety analysis. Using a detailed and accurate pulsing sequence is required to obtain an accurate picture of the possible safety hazard posed by the irradiated structure of the divertor in the case of the accidental release of some of its radioactive inventory. In addition, a

reliable estimate of the level of decay heat generated in the divertor is needed to accurately calculate the expected temperature rise of its structure during a Loss of Coolant Accident (LOCA) and/or a Loss of Flow Accident (LOFA). This temperature rise would also influence the level of possible radioactive release during a severe accident.

The increase in the divertor temperature during a LOCA/LOFA needs to be controlled in order to limit the mobilization of activation products via oxidation driven volatility. Limiting the increase in temperature would also limit the possible mobilization of tritium present in the plasma facing components. In addition, controlling the rise in temperature would also help in avoiding the possible formation of large amounts of hydrogen from beryllium-steam reactions under severe accident conditions. Finally, it is also important to limit any rise in the structure temperature below temperatures deemed of special concern from a structural analysis point of view.

Depending on the material used in the analysis, the short and mid-term radioactivity could be influenced by the details of the overall pulsing sequence, in particular, for isotopes with half-lives larger than the final pulse width but smaller than the total operation time [16]. The DKR-PULSAR2.0 code used in this analysis applies an efficient mathematical model of pulsing sequences allowing for the detailed modeling of all possible pulsing scenarios [17]. The code also allows for the modeling of indefinite number of pulses and intervals in a single computer run.

To examine the effect of pulsing sequences on the decay heat generation, the calculations were performed for the following two operational scenarios:

**I. SA1:** This scenario corresponds to a total machine fluence of  $0.3 \text{ MW}\cdot\text{a}/\text{m}^2$ . It has a long term availability of 25% and a final month availability of 50%. A burn pulse length of one hour producing 1500 MW of fusion power is used in this scenario. The SA1 scenario is modeled as follows:

- i. The long term span, which has a total duration of about 13.6 months, was modeled by a group of 375 pulses of one hour width with one hour dwell time between pulses. This group of pulses is repeated seven times with 750 hours of additional cooling time between them. This maintains an overall long term availability of 25%.
- ii. The last month corresponds to the final group of pulses. It includes 375 pulses of one hour width and one hour of dwell time between pulses, thus maintaining a short term availability of 50%.

**II. M5:** This scenario corresponds to a total fluence of  $0.1 \text{ MW}\cdot\text{a}/\text{m}^2$ . It has a long term availability of only 4% and a last month availability of 50%. A 1000 second burn producing 1500 MW of fusion power is used. The scenario is modeled as follows:

- i. 1900 pulses of 1000 second width with 25000 second dwell time between pulses for a total duration of 18.8 months.
- ii. An additional month is modeled with 1250 pulses of 1000 second width and 1000 seconds of dwell time between pulses. This maintains a short term availability of 50%.

The elemental composition of the materials [18] used in the analysis includes all possible impurities that may influence the long term radioactivity generated in the divertor. The activation calculations have been performed for the zones defined in Table 2. The results for zones in 9 different areas of the divertor are reported and analyzed in this report. These areas are:

- a. Dome PFC
- b. Dome body
- c. Central body
- d. Wings
- e. Outer leg
- f. Inner leg
- g. Outer vertical target
- h. Inner vertical target
- i. Rails

## 6. ACTIVATION RESULTS

Activation and decay heat values are calculated using the neutron fluxes produced by the MCNP-4A calculations for the different zones of the divertor. The activation and decay heat values are calculated for 12 different times following shutdown, ranging from zero to 1000 years. In addition, all nuclides contributing over 10% of the activity or decay heat at any of these 12 times are identified. The same calculational approach is used with the two operational scenarios previously discussed. The following 17 zones are selected for detailed presentation and analysis of results. The numbering of these zones follows the same order given in Figs. 2-4 and Table 2. Materials contained in each zone are given between brackets.

### I. Dome PFC:

- **Zone 1 (100% W)**

This zone represents the top 1 cm tungsten PFC layer of the divertor dome. As shown in Tables 5 and 39,  $^{183m}W$  ( $T_{1/2} = 5.2$  s) is the dominant contributor to the activity induced at shutdown for both operational scenarios. The  $^{187}W$  ( $T_{1/2} = 23.9$  h) is the other major contributor to activity. During the first day following shutdown,  $^{187}W$  and  $^{185}W$  ( $T_{1/2} = 75.1$  d) dominate the induced activity.  $^{185}W$  and  $^{181}W$  are the major contributors to activity one year following shutdown. At 10 years following shutdown,  $^{179}Ta$  ( $T_{1/2} = 665$  d) generates more than 60% of the zone's activity.  $^{60}Co$  ( $T_{1/2} = 5.27$  y) is the other major contributor to activity at the same time. Activities induced for times greater than 10 years are dominated by  $^{39}Ar$  ( $T_{1/2} = 269$  y),  $^{63}Ni$  ( $T_{1/2} = 100$  y),  $^{91}Nb$  ( $T_{1/2} = 10,000$  y), and  $^{14}C$  ( $T_{1/2} = 5730$  y). The same nuclides dominate the activities induced at all times following shutdown for both operational scenarios. Figure 16 shows the variation in activity as a function of time for the two scenarios. It is clear that the results are nearly identical for short term activity since the availability is the same during the last month of operation in both operation scenarios. On the other hand, the long term activity determined by the total fluence is lower by about a factor of 3 for the M5 scenario. The activity and decay heat results for all the zones confirm this observation.

All tungsten radionuclides are generated by  $(n,\gamma)$  and  $(n,2n)$  reactions with natural tungsten included in the calculation. The importance of using the correct self-shielded cross sections for the production of  $^{187}W$  lies in the fact that the daughter nuclides of  $^{187}W$  (produced via multi-step reactions and/or decay paths) will also be correctly predicted. All other contributors to activity

following shutdown are produced by nuclear interactions with impurities included in the tungsten chemical composition.  $^{179}\text{Ta}$  is produced by the  $^{180}\text{Ta}(\text{n},2\text{n})$  reaction,  $^{60}\text{Co}$  is produced by  $^{59}\text{Co}(\text{n},\gamma)$  reaction,  $^{39}\text{Ar}$  is mostly produced via the  $^{39}\text{K}(\text{n},\text{p})$  pathway,  $^{63}\text{Ni}$  is mostly generated by the  $^{62}\text{Ni}(\text{n},\gamma)$  reaction,  $^{91}\text{Nb}$  is produced by the  $^{92}\text{Mo}(\text{n},\text{d})$  pathway, and  $^{14}\text{C}$  is largely generated by the  $^{14}\text{N}(\text{n},\gamma)$  reaction. Chemical composition of the tungsten alloy used in this analysis contains as impurities 10 wppm of each of tantalum, cobalt, potassium, niobium, and nitrogen. It also contains 20 wppm and 100 wppm of nickel and molybdenum, respectively.

Figure 17 shows the decay heat generated in zone 1 as a function of time following shutdown. The  $^{187}\text{W}$  isotope is even a larger contributor to the decay heat than activity generated following shutdown. It produces about 90% of the decay heat up to 1 day following shutdown. Similar to the induced activity,  $^{185}\text{W}$  and  $^{181}\text{W}$  dominate the induced decay heat in the period between 1 week and 1 year.  $^{60}\text{Co}$  appears as nearly the sole contributor to the decay heat at 10 years after shutdown.  $^{108\text{m}}\text{Ag}$  ( $T_{1/2} = 130$  y) produced by  $^{107}\text{Ag}(\text{n},\gamma)$  and  $^{109}\text{Ag}(\text{n},2\text{n})$  reactions with the silver impurities (5 wppm) in the tungsten alloy is the major contributor to the decay heat after 100 years from shutdown. At times greater than 100 years, the decay heat is dominated by  $^{39}\text{Ar}$ ,  $^{14}\text{C}$ , and  $^{94}\text{Nb}$  ( $T_{1/2} = 20,000$  y) which is produced as a result of the  $^{93}\text{Nb}(\text{n},\gamma)$  and  $^{94}\text{Mo}(\text{n},\text{p})$  reactions. Tables 6 and 40 list all major contributors to the decay heat for the SA1 and M5 scenarios, respectively.

Finally, it is important to emphasize that the dominance of the  $^{187}\text{W}$  contribution to the divertor PFC decay heat is also affected by the accuracy of the three-dimensional model used in the analysis. A different study [19] showed that using a homogeneous composition of W and Cu + H<sub>2</sub>O (zones 1 and 2 in this analysis) to represent the divertor's PFC region along with homogeneous non-self-shielded data resulted in overestimating the tungsten decay heat produced at one hour cooling times by a factor of three.

- **Zone 2** (75% GlidCop Cu and 25% H<sub>2</sub>O)

This zone represents the heat sink layer behind the dome PFC. As shown in Tables 7 and 41, the copper isotopes,  $^{64}\text{Cu}$  ( $T_{1/2} = 12.71$  h),  $^{62}\text{Cu}$  ( $T_{1/2} = 9.74$  m), and  $^{66}\text{Cu}$  ( $T_{1/2} = 5.1$  m) dominate the induced activity during the first hour following shutdown for both operational scenarios.  $^{64}\text{Cu}$  continues to be the sole dominant isotope during the first few days. The three copper isotopes are produced by (n,γ) and (n,2n) interactions with the two stable copper isotopes,  $^{63}\text{Cu}$  and  $^{65}\text{Cu}$ . In addition, the  $^{63}\text{Cu}(\text{n},\text{p})$  reaction results in the production of  $^{63}\text{Ni}$  which dominates the induced activity for times greater than one week following shutdown, regardless of the pulsing scenario.

The decay heat generated in zone 2 after shutdown is dominated by the same 3 copper isotopes,  $^{64}\text{Cu}$ ,  $^{62}\text{Cu}$ , and  $^{66}\text{Cu}$ , during the first few days. Decay heat generated after the first week is mostly produced by impurities contained in the GlidCop Cu alloy. As shown in Table 8 and 42, except for  $^{63}\text{Ni}$ , the decay heat for times greater than the first week is dominated by  $^{60}\text{Co}$  up to ten years and  $^{110\text{m}}\text{Ag}$  ( $T_{1/2} = 252$  d) up to a year. The  $^{60}\text{Co}$  and  $^{110\text{m}}\text{Ag}$  isotopes are produced by  $(n,\gamma)$  reactions with the two stable nuclides  $^{59}\text{Co}$  and  $^{109}\text{Ag}$ , respectively. The temporal variation of activity and decay heat generated by the two operational scenarios are shown in Figs. 18 and 19, respectively.

## II. Dome Body:

- **Zone 4** (85% GlidCop Cu and 15% H<sub>2</sub>O)

Figures 20 and 21 show the activity and decay heat values generated in this zone. The activity and decay heat are dominated by radioactive products of the GlidCop Cu alloy. As shown in Tables 9, 10, 43 and 44, radioisotopes dominating the activity and decay heat in zone 2 are also, for the most part, the major contributors to zone 4.

- **Zone 7** (75% 316 SS-LN and 25% H<sub>2</sub>O)

Like most steel alloys, the activity and decay heat are dominated in short and mid-terms by the two manganese isotopes  $^{56}\text{Mn}$  and  $^{54}\text{Mn}$ . Figures 22 and 23 show the activity and decay heat values generated in the zone. As shown in Tables 11, 12, 45, and 46,  $^{56}\text{Mn}$  ( $T_{1/2} = 2.58$  h) is the major contributor to the activity and decay heat during the first few hours following shutdown. On the other hand,  $^{54}\text{Mn}$  ( $T_{1/2} = 312.5$  d) is the major contributor to the decay heat up to a year. The manganese isotopes are nearly produced equally by the two following pathways:

$^{54}\text{Mn}$  via  $^{55}\text{Mn}$  ( $n,2n$ ) and  $^{54}\text{Fe}(n,p)$  reactions

$^{56}\text{Mn}$  via  $^{55}\text{Mn}$  ( $n,\gamma$ ) and  $^{56}\text{Fe}(n,p)$  reactions

Other contributors to activity are  $^{51}\text{Cr}$  ( $T_{1/2} = 27.71$  d) during the first month,  $^{55}\text{Fe}$  ( $T_{1/2} = 2.7$  y) during the first 10 years,  $^{63}\text{Ni}$  during the first 100 years, and  $^{59}\text{Ni}$  ( $T_{1/2} = 80,000$  y) for times more than 1000 years. The mid and long-term decay heat is generated by  $^{58}\text{Co}$  ( $T_{1/2} = 70.8$  d) and  $^{60}\text{Co}$  during the first year.  $^{63}\text{Ni}$  dominated during the first 100 years.  $^{59}\text{Ni}$  and  $^{14}\text{C}$  dominate at 1000 years from shutdown.

The  $^{51}\text{Cr}$  isotope is mostly produced by the  $^{50}\text{Cr}(\text{n},\gamma)$  and  $^{52}\text{Cr}(\text{n},2\text{n})$  reactions.  $^{55}\text{Fe}$  is a product of the  $^{54}\text{Fe}(\text{n},\gamma)$  and  $^{56}\text{Fe}(\text{n},2\text{n})$  reactions. While,  $^{63}\text{Ni}$  is mainly produced by  $^{62}\text{Ni}(\text{n},\gamma)$  reaction,  $^{59}\text{Ni}$  could be produced by either of the  $^{58}\text{Ni}(\text{n},\gamma)$  or  $^{60}\text{Ni}(\text{n},2\text{n})$  reactions.  $^{58}\text{Ni}$  is also the major contributor to the production of  $^{58}\text{Co}$ . The other contributor to the production of  $^{58}\text{Co}$  is  $^{59}\text{Co}$  which also produces  $^{60}\text{Co}$  via the  $(\text{n},\gamma)$  pathway. The  $^{14}\text{C}$  isotope is produced by the  $^{14}\text{N}(\text{n},\text{p})$  reaction.

### **III. Central Body:**

- **Zone 16** (80% 316 SS-LN and 20%  $\text{H}_2\text{O}$ )

As in zone 7, the activity and decay heat are dominated by the 316 SS-LN alloy. As shown in Tables 13, 14, 47, and 48, the activity and decay heat are dominated by the same isotopes mentioned in the previous discussion of zone 7. Figures 24 and 25 show the variation in the activity and decay heat as a function of time following shutdown.

### **IV. Wings:**

- **Zone 24 and Zone 26** (16% W, 79% Cu and 5%  $\text{H}_2\text{O}$ )

Zones 24 and 26 represent the outer and inner wings of the divertor, respectively. Activities and decay heat values in both zones are dominated by the same radionuclides.  $^{64}\text{Cu}$  and  $^{187}\text{W}$  dominate the activity and decay heat during the first day following shutdown.  $^{181}\text{W}$  and  $^{185}\text{W}$  dominate during the first year.  $^{60}\text{Co}$  and  $^{63}\text{Ni}$  dominate at times greater than a year. Except for the tungsten isotopes, all other isotopes are the products of the GlidCop Cu alloy. Figs. 26-29 and Tables 15-18 and 49-52, show the different aspects of activity and decay heat generation in the two zones.

### **V. Outer Leg:**

- **Zone 41** (80% 316 SS-LN and 20%  $\text{H}_2\text{O}$ )

Dominant contributors to activity and decay heat following shutdown are similar to those discussed in the results of zone 16. Figures 30 and 31 and Tables 19, 20, 53, and 54 show the detailed results for zone 41 for the two operational scenarios.

## **VI. Inner Leg:**

- **Zone 60** (80% 316 SS-LN and 20% H<sub>2</sub>O)

Tables 21, 22, 55, and 56 show the dominant nuclides for activity and decay heat. Figures 32 and 33 show the activity and decay heat generated after shutdown. Major contributors to activity and decay heat are similar to those mentioned in the discussion of the results of zone 16. The levels of activity and decay heat generated in the inner leg are lower than the levels induced in the outer leg due to the fact that the inner leg is exposed to a lower neutron flux.

## **VII. Outer Vertical Target:**

- **Zone 67 and Zone 68** (100% W)

These two zones represent the tungsten armor of the outer vertical target. The tungsten at the top of the outer vertical target (zone 67) experiences a higher level of activation in comparison to the lower part of the target (zone 68). As shown in Tables 23-26 and 57-60, the nuclides dominating the activity and decay heat are identical to those dominating the 1 cm tungsten layer of the dome's PFC. Figures 34-37 show the activity and decay heat variation as a function of time following shutdown.

- **Zone 73** (89% C, 4% GlidCop Cu and 7% H<sub>2</sub>O)

The zone represents the armor of the lower section of the outer vertical target. Carbon activity and decay heat is considerably low resulting in the copper alloy being the major source of activity and decay heat generated in the zone. <sup>66</sup>Cu and <sup>64</sup>Cu dominate during the first week after shutdown and <sup>63</sup>Ni dominates at longer times. <sup>110m</sup>Ag dominates the decay heat in the period between one week and one year. Tables 27, 28, 61, and 62 show the major contributors. Figures 38 and 39 show the temporal variation of activity and decay heat.

## **VIII. Inner Vertical Target:**

- **Zone 76 and Zone 77** (100% W)

The zones represent the tungsten armor of the inner vertical target. Dominant nuclides are similar to zones 67 and 68. Another similarity is apparent in the fact that tungsten experiences a higher level of activation and decay heat in the upper section of the inner vertical target (zone 76) than the level experienced by the lower section (zone 77). Major contributors are listed in Tables 29-32 and 63-66. Variation of activities and decay heat as a function of time following shutdown are shown in Figs. 40-43.

- **Zone 82** (89% C, 4% GlidCop Cu, and 7% H<sub>2</sub>O)

This zone is similar to zone 73. Figures 44-45 show activity and decay heat variation. Tables 33-34 and 67-68 list dominant nuclides for the SA1 and M5 scenarios.

The levels of activity and decay heat generated in the inner vertical target is lower than the levels induced in the outer vertical target due to the fact that the inner vertical target is exposed to a lower neutron flux than the outer vertical target.

## **IX. Rails:**

- **Zone 104 and Zone 105** (100% 316 SS-LN)

The zones are made of 100% steel and as in zone 7, the manganese isotopes are the dominant source of activity and decay heat following shutdown. A detailed description of dominant nuclides is provided in the discussion of zone 7. Tables 35-38 and 69-72 list dominant nuclides. Figures 46-49 show activity and decay heat variation for both zones under the two operational scenarios. The neutron flux in the rails is very small due to the shielding provided by the divertor cassette. As a result the activity and decay heat levels generated in the rails are extremely low particularly for the outer rail (zone 104).

Tables 73 and 74 provide a summary of the specific activities and decay heat generated in all zones as a function of time following shutdown for the SA1 scenario, respectively. A similar summary is provided for the M5 operational scenario in Tables 75 and 76.

Table 5. Major Contributors to Activity Induced in Dome PFC (Zone 1) for SA1 Scenario (in percent)

Time	0	1 m	10 m	1 h	6 h	1 d	1w	1 mo	1 y	10 y	100 y	1000 y
c 14	5.644E-08	9.886E-08	1.084E-07	1.105E-07	1.211E-07	1.612E-07	3.25E-07	4.08E-07	5.46E-06	2.32E-02	4.91E+00	1.95E+01
ar 39	3.453E-07	6.048E-07	6.633E-07	6.760E-07	7.407E-07	9.859E-07	1.99E-06	2.49E-06	3.33E-05	1.38E-01	2.35E+01	1.03E+01
co 60	2.605E-04	4.564E-04	5.005E-04	5.101E-04	5.589E-04	7.437E-04	1.50E-03	1.86E-03	2.21E-02	2.87E+01	4.42E-02	0.00E+00
ni 63	4.521E-07	7.919E-07	8.684E-07	8.851E-07	9.698E-07	1.291E-06	2.61E-06	3.26E-06	4.35E-05	1.73E-01	1.99E+01	1.76E-01
nb 93m	2.394E-06	4.194E-06	4.599E-06	4.687E-06	5.136E-06	6.836E-06	1.38E-05	1.72E-05	2.22E-04	6.48E-01	6.82E+00	1.48E+01
nb 91	2.251E-07	3.943E-07	4.325E-07	4.408E-07	4.829E-07	6.428E-07	1.30E-06	1.63E-06	2.18E-05	9.16E-02	1.79E+01	3.17E+01
mo 93	5.606E-08	9.820E-08	1.077E-07	1.098E-07	1.203E-07	1.601E-07	3.23E-07	4.05E-07	5.43E-06	2.30E-02	4.84E+00	1.80E+01
ta179	6.773E-03	1.187E-02	1.301E-02	1.326E-02	1.453E-02	1.933E-02	3.88E-02	4.74E-02	4.48E-01	6.12E+01	1.55E-11	0.00E+00
w 181	4.649E+00	8.145E+00	8.931E+00	9.101E+00	9.960E+00	1.320E+01	2.58E+01	2.82E+01	5.57E+01	1.61E-03	0.00E+00	0.00E+00
w 183m	4.034E+01	2.418E-02	1.708E-33	0.000E+00	0.000E+00	0.000E+00	0.00E+00	0.00E+00	0.00E+00	0.00E+00	0.00E+00	0.00E+00
w 185	1.310E+01	2.295E+01	2.517E+01	2.564E+01	2.804E+01	3.707E+01	7.08E+01	7.14E+01	4.33E+01	1.16E-08	0.00E+00	0.00E+00
w 187	3.274E+01	5.733E+01	6.260E+01	6.228E+01	5.903E+01	4.664E+01	1.45E+00	1.51E-07	0.00E+00	0.00E+00	0.00E+00	0.00E+00

Table 6. Major Contributors to Decay Heat Induced in Dome PFC (Zone 1) for SA1 Scenario (in percent)

Time	0	1 m	10 m	1 h	6 h	1 d	1w	1 mo	1 y	10 y	100 y	1000 y
c 14	7.026E-09	1.022E-08	1.062E-08	1.088E-08	1.242E-08	1.968E-08	1.31E-07	1.86E-07	3.03E-06	1.48E-03	1.09E+00	1.16E+01
ar 39	1.901E-07	2.767E-07	2.874E-07	2.944E-07	3.362E-07	5.326E-07	3.55E-06	5.03E-06	8.17E-05	3.92E-02	2.30E+01	2.69E+01
co 60	1.705E-03	2.481E-03	2.577E-03	2.640E-03	3.015E-03	4.775E-03	3.17E-02	4.46E-02	6.44E-01	9.66E+01	5.14E-01	0.00E+00
nb 94	2.032E-08	2.957E-08	3.072E-08	3.147E-08	3.593E-08	5.693E-08	3.79E-07	5.38E-07	8.75E-06	4.29E-03	3.17E+00	3.66E+01
ag108m	7.296E-07	1.062E-06	1.103E-06	1.130E-06	1.290E-06	2.044E-06	1.36E-05	1.93E-05	3.12E-04	1.46E-01	6.62E+01	5.78E+00
w 181	5.581E-01	8.122E-01	8.437E-01	8.640E-01	9.855E-01	1.555E+00	1.00E+01	1.24E+01	2.97E+01	9.96E-05	0.00E+00	0.00E+00
w 183m	3.001E+01	1.494E-02	9.999E-34	0.000E+00	0.000E+00	0.00E+00	0.00E+00	0.00E+00	0.00E+00	0.00E+00	0.00E+00	0.00E+00
w 185	4.186E+00	6.091E+00	6.327E+00	6.479E+00	7.385E+00	1.162E+01	7.32E+01	8.36E+01	6.16E+01	1.91E-09	0.00E+00	0.00E+00
w 187	5.949E+01	8.653E+01	8.950E+01	8.949E+01	8.841E+01	8.314E+01	8.53E+00	1.01E-06	0.00E+00	0.00E+00	0.00E+00	0.00E+00

Table 7. Major Contributors to Activity Induced in Dome PFC (Zone 2) for SA1 Scenario (in percent)

Time	0	1 m	10 m	1 h	6 h	1 d	1w	1 mo	1 y	10 y	100 y	1000 y
ni 63	1.014E-02	1.060E-02	1.350E-02	1.729E-02	2.288E-02	6.129E-02	4.39E+01	6.81E+01	8.49E+01	9.55E+01	9.99E+01	9.94E+01
cu 62	1.849E+01	1.799E+01	1.205E+01	4.347E-01	2.867E-10	2.489E-43	0.00E+00	0.00E+00	0.00E+00	0.00E+00	0.00E+00	0.00E+00
cu 64	6.137E+01	6.410E+01	8.098E+01	9.910E+01	9.978E+01	9.980E+01	2.70E+01	1.79E-12	0.00E+00	0.00E+00	0.00E+00	0.00E+00
cu 66	1.899E+01	1.732E+01	6.476E+00	9.147E-03	2.966E-09	6.320E-09	7.26E-07	8.85E-10	0.00E+00	0.00E+00	0.00E+00	0.00E+00

Table 8. Major Contributors to Decay Heat Induced in Dome PFC (Zone 2) for SA1 Scenario (in percent)

Time	0	1 m	10 m	1 h	6 h	1 d	1w	1 mo	1 y	10 y	100 y	1000 y
co 60	1.109E-03	1.234E-03	2.107E-03	5.058E-03	6.935E-03	1.860E-02	7.56E+00	1.31E+01	3.67E+01	6.11E+01	2.13E-03	0.00E+00
ni 63	1.984E-04	2.209E-04	3.771E-04	9.053E-04	1.241E-03	3.329E-03	1.36E+00	2.37E+00	7.43E+00	3.80E+01	9.94E+01	9.42E+01
cu 62	4.822E+01	4.998E+01	4.487E+01	3.033E+00	2.072E-09	1.801E-42	0.00E+00	0.00E+00	0.00E+00	0.00E+00	0.00E+00	0.00E+00
cu 64	2.195E+01	2.441E+01	4.133E+01	9.479E+01	9.887E+01	9.903E+01	1.53E+01	1.14E-12	0.00E+00	0.00E+00	0.00E+00	0.00E+00
cu 66	2.502E+01	2.431E+01	1.218E+01	3.225E-02	1.083E-08	2.311E-08	1.51E-06	2.07E-09	0.00E+00	0.00E+00	0.00E+00	0.00E+00
as 74	2.784E-03	3.100E-03	5.290E-03	1.268E-02	1.725E-02	4.493E-02	1.45E+01	1.01E+01	6.70E-05	0.00E+00	0.00E+00	0.00E+00
ag110m	3.124E-03	3.478E-03	5.937E-03	1.425E-02	1.953E-02	5.228E-02	2.09E+01	3.43E+01	4.28E+01	2.56E-02	3.14E-41	0.00E+00
sb124	2.970E-03	3.306E-03	5.643E-03	1.354E-02	1.853E-02	4.926E-02	1.87E+01	2.50E+01	1.68E+00	3.60E-16	0.00E+00	0.00E+00

Table 9. Major Contributors to Activity Induced in Dome Body (Zone 4) for SA1 Scenario (in percent)

Time	0	1 m	10 m	1 h	6 h	1 d	1w	1 mo	1 y	10 y	100 y	1000 y
ni 63	6.243E-03	6.499E-03	8.105E-03	9.804E-03	1.293E-02	3.462E-02	3.09E+01	5.60E+01	7.96E+01	9.53E+01	1.00E+02	9.96E+01
cu 64	6.695E+01	6.963E+01	8.613E+01	9.954E+01	9.986E+01	9.984E+01	3.38E+01	2.61E-12	0.00E+00	0.00E+00	0.00E+00	0.00E+00
cu 66	2.311E+01	2.099E+01	7.685E+00	1.025E-02	1.349E-09	2.874E-09	4.12E-07	5.86E-10	0.00E+00	0.00E+00	0.00E+00	0.00E+00
ag110m	1.419E-03	1.477E-03	1.842E-03	2.228E-03	2.937E-03	7.848E-03	6.90E+00	1.17E+01	6.61E+00	9.24E-04	4.56E-43	0.00E+00
sb124	1.672E-03	1.740E-03	2.170E-03	2.624E-03	3.453E-03	9.164E-03	7.65E+00	1.06E+01	3.23E-01	1.61E-17	0.00E+00	0.00E+00

Table 10. Major Contributors to Decay Heat Induced in Dome Body (Zone 4) for SA1 Scenario (in percent)

Time	0	1 m	10 m	1 h	6 h	1 d	1w	1 mo	1 y	10 y	100 y	1000 y
co 60	1.542E-03	1.684E-03	2.832E-03	5.336E-03	7.157E-03	1.915E-02	7.62E+00	1.23E+01	3.45E+01	7.40E+01	3.88E-03	0.00E+00
ni 63	1.517E-04	1.657E-04	2.786E-04	5.248E-04	7.040E-04	1.884E-03	7.52E-01	1.22E+00	3.84E+00	2.53E+01	9.92E+01	9.44E+01
cu 62	3.007E+01	3.058E+01	2.704E+01	1.434E+00	9.585E-10	8.314E-43	0.00E+00	0.00E+00	0.00E+00	0.00E+00	0.00E+00	0.00E+00
cu 64	2.972E+01	3.242E+01	5.408E+01	9.734E+01	9.931E+01	9.926E+01	1.50E+01	1.04E-12	0.00E+00	0.00E+00	0.00E+00	0.00E+00
cu 66	3.781E+01	3.603E+01	1.779E+01	3.695E-02	4.946E-09	1.053E-08	6.74E-07	8.61E-10	0.00E+00	0.00E+00	0.00E+00	0.00E+00
ag110m	5.660E-03	6.180E-03	1.039E-02	1.958E-02	2.625E-02	7.009E-02	2.75E+01	4.19E+01	5.24E+01	4.04E-02	7.43E-41	0.00E+00
sb124	5.300E-03	5.787E-03	9.731E-03	1.833E-02	2.452E-02	6.507E-02	2.42E+01	3.01E+01	2.03E+00	5.59E-16	0.00E+00	0.00E+00

Table 11. Major Contributors to Activity Induced in Dome Body (Zone 7) for SA1 Scenario (in percent)

Time	0	1 m	10 m	1 h	6 h	1 d	1w	1 mo	1 y	10 y	100 y	1000 y
c 14	6.114E-05	6.235E-05	6.730E-05	8.170E-05	1.555E-04	2.417E-04	3.05E-04	4.65E-04	1.80E-03	1.80E-02	3.00E-01	1.15E+01
cr 51	1.534E+01	1.564E+01	1.688E+01	2.047E+01	3.873E+01	5.911E+01	6.42E+01	5.44E+01	4.80E-02	8.05E-37	0.00E+00	0.00E+00
mn 56	6.018E+01	6.109E+01	6.333E+01	6.144E+01	3.046E+01	3.744E-01	7.19E-18	0.00E+00	0.00E+00	0.00E+00	0.00E+00	0.00E+00
fe 55	3.265E+00	3.330E+00	3.594E+00	4.363E+00	8.296E+00	1.290E+01	1.62E+01	2.43E+01	7.48E+01	7.59E+01	1.55E-07	0.00E+00
co 60	1.649E-01	1.681E-01	1.814E-01	2.203E-01	4.189E-01	6.513E-01	8.21E-01	1.24E+00	4.27E+00	1.30E+01	1.57E-03	0.00E+00
ni 59	3.179E-04	3.242E-04	3.499E-04	4.248E-04	8.079E-04	1.257E-03	1.59E-03	2.42E-03	9.38E-03	9.35E-02	1.57E+00	6.69E+01
ni 63	3.930E-02	4.007E-02	4.325E-02	5.251E-02	9.986E-02	1.553E-01	1.96E-01	2.99E-01	1.15E+00	1.08E+01	9.76E+01	8.32E+00

Table 12. Major Contributors to Decay Heat Induced in Dome Body (Zone 7) for SA1 Scenario (in percent)

Time	0	1 m	10 m	1 h	6 h	1 d	1w	1 mo	1 y	10 y	100 y	1000 y
c 14	1.646E-06	1.712E-06	1.845E-06	2.304E-06	7.227E-06	4.566E-05	8.58E-05	1.14E-04	4.10E-04	2.58E-03	8.64E-01	3.68E+01
cr 51	3.101E-01	3.225E-01	3.475E-01	4.337E-01	1.353E+00	8.389E+00	1.36E+01	1.01E+01	8.19E-03	8.67E-38	0.00E+00	0.00E+00
mn 54	3.164E-01	3.290E-01	3.546E-01	4.429E-01	1.388E+00	8.756E+00	1.62E+01	2.06E+01	3.51E+01	1.49E-01	1.00E-30	0.00E+00
mn 56	8.263E+01	8.553E+01	8.854E+01	8.839E+01	7.225E+01	3.607E+00	1.03E-16	0.00E+00	0.00E+00	0.00E+00	0.00E+00	0.00E+00
fe 59	2.230E-01	2.319E-01	2.499E-01	3.120E-01	9.754E-01	6.091E+00	1.04E+01	9.66E+00	1.90E-01	7.45E-23	0.00E+00	0.00E+00
co 58m	5.457E+00	5.667E+00	6.039E+00	7.080E+00	1.519E+01	2.445E+01	8.16E-04	3.01E-22	0.00E+00	0.00E+00	0.00E+00	0.00E+00
co 58	6.898E-01	7.172E-01	7.730E-01	9.652E-01	3.021E+00	1.895E+01	3.36E+01	3.56E+01	4.86E+00	3.51E-13	0.00E+00	0.00E+00
co 60	2.333E-01	2.426E-01	2.615E-01	3.266E-01	1.024E+00	6.468E+00	1.21E+01	1.61E+01	5.10E+01	9.80E+01	2.39E-01	0.00E+00
ni 59	1.273E-06	1.324E-06	1.427E-06	1.783E-06	5.591E-06	3.532E-05	6.64E-05	8.86E-05	3.18E-04	2.00E-03	6.76E-01	3.18E+01
ni 63	3.666E-04	3.812E-04	4.108E-04	5.131E-04	1.609E-03	1.017E-02	1.91E-02	2.55E-02	9.08E-02	5.36E-01	9.75E+01	9.20E+00
mo 99	5.968E-01	6.204E-01	6.677E-01	8.267E-01	2.460E+00	1.286E+01	5.32E+00	1.92E-02	1.41E-38	0.00E+00	0.00E+00	0.00E+00

Table 13. Major Contributors to Activity Induced in Central Body (Zone 16) for SA1 Scenario (in percent)

Time	0	1 m	10 m	1 h	6 h	1 d	1w	1 mo	1 y	10 y	100 y	1000 y
c 14	6.156E-05	6.242E-05	6.716E-05	8.243E-05	1.635E-04	2.646E-04	3.46E-04	5.54E-04	2.50E-03	2.17E-02	3.00E-01	1.17E+01
cr 51	1.475E+01	1.495E+01	1.609E+01	1.973E+01	3.892E+01	6.181E+01	6.96E+01	6.19E+01	6.34E-02	9.28E-37	0.00E+00	0.00E+00
mn 56	6.310E+01	6.369E+01	6.583E+01	6.457E+01	3.338E+01	4.269E-01	8.50E-18	0.00E+00	0.00E+00	0.00E+00	0.00E+00	0.00E+00
fe 55	2.484E+00	2.519E+00	2.710E+00	3.327E+00	6.596E+00	1.067E+01	1.39E+01	2.19E+01	7.82E+01	6.93E+01	1.17E-07	0.00E+00
co 60	1.845E-01	1.870E-01	2.013E-01	2.470E-01	4.898E-01	7.925E-01	1.04E+00	1.64E+00	6.56E+00	1.74E+01	1.75E-03	0.00E+00
ni 59	3.223E-04	3.268E-04	3.516E-04	4.316E-04	8.559E-04	1.385E-03	1.81E-03	2.90E-03	1.31E-02	1.14E-01	1.59E+00	6.85E+01
ni 63	3.956E-02	4.011E-02	4.316E-02	5.297E-02	1.051E-01	1.700E-01	2.23E-01	3.56E-01	1.59E+00	1.30E+01	9.77E+01	8.46E+00

Table 14. Major Contributors to Decay Heat Induced in Central Body (Zone 16) for SA1 Scenario (in percent)

Time	0	1 m	10 m	1 h	6 h	1 d	1w	1 mo	1 y	10 y	100 y	1000 y
c 14	1.678E-06	1.711E-06	1.827E-06	2.292E-06	7.546E-06	5.561E-05	1.04E-04	1.45E-04	4.85E-04	2.33E-03	8.65E-01	3.74E+01
cr 51	3.019E-01	3.080E-01	3.288E-01	4.121E-01	1.349E+00	9.760E+00	1.58E+01	1.22E+01	9.25E-03	7.49E-38	0.00E+00	0.00E+00
mn 54	1.694E-01	1.728E-01	1.845E-01	2.315E-01	7.616E-01	5.603E+00	1.04E+01	1.37E+01	2.18E+01	7.07E-02	5.26E-31	0.00E+00
mn 56	8.771E+01	8.907E+01	9.134E+01	9.158E+01	7.858E+01	4.576E+00	1.31E-16	0.00E+00	0.00E+00	0.00E+00	0.00E+00	0.00E+00
fe 59	2.451E-01	2.500E-01	2.669E-01	3.347E-01	1.098E+00	7.999E+00	1.37E+01	1.32E+01	2.42E-01	7.26E-23	0.00E+00	0.00E+00
co 58m	3.407E+00	3.471E+00	3.664E+00	4.314E+00	9.714E+00	1.824E+01	6.08E-04	2.34E-22	0.00E+00	0.00E+00	0.00E+00	0.00E+00
co 58	4.500E-01	4.590E-01	4.901E-01	6.146E-01	2.019E+00	1.477E+01	2.61E+01	2.90E+01	3.68E+00	2.03E-13	0.00E+00	0.00E+00
co 60	2.643E-01	2.696E-01	2.878E-01	3.611E-01	1.189E+00	8.757E+00	1.64E+01	2.27E+01	6.70E+01	9.86E+01	2.65E-01	0.00E+00
ni 59	1.307E-06	1.333E-06	1.423E-06	1.785E-06	5.878E-06	4.332E-05	8.13E-05	1.13E-04	3.78E-04	1.82E-03	6.81E-01	3.26E+01
ni 63	3.735E-04	3.810E-04	4.069E-04	5.104E-04	1.680E-03	1.238E-02	2.32E-02	3.24E-02	1.07E-01	4.85E-01	9.76E+01	9.37E+00
mo 99	7.264E-01	7.409E-01	7.898E-01	9.821E-01	3.068E+00	1.871E+01	7.73E+00	2.91E-02	1.99E-38	0.00E+00	0.00E+00	0.00E+00

Table 15. Major Contributors to Activity Induced in Wings (Zone 24) for SA1 Scenario (in percent)

Time	0	1 m	10 m	1 h	6 h	1 d	1w	1 mo	1 y	10 y	100 y	1000 y
ni 63	8.297E-03	1.001E-02	1.221E-02	1.486E-02	1.862E-02	3.788E-02	1.59E-01	1.97E-01	2.73E+00	9.52E+01	9.99E+01	9.90E+01
cu 62	1.520E+01	1.708E+01	1.095E+01	3.753E-01	2.344E-10	1.545E-43	0.00E+00	0.00E+00	0.00E+00	0.00E+00	0.00E+00	0.00E+00
cu 64	4.230E+01	5.101E+01	6.168E+01	7.174E+01	6.839E+01	5.194E+01	8.23E-02	4.38E-15	0.00E+00	0.00E+00	0.00E+00	0.00E+00
cu 66	1.043E+01	1.099E+01	3.932E+00	5.279E-03	2.644E-09	4.278E-09	2.87E-09	2.81E-12	0.00E+00	0.00E+00	0.00E+00	0.00E+00
w 181	1.177E+00	1.421E+00	1.732E+00	2.109E+00	2.639E+00	5.345E+00	2.16E+01	2.36E+01	4.83E+01	1.22E-05	0.00E+00	0.00E+00
w 183m	1.391E+01	5.744E-03	4.510E-34	0.000E+00	0.000E+00	0.000E+00	0.000E+00	0.00E+00	0.00E+00	0.00E+00	0.00E+00	0.00E+00
w 185	4.227E+00	5.102E+00	6.219E+00	7.568E+00	9.467E+00	1.912E+01	7.58E+01	7.60E+01	4.79E+01	1.12E-10	0.00E+00	0.00E+00
w 187	1.004E+01	1.212E+01	1.471E+01	1.748E+01	1.895E+01	2.287E+01	1.48E+00	1.53E-07	0.00E+00	0.00E+00	0.00E+00	0.00E+00

Table 16. Major Contributors to Decay Heat Induced in Wings (Zone 24) for SA1 Scenario (in percent)

Time	0	1 m	10 m	1 h	6 h	1 d	1w	1 mo	1 y	10 y	100 y	1000 y
co 60	8.869E-04	1.008E-03	1.570E-03	3.107E-03	3.986E-03	8.324E-03	1.02E-01	1.39E-01	2.06E+00	5.62E+01	1.76E-03	0.00E+00
ni 63	1.924E-04	2.186E-04	3.407E-04	6.739E-04	8.647E-04	1.806E-03	2.21E-02	3.05E-02	5.07E-01	4.24E+01	9.93E+01	9.14E+01
cu 62	4.696E+01	4.969E+01	4.072E+01	2.268E+00	1.450E-09	9.817E-43	0.00E+00	0.00E+00	0.00E+00	0.00E+00	0.00E+00	0.00E+00
cu 64	1.792E+01	2.034E+01	3.144E+01	5.943E+01	5.800E+01	4.525E+01	2.09E-01	1.24E-14	0.00E+00	0.00E+00	0.00E+00	0.00E+00
cu 66	1.629E+01	1.615E+01	7.389E+00	1.612E-02	8.266E-09	1.374E-08	2.69E-08	2.93E-11	0.00E+00	0.00E+00	0.00E+00	0.00E+00
w 181	7.599E-02	8.634E-02	1.345E-01	2.661E-01	3.410E-01	7.094E-01	8.38E+00	1.01E+01	2.50E+01	1.51E-05	0.00E+00	0.00E+00
w 185	7.260E-01	8.249E-01	1.285E+00	2.542E+00	3.255E+00	6.754E+00	7.81E+01	8.69E+01	6.58E+01	3.70E-10	0.00E+00	0.00E+00
w 187	9.810E+00	1.114E+01	1.729E+01	3.338E+01	3.706E+01	4.595E+01	8.65E+00	9.94E-07	0.00E+00	0.00E+00	0.00E+00	0.00E+00

Table 17. Major Contributors to Activity Induced in Wings (Zone 26) for SA1 Scenario (in percent)

Time	0	1 m	10 m	1 h	6 h	1 d	1w	1 mo	1 y	10 y	100 y	1000 y
ni 63	8.365E-03	1.010E-02	1.240E-02	1.520E-02	1.901E-02	3.819E-02	1.50E-01	1.87E-01	2.62E+00	9.50E+01	9.99E+01	9.90E+01
cu 62	1.581E+01	1.777E+01	1.147E+01	3.960E-01	2.467E-10	1.607E-43	0.00E+00	0.00E+00	0.00E+00	0.00E+00	0.00E+00	0.00E+00
cu 64	4.114E+01	4.964E+01	6.043E+01	7.079E+01	6.733E+01	5.052E+01	7.53E-02	4.01E-15	0.00E+00	0.00E+00	0.00E+00	0.00E+00
cu 66	1.069E+01	1.126E+01	4.058E+00	5.486E-03	2.779E-09	4.441E-09	2.81E-09	2.74E-12	0.00E+00	0.00E+00	0.00E+00	0.00E+00
w 181	1.214E+00	1.466E+00	1.799E+00	2.205E+00	2.755E+00	5.510E+00	2.10E+01	2.28E+01	4.74E+01	1.25E-05	0.00E+00	0.00E+00
w 183m	1.384E+01	5.721E-03	4.523E-34	0.000E+00	0.000E+00	0.000E+00	0.00E+00	0.00E+00	0.00E+00	0.00E+00	0.00E+00	0.00E+00
w 185	4.542E+00	5.484E+00	6.731E+00	8.250E+00	1.030E+01	2.054E+01	7.66E+01	7.67E+01	4.90E+01	1.19E-10	0.00E+00	0.00E+00
w 187	9.984E+00	1.205E+01	1.473E+01	1.907E+01	2.274E+01	1.38E+00	1.43E-07	0.00E+00	0.00E+00	0.00E+00	0.00E+00	0.00E+00

Table 18. Major Contributors to Decay Heat Induced in Wings (Zone 26) for SA1 Scenario (in percent)

Time	0	1 m	10 m	1 h	6 h	1 d	1w	1 mo	1 y	10 y	100 y	1000 y
co 60	9.333E-04	1.060E-03	1.667E-03	3.381E-03	4.339E-03	9.012E-03	1.03E-01	1.40E-01	2.09E+00	5.76E+01	1.87E-03	0.00E+00
ni 63	1.905E-04	2.164E-04	3.402E-04	6.901E-04	8.858E-04	1.840E-03	2.10E-02	2.88E-02	4.82E-01	4.09E+01	9.93E+01	9.12E+01
cu 62	4.797E+01	5.073E+01	4.195E+01	2.396E+00	1.532E-09	1.032E-42	0.00E+00	0.00E+00	0.00E+00	0.00E+00	0.00E+00	0.00E+00
cu 64	1.712E+01	1.943E+01	3.029E+01	5.870E+01	5.731E+01	4.447E+01	1.92E-01	1.13E-14	0.00E+00	0.00E+00	0.00E+00	0.00E+00
cu 66	1.639E+01	1.625E+01	7.496E+00	1.677E-02	8.718E-09	1.441E-08	2.64E-08	2.84E-11	0.00E+00	0.00E+00	0.00E+00	0.00E+00
w 181	7.693E-02	8.738E-02	1.374E-01	2.786E-01	3.572E-01	7.389E-01	8.15E+00	9.78E+00	2.43E+01	1.50E-05	0.00E+00	0.00E+00
w 185	7.660E-01	8.702E-01	1.368E+00	2.774E+00	3.554E+00	7.332E+00	7.92E+01	8.75E+01	6.67E+01	3.81E-10	0.00E+00	0.00E+00
w 187	9.578E+00	1.087E+01	1.702E+01	3.371E+01	3.743E+01	4.615E+01	8.12E+00	9.26E-07	0.00E+00	0.00E+00	0.00E+00	0.00E+00

Table 19. Major Contributors to Activity Induced in Outer Leg (Zone 41) for SA1 Scenario (in percent)

Time	0	1 m	10 m	1 h	6 h	1 d	1w	1 mo	1 y	10 y	100 y	1000 y
c 14	6.326E-05	6.397E-05	6.861E-05	8.445E-05	1.702E-04	2.792E-04	3.72E-04	6.13E-04	3.07E-03	2.42E-02	2.99E-01	1.19E+01
cr 51	1.488E+01	1.505E+01	1.614E+01	1.985E+01	3.979E+01	6.406E+01	7.34E+01	6.73E+01	7.66E-02	1.02E-36	0.00E+00	0.00E+00
mn 56	6.451E+01	6.495E+01	6.690E+01	6.582E+01	3.457E+01	4.482E-01	9.07E-18	0.00E+00	0.00E+00	0.00E+00	0.00E+00	0.00E+00
fe 55	2.177E+00	2.202E+00	2.362E+00	2.907E+00	5.857E+00	9.604E+00	1.27E+01	2.07E+01	8.20E+01	6.60E+01	9.96E-08	0.00E+00
co 60	1.863E-01	1.884E-01	2.021E-01	2.487E-01	5.012E-01	8.221E-01	1.09E+00	1.79E+00	7.93E+00	1.92E+01	1.72E-03	0.00E+00
ni 59	3.324E-04	3.361E-04	3.605E-04	4.437E-04	8.942E-04	1.467E-03	1.95E-03	3.22E-03	1.61E-02	1.27E-01	1.59E+00	6.97E+01
ni 63	4.076E-02	4.122E-02	4.421E-02	5.442E-02	1.097E-01	1.799E-01	2.39E-01	3.95E-01	1.97E+00	1.46E+01	9.78E+01	8.59E+00

Table 20. Major Contributors to Decay Heat Induced in Outer Leg (Zone 41) for SA1 Scenario (in percent)

Time	0	1 m	10 m	1 h	6 h	1 d	1w	1 mo	1 y	10 y	100 y	1000 y
c 14	1.738E-06	1.760E-06	1.870E-06	2.352E-06	7.977E-06	6.574E-05	1.23E-04	1.78E-04	5.71E-04	2.37E-03	8.63E-01	3.82E+01
cr 51	3.072E-01	3.111E-01	3.304E-01	4.151E-01	1.401E+00	1.133E+01	1.82E+01	1.47E+01	1.07E-02	7.50E-38	0.00E+00	0.00E+00
mn 54	8.843E-02	8.957E-02	9.515E-02	1.196E-01	4.056E-01	3.337E+00	6.15E+00	8.48E+00	1.29E+01	3.63E-02	2.65E-31	0.00E+00
mn 56	9.041E+01	9.116E+01	9.301E+01	9.347E+01	8.264E+01	5.382E+00	1.53E-16	0.00E+00	0.00E+00	0.00E+00	0.00E+00	0.00E+00
fe 59	2.586E-01	2.619E-01	2.782E-01	3.496E-01	1.182E+00	9.629E+00	1.64E+01	1.65E+01	2.90E-01	7.54E-23	0.00E+00	0.00E+00
co 58m	2.119E+00	2.143E+00	2.251E+00	2.657E+00	6.164E+00	1.294E+01	4.30E-04	1.72E-22	0.00E+00	0.00E+00	0.00E+00	0.00E+00
co 58	3.042E-01	3.081E-01	3.272E-01	4.113E-01	1.392E+00	1.139E+01	2.01E+01	2.32E+01	2.82E+00	1.35E-13	0.00E+00	0.00E+00
co 60	2.691E-01	2.726E-01	2.895E-01	3.641E-01	1.235E+00	1.017E+01	1.90E+01	2.73E+01	7.75E+01	9.87E+01	2.60E-01	0.00E+00
ni 59	1.359E-06	1.376E-06	1.462E-06	1.838E-06	6.235E-06	5.139E-05	9.60E-05	1.39E-04	4.46E-04	1.86E-03	6.82E-01	3.34E+01
ni 63	3.880E-04	3.930E-04	4.175E-04	5.250E-04	1.781E-03	1.468E-02	2.74E-02	3.98E-02	1.27E-01	4.95E-01	9.77E+01	9.58E+00
mo 99	7.869E-01	7.969E-01	8.452E-01	1.054E+00	3.391E+00	2.313E+01	9.51E+00	3.73E-02	2.46E-38	0.00E+00	0.00E+00	0.00E+00

Table 21. Major Contributors to Activity Induced in Inner Leg (Zone 60) for SA1 Scenario (in percent)

Time	0	1 m	10 m	1 h	6 h	1 d	1w	1 mo	1 y	10 y	100 y	1000 y
c 14	6.329E-05	6.395E-05	6.854E-05	8.462E-05	1.724E-04	2.851E-04	3.82E-04	6.40E-04	3.32E-03	2.48E-02	2.98E-01	1.18E+01
cr 51	1.490E+01	1.506E+01	1.614E+01	1.991E+01	4.035E+01	6.548E+01	7.55E+01	7.03E+01	8.29E-02	1.04E-36	0.00E+00	0.00E+00
mn 56	6.527E+01	6.566E+01	6.759E+01	6.669E+01	3.541E+01	4.628E-01	9.44E-18	0.00E+00	0.00E+00	0.00E+00	0.00E+00	0.00E+00
fe 55	2.081E+00	2.103E+00	2.253E+00	2.782E+00	5.667E+00	9.366E+00	1.25E+01	2.06E+01	8.48E+01	6.45E+01	9.46E-08	0.00E+00
co 60	1.927E-01	1.947E-01	2.087E-01	2.576E-01	5.248E-01	8.676E-01	1.16E+00	1.93E+00	8.87E+00	2.03E+01	1.77E-03	0.00E+00
ni 59	3.353E-04	3.388E-04	3.631E-04	4.483E-04	9.133E-04	1.510E-03	2.02E-03	3.39E-03	1.76E-02	1.31E-01	1.59E+00	7.00E+01
ni 63	4.102E-02	4.145E-02	4.443E-02	5.485E-02	1.117E-01	1.848E-01	2.48E-01	4.15E-01	2.14E+00	1.50E+01	9.78E+01	8.61E+00

Table 22. Major Contributors to Decay Heat Induced in Inner Leg (Zone 60) for SA1 Scenario (in percent)

Time	0	1 m	10 m	1 h	6 h	1 d	1w	1 mo	1 y	10 y	100 y	1000 y
c 14	1.751E-06	1.769E-06	1.875E-06	2.363E-06	8.217E-06	7.544E-05	1.40E-04	2.10E-04	6.14E-04	2.30E-03	8.58E-01	3.81E+01
cr 51	3.097E-01	3.129E-01	3.317E-01	4.176E-01	1.444E+00	1.301E+01	2.08E+01	1.73E+01	1.15E-02	7.27E-38	0.00E+00	0.00E+00
mn 56	9.209E+01	9.263E+01	9.431E+01	9.500E+01	8.608E+01	6.245E+00	1.76E-16	0.00E+00	0.00E+00	0.00E+00	0.00E+00	0.00E+00
fe 59	2.637E-01	2.664E-01	2.824E-01	3.557E-01	1.233E+00	1.119E+01	1.89E+01	1.97E+01	3.16E-01	7.39E-23	0.00E+00	0.00E+00
co 58	1.586E-01	1.602E-01	1.698E-01	2.140E-01	7.424E-01	6.766E+00	1.18E+01	1.41E+01	1.57E+00	6.78E-14	0.00E+00	0.00E+00
co 60	2.802E-01	2.831E-01	3.001E-01	3.782E-01	1.315E+00	1.207E+01	2.23E+01	3.32E+01	8.62E+01	9.88E+01	2.68E-01	0.00E+00
ni 59	1.380E-06	1.394E-06	1.478E-06	1.863E-06	6.476E-06	5.946E-05	1.10E-04	1.65E-04	4.84E-04	1.81E-03	6.84E-01	3.35E+01
ni 63	3.932E-04	3.973E-04	4.211E-04	5.308E-04	1.845E-03	1.694E-02	3.14E-02	4.71E-02	1.37E-01	4.83E-01	9.77E+01	9.61E+00
mo 99	8.133E-01	8.216E-01	8.695E-01	1.086E+00	3.583E+00	2.723E+01	1.11E+01	4.50E-02	2.71E-38	0.00E+00	0.00E+00	0.00E+00
ta182	1.035E-01	1.046E-01	1.109E-01	1.397E-01	4.851E-01	4.433E+00	7.93E+00	1.03E+01	4.01E+00	3.69E-08	3.24E-13	1.60E-11

Table 23. Major Contributors to Activity Induced in Outer Vertical Target (Zone 67) for SA1 Scenario (in percent)

Time	0	1 m	10 m	1 h	6 h	1 d	1w	1 mo	1 y	10 y	100 y	1000 y
c 14	4.594E-08	8.515E-08	9.247E-08	9.421E-08	1.032E-07	1.373E-07	2.73E-07	3.40E-07	4.77E-06	1.99E-02	4.71E+00	1.85E+01
ar 39	2.951E-07	5.470E-07	5.941E-07	6.053E-07	6.631E-07	8.821E-07	1.76E-06	2.18E-06	3.06E-05	1.25E-01	2.37E+01	1.02E+01
co 60	3.135E-04	5.811E-04	6.311E-04	6.430E-04	7.043E-04	9.367E-04	1.86E-03	2.30E-03	2.86E-02	3.65E+01	6.26E-02	0.00E+00
ni 63	3.736E-07	6.924E-07	7.520E-07	7.661E-07	8.393E-07	1.116E-06	2.22E-06	2.76E-06	3.86E-05	1.51E-01	1.94E+01	1.69E-01
nb 93m	2.016E-06	3.736E-06	4.057E-06	4.134E-06	4.529E-06	6.024E-06	1.20E-05	1.49E-05	2.01E-04	5.77E-01	7.13E+00	1.59E+01
nb 91	1.868E-07	3.462E-07	3.760E-07	3.831E-07	4.197E-07	5.582E-07	1.11E-06	1.38E-06	1.94E-05	8.03E-02	1.75E+01	3.06E+01
mo 93	5.176E-08	9.593E-08	1.042E-07	1.061E-07	1.163E-07	1.547E-07	3.08E-07	3.83E-07	5.38E-06	2.24E-02	5.26E+00	1.93E+01
ta179	5.713E-03	1.059E-02	1.150E-02	1.172E-02	1.284E-02	1.706E-02	3.38E-02	4.10E-02	4.05E-01	5.45E+01	1.54E-11	0.00E+00
w 181	4.015E+00	7.443E+00	8.083E+00	8.233E+00	9.009E+00	1.193E+01	2.30E+01	2.50E+01	5.17E+01	1.47E-03	0.00E+00	0.00E+00
w 183m	4.387E+01	2.783E-02	1.947E-33	0.000E+00	0.000E+00	0.000E+00	0.00E+00	0.00E+00	0.00E+00	0.00E+00	0.00E+00	0.00E+00
w 185	1.337E+01	2.479E+01	2.692E+01	2.742E+01	2.998E+01	3.960E+01	7.46E+01	7.47E+01	4.75E+01	1.25E-08	0.00E+00	0.00E+00
w 187	3.146E+01	5.828E+01	6.301E+01	6.267E+01	5.940E+01	4.690E+01	1.44E+00	1.49E-07	0.00E+00	0.00E+00	0.00E+00	0.00E+00

Table 24. Major Contributors to Decay Heat Induced in Outer Vertical Target (Zone 67) for SA1 Scenario (in percent)

Time	0	1 m	10 m	1 h	6 h	1 d	1w	1 mo	1 y	10 y	100 y	1000 y
c 14	5.778E-09	8.762E-09	9.068E-09	9.288E-09	1.061E-08	1.683E-08	1.11E-07	1.52E-07	2.56E-06	1.01E-03	1.00E+00	1.02E+01
ar 39	1.642E-07	2.490E-07	2.577E-07	2.639E-07	3.015E-07	4.783E-07	3.15E-06	4.33E-06	7.26E-05	2.81E-02	2.23E+01	2.49E+01
co 60	2.073E-03	3.143E-03	3.253E-03	3.332E-03	3.806E-03	6.036E-03	3.96E-02	5.40E-02	8.06E-01	9.76E+01	7.00E-01	0.00E+00
nb 94	2.181E-08	3.308E-08	3.423E-08	3.506E-08	4.005E-08	6.354E-08	4.18E-07	5.75E-07	9.67E-06	3.83E-03	3.81E+00	4.21E+01
ag108m	6.536E-07	9.912E-07	1.026E-06	1.051E-06	1.200E-06	1.904E-06	1.25E-05	1.72E-05	2.88E-04	1.09E-01	6.64E+01	5.55E+00
w 181	4.870E-01	7.385E-01	7.643E-01	7.826E-01	8.929E-01	1.411E+00	8.97E+00	1.08E+01	2.67E+01	7.22E-05	0.00E+00	0.00E+00
w 183m	3.297E+01	1.711E-02	1.141E-33	0.000E+00	0.000E+00	0.000E+00	0.00E+00	0.00E+00	0.00E+00	0.00E+00	0.00E+00	0.00E+00
w 185	4.316E+00	6.546E+00	6.774E+00	6.936E+00	7.908E+00	1.246E+01	7.76E+01	8.59E+01	6.54E+01	1.64E-09	0.00E+00	0.00E+00
w 187	5.774E+01	8.753E+01	9.019E+01	9.017E+01	8.911E+01	8.391E+01	8.51E+00	9.72E-07	0.00E+00	0.00E+00	0.00E+00	0.00E+00

Table 25. Major Contributors to Activity Induced in Outer Vertical Target (Zone 68) for SA1 Scenario (in percent)

Time	0	1 m	10 m	1 h	6 h	1 d	1w	1 mo	1 y	10 y	100 y	1000 y
c 14	5.221E-08	9.691E-08	1.045E-07	1.064E-07	1.165E-07	1.546E-07	3.07E-07	3.83E-07	5.56E-06	2.36E-02	5.50E+00	2.12E+01
ar 39	2.864E-07	5.317E-07	5.734E-07	5.839E-07	6.393E-07	8.485E-07	1.68E-06	2.10E-06	3.04E-05	1.26E-01	2.36E+01	9.98E+00
co 60	3.262E-04	6.055E-04	6.529E-04	6.649E-04	7.279E-04	9.658E-04	1.91E-03	2.37E-03	3.04E-02	3.95E+01	6.70E-02	0.00E+00
ni 63	3.910E-07	7.259E-07	7.827E-07	7.971E-07	8.727E-07	1.158E-06	2.30E-06	2.87E-06	4.13E-05	1.65E-01	2.09E+01	1.78E-01
nb 93m	2.232E-06	4.144E-06	4.468E-06	4.550E-06	4.981E-06	6.611E-06	1.31E-05	1.63E-05	2.28E-04	6.64E-01	7.76E+00	1.64E+01
nb 91	1.635E-07	3.035E-07	3.273E-07	3.333E-07	3.649E-07	4.843E-07	9.61E-07	1.20E-06	1.74E-05	7.31E-02	1.58E+01	2.70E+01
mo 93	5.302E-08	9.842E-08	1.061E-07	1.081E-07	1.183E-07	1.570E-07	3.12E-07	3.89E-07	5.64E-06	2.39E-02	5.54E+00	1.99E+01
ta179	5.250E-03	9.746E-03	1.051E-02	1.070E-02	1.172E-02	1.554E-02	3.07E-02	3.74E-02	3.82E-01	5.21E+01	1.46E-11	0.00E+00
w 181	3.700E+00	6.869E+00	7.406E+00	7.541E+00	8.246E+00	1.090E+01	2.09E+01	2.28E+01	4.88E+01	1.41E-03	0.00E+00	0.00E+00
w 183m	4.414E+01	2.804E-02	1.948E-33	0.000E+00	0.000E+00	0.000E+00	0.00E+00	0.00E+00	0.00E+00	0.00E+00	0.00E+00	0.00E+00
w 185	1.388E+01	2.577E+01	2.779E+01	2.829E+01	3.091E+01	4.075E+01	7.65E+01	7.69E+01	5.05E+01	1.35E-08	0.00E+00	0.00E+00
w 187	3.150E+01	5.844E+01	6.274E+01	6.237E+01	5.907E+01	4.654E+01	1.42E+00	1.48E-07	0.00E+00	0.00E+00	0.00E+00	0.00E+00

Table 26. Major Contributors to Decay Heat Induced in Outer Vertical Target (Zone 68) for SA1 Scenario (in percent)

Time	0	1 m	10 m	1 h	6 h	1 d	1w	1 mo	1 y	10 y	100 y	1000 y
c 14	6.563E-09	9.968E-09	1.029E-08	1.053E-08	1.203E-08	1.903E-08	1.23E-07	1.70E-07	2.95E-06	1.11E-03	1.18E+00	1.10E+01
ar 39	1.593E-07	2.419E-07	2.497E-07	2.557E-07	2.919E-07	4.619E-07	2.99E-06	4.13E-06	7.15E-05	2.63E-02	2.25E+01	2.30E+01
co 60	2.155E-03	3.274E-03	3.379E-03	3.460E-03	3.949E-03	6.248E-03	4.03E-02	5.53E-02	8.50E-01	9.79E+01	7.58E-01	0.00E+00
nb 94	2.496E-08	3.791E-08	4.007E-08	4.574E-08	7.239E-08	4.68E-07	4.68E-07	1.12E-05	4.22E-03	4.54E+00	4.58E+01	4.97E+00
ag108m	6.160E-07	9.357E-07	9.658E-07	9.889E-07	1.129E-06	1.787E-06	1.16E-05	1.60E-05	2.76E-04	9.88E-02	6.52E+01	4.97E+00
w 181	4.485E-01	6.812E-01	7.031E-01	7.198E-01	8.207E-01	1.293E+00	8.08E+00	9.78E+00	2.50E+01	6.41E-05	0.00E+00	0.00E+00
w 183m	3.315E+01	1.723E-02	1.146E-33	0.000E+00	0.000E+00	0.000E+00	0.00E+00	0.00E+00	0.00E+00	0.00E+00	0.00E+00	0.00E+00
w 185	4.478E+00	6.802E+00	7.021E+00	7.186E+00	8.188E+00	1.287E+01	7.87E+01	8.77E+01	6.88E+01	1.64E-09	0.00E+00	0.00E+00
w 187	5.778E+01	8.772E+01	9.016E+01	9.011E+01	8.899E+01	8.359E+01	8.33E+00	9.58E-07	0.00E+00	0.00E+00	0.00E+00	0.00E+00

Table 27. Major Contributors to Activity Induced in Outer Vertical Target (Zone 73) for SA1 Scenario (in percent)

Time	0	1 m	10 m	1 h	6 h	1 d	1w	1 mo	1 y	10 y	100 y	1000 y
c 14	9.758E-07	1.020E-06	1.255E-06	1.482E-06	1.952E-06	5.226E-06	5.47E-03	1.08E-02	1.53E-02	2.00E-02	4.09E-02	1.54E+01
ni 63	4.693E-03	4.906E-03	6.036E-03	7.126E-03	9.387E-03	2.513E-02	2.63E+01	5.18E+01	7.29E+01	9.00E+01	9.98E+01	8.32E+01
cu 64	6.935E+01	7.243E+01	8.839E+01	9.970E+01	9.990E+01	9.988E+01	3.95E+01	3.33E-12	0.00E+00	0.00E+00	0.00E+00	0.00E+00
cu 66	2.398E+01	2.187E+01	7.900E+00	1.028E-02	7.480E-10	1.593E-09	2.67E-07	4.14E-10	0.00E+00	0.00E+00	0.00E+00	0.00E+00
ag110m	1.094E-03	1.143E-03	1.407E-03	1.661E-03	5.841E-03	6.01E+00	1.11E+01	6.21E+00	8.95E-04	4.67E-43	0.00E+00	

Table 28. Major Contributors to Decay Heat Induced in Outer Vertical Target (Zone 73) for SA1 Scenario (in percent)

Time	0	1 m	10 m	1 h	6 h	1 d	1w	1 mo	1 y	10 y	100 y	1000 y
be 10	2.118E-08	2.472E-08	4.092E-08	6.873E-08	9.145E-08	2.447E-07	1.25E-04	2.10E-04	6.20E-04	4.06E-03	3.53E-02	1.02E+01
c 14	7.117E-08	8.304E-08	1.375E-07	2.309E-07	3.072E-07	8.222E-07	4.19E-04	7.05E-04	2.08E-03	1.36E-02	1.17E-01	3.04E+01
co 60	1.514E-03	1.766E-03	2.925E-03	4.912E-03	6.535E-03	1.748E-02	8.88E+00	1.48E+01	3.88E+01	7.78E+01	4.86E-03	0.00E+00
ni 63	1.186E-04	1.384E-04	2.291E-04	3.847E-04	5.119E-04	1.370E-03	6.97E-01	1.17E+00	3.44E+00	2.12E+01	9.90E+01	5.69E+01
cu 62	1.873E+01	2.035E+01	1.772E+01	8.380E-01	5.556E-10	4.818E-43	0.00E+00	0.00E+00	0.00E+00	0.00E+00	0.00E+00	0.00E+00
cu 64	3.201E+01	3.732E+01	6.128E+01	9.833E+01	9.952E+01	9.946E+01	1.92E+01	1.38E-12	0.00E+00	0.00E+00	0.00E+00	0.00E+00
cu 66	4.079E+01	4.154E+01	2.019E+01	3.738E-02	2.747E-09	5.847E-09	4.78E-07	6.32E-10	0.00E+00	0.00E+00	0.00E+00	0.00E+00
ag110m	4.536E-03	5.293E-03	8.763E-03	1.472E-02	1.957E-02	5.226E-02	2.62E+01	4.13E+01	4.82E+01	3.46E-02	7.61E-41	0.00E+00
sb124	4.034E-03	4.707E-03	7.793E-03	1.308E-02	1.737E-02	4.608E-02	2.19E+01	2.82E+01	1.77E+00	4.56E-16	0.00E+00	0.00E+00

Table 29. Major Contributors to Activity Induced in Inner Vertical Target (Zone 76) for SA1 Scenario (in percent)

Time	0	1 m	10 m	1 h	6 h	1 d	1w	1 mo	1 y	10 y	100 y	1000 y
c 14	5.240E-08	9.146E-08	9.392E-08	9.567E-08	1.059E-07	1.466E-07	3.45E-07	4.37E-07	7.65E-06	3.94E-02	8.67E+00	3.26E+01
ar 39	1.909E-07	3.332E-07	3.422E-07	3.485E-07	3.857E-07	5.341E-07	1.26E-06	1.59E-06	2.78E-05	1.40E-01	2.47E+01	1.02E+01
co 60	3.244E-04	5.661E-04	5.814E-04	5.922E-04	6.552E-04	9.072E-04	2.13E-03	2.67E-03	4.15E-02	6.54E+01	1.05E-01	0.00E+00
ni 63	3.363E-07	5.869E-07	6.028E-07	6.139E-07	6.794E-07	9.408E-07	2.21E-06	2.80E-06	4.88E-05	2.36E-01	2.82E+01	2.35E-01
nb 93m	2.022E-06	3.530E-06	3.625E-06	3.692E-06	4.086E-06	5.657E-06	1.33E-05	1.68E-05	2.83E-04	9.98E-01	9.31E+00	1.66E+01
nb 91	4.980E-08	8.691E-08	8.926E-08	9.092E-08	1.006E-07	1.393E-07	3.28E-07	4.15E-07	7.27E-06	3.71E-02	7.53E+00	1.26E+01
mo 93	3.513E-08	6.131E-08	6.296E-08	6.413E-08	7.097E-08	9.828E-08	2.31E-07	2.93E-07	5.13E-06	2.64E-02	5.76E+00	2.02E+01
ta179	1.740E-03	3.038E-03	3.120E-03	3.178E-03	3.516E-03	4.866E-03	1.14E-02	1.41E-02	1.74E-01	2.87E+01	7.58E-12	0.00E+00
w 181	1.625E+00	2.837E+00	2.913E+00	2.967E+00	3.279E+00	4.522E+00	1.03E+01	1.14E+01	2.94E+01	1.03E-03	0.00E+00	0.00E+00
w 183m	4.199E+01	2.508E-02	1.659E-33	0.000E+00	0.000E+00	0.000E+00	0.000E+00	0.000E+00	0.000E+00	0.00E+00	0.00E+00	0.00E+00
w 185	1.406E+01	2.454E+01	2.520E+01	2.566E+01	2.834E+01	3.897E+01	8.67E+01	8.85E+01	7.01E+01	2.28E-08	0.00E+00	0.00E+00
w 187	3.942E+01	6.877E+01	7.032E+01	6.991E+01	6.693E+01	5.501E+01	1.99E+00	2.10E-07	0.00E+00	0.00E+00	0.00E+00	0.00E+00

Table 30. Major Contributors to Decay Heat Induced in Inner Vertical Target (Zone 76) for SA1 Scenario (in percent)

Time	0	1 m	10 m	1 h	6 h	1 d	1w	1 mo	1 y	10 y	100 y	1000 y
c 14	5.942E-09	8.348E-09	8.452E-09	8.650E-09	9.902E-09	1.589E-08	1.27E-07	1.81E-07	3.49E-06	1.14E-03	1.91E+00	1.24E+01
ar 39	9.575E-08	1.345E-07	1.362E-07	1.394E-07	1.596E-07	2.560E-07	2.05E-06	2.91E-06	5.62E-05	1.78E-02	2.41E+01	1.71E+01
co 60	1.933E-03	2.716E-03	2.750E-03	2.814E-03	3.222E-03	5.169E-03	4.12E-02	5.81E-02	9.97E-01	9.92E+01	1.21E+00	0.00E+00
nb 94	2.575E-08	3.618E-08	3.662E-08	3.748E-08	4.291E-08	6.886E-08	5.51E-07	7.83E-07	1.51E-05	4.92E-03	8.35E+00	5.85E+01
ag108m	3.094E-07	4.347E-07	4.401E-07	4.504E-07	5.156E-07	8.274E-07	6.62E-06	9.40E-06	1.81E-04	5.60E-02	5.83E+01	3.10E+00
w 181	1.777E-01	2.497E-01	2.528E-01	2.586E-01	2.957E-01	4.726E-01	3.65E+00	4.54E+00	1.29E+01	2.87E-05	0.00E+00	0.00E+00
w 183m	2.845E+01	1.368E-02	8.922E-34	0.000E+00	0.000E+00	0.000E+00	0.00E+00	0.00E+00	0.00E+00	0.00E+00	0.00E+00	0.00E+00
w 185	4.091E+00	5.747E+00	5.818E+00	5.952E+00	6.801E+00	1.084E+01	8.20E+01	9.39E+01	8.22E+01	1.69E-09	0.00E+00	0.00E+00
w 187	6.524E+01	9.161E+01	9.234E+01	9.225E+01	9.136E+01	8.702E+01	1.07E+01	1.27E-06	0.00E+00	0.00E+00	0.00E+00	0.00E+00

Table 31. Major Contributors to Activity Induced in Inner Vertical Target (Zone 77) for SA1 Scenario (in percent)

Time	0	1 m	10 m	1 h	6 h	1 d	1w	1 mo	1 y	10 y	100 y	1000 y
c 14	6.273E-08	1.053E-07	1.078E-07	1.098E-07	1.213E-07	1.671E-07	3.83E-07	4.84E-07	8.75E-06	3.91E-02	9.97E+00	3.72E+01
ar 39	1.884E-07	3.163E-07	3.239E-07	3.298E-07	3.645E-07	5.020E-07	1.15E-06	1.45E-06	2.62E-05	1.15E-01	2.34E+01	9.61E+00
co 60	4.436E-04	7.447E-04	7.626E-04	7.764E-04	8.579E-04	1.181E-03	2.70E-03	3.39E-03	5.43E-02	7.42E+01	1.37E-01	0.00E+00
ni 63	4.003E-07	6.721E-07	6.881E-07	7.007E-07	7.743E-07	1.066E-06	2.44E-06	3.09E-06	5.55E-05	2.33E-01	3.23E+01	2.67E-01
nb 93m	2.221E-06	3.727E-06	3.817E-06	3.886E-06	4.294E-06	5.914E-06	1.35E-05	1.71E-05	2.97E-04	9.08E-01	9.62E+00	1.67E+01
mo 93	3.697E-08	6.207E-08	6.355E-08	6.471E-08	7.151E-08	9.849E-08	2.26E-07	2.86E-07	5.16E-06	2.30E-02	5.83E+00	2.03E+01
ta179	1.584E-03	2.659E-03	2.723E-03	2.773E-03	3.064E-03	4.216E-03	9.61E-03	1.19E-02	1.51E-01	2.17E+01	6.63E-12	0.00E+00
w 181	1.495E+00	2.510E+00	2.570E+00	2.616E+00	2.887E+00	3.960E+00	8.77E+00	9.70E+00	2.58E+01	7.87E-04	0.00E+00	0.00E+00
w 183m	3.976E+01	2.284E-02	1.507E-33	0.000E+00	0.000E+00	0.00E+00	0.00E+00	0.00E+00	0.00E+00	0.00E+00	0.00E+00	0.00E+00
w 185	1.548E+01	2.598E+01	2.660E+01	2.707E+01	2.986E+01	4.084E+01	8.86E+01	9.02E+01	7.38E+01	2.08E-08	0.00E+00	0.00E+00
w 187	4.066E+01	6.822E+01	6.955E+01	6.913E+01	6.609E+01	5.403E+01	1.91E+00	2.01E-07	0.00E+00	0.00E+00	0.00E+00	0.00E+00

Table 32. Major Contributors to Decay Heat Induced in Inner Vertical Target (Zone 77) for SA1 Scenario (in percent)

Time	0	1 m	10 m	1 h	6 h	1 d	1w	1 mo	1 y	10 y	100 y	1000 y
c 14	7.058E-09	9.687E-09	9.799E-09	1.003E-08	1.147E-08	1.837E-08	1.41E-07	1.99E-07	3.91E-06	9.96E-04	2.21E+00	1.35E+01
ar 39	9.378E-08	1.287E-07	1.302E-07	1.332E-07	1.524E-07	2.441E-07	1.88E-06	2.64E-06	5.18E-05	1.29E-02	2.30E+01	1.54E+01
co 60	2.624E-03	3.601E-03	3.643E-03	3.728E-03	4.265E-03	6.829E-03	5.24E-02	7.31E-02	1.27E+00	9.94E+01	1.60E+00	0.00E+00
nb 94	2.900E-08	3.980E-08	4.026E-08	4.120E-08	4.714E-08	7.550E-08	5.81E-07	8.17E-07	1.61E-05	4.10E-03	9.16E+00	6.06E+01
ag108m	3.137E-07	4.305E-07	4.355E-07	4.456E-07	5.099E-07	8.166E-07	6.28E-06	8.83E-06	1.73E-04	4.20E-02	5.76E+01	2.88E+00
w 181	1.622E-01	2.226E-01	2.252E-01	2.304E-01	2.633E-01	4.198E-01	3.12E+00	3.84E+00	1.11E+01	1.93E-05	0.00E+00	0.00E+00
w 183m	2.673E+01	1.256E-02	8.181E-34	0.000E+00	0.000E+00	0.00E+00	0.00E+00	0.00E+00	0.00E+00	0.00E+00	0.00E+00	0.00E+00
w 185	4.469E+00	6.133E+00	6.203E+00	6.345E+00	7.247E+00	1.153E+01	8.39E+01	9.50E+01	8.45E+01	1.36E-09	0.00E+00	0.00E+00
w 187	6.677E+01	9.160E+01	9.225E+01	9.215E+01	9.122E+01	8.671E+01	1.03E+01	1.20E-06	0.00E+00	0.00E+00	0.00E+00	0.00E+00

Table 33. Major Contributors to Activity Induced in Inner Vertical Target (Zone 82) for SA1 Scenario (in percent)

Time	0	1 m	10 m	1 h	6 h	1 d	1w	1 mo	1 y	10 y	100 y	1000 y
c 14	1.075E-06	1.118E-06	1.376E-06	1.590E-06	2.091E-06	5.598E-06	7.16E-03	1.81E-02	3.51E-02	5.62E-02	1.13E-01	3.36E+01
co 60	4.836E-04	5.029E-04	6.188E-04	7.152E-04	9.405E-04	2.517E-03	3.21E+00	8.06E+00	1.38E+01	6.79E+00	9.91E-05	0.00E+00
ni 63	1.872E-03	1.947E-03	2.395E-03	2.769E-03	3.642E-03	9.747E-03	1.25E+01	3.15E+01	6.07E+01	9.15E+01	9.98E+01	6.57E+01
cu 64	7.135E+01	7.413E+01	9.047E+01	9.991E+01	9.994E+01	9.990E+01	4.84E+01	5.23E-12	0.00E+00	0.00E+00	0.00E+00	0.00E+00
cu 66	2.771E+01	2.515E+01	9.081E+00	1.158E-02	5.581E-11	1.188E-10	2.44E-08	4.85E-11	0.00E+00	0.00E+00	0.00E+00	0.00E+00
ag110m	1.232E-03	1.281E-03	1.576E-03	1.822E-03	2.395E-03	6.396E-03	8.05E+00	1.91E+01	1.46E+01	2.57E-03	1.32E-42	0.00E+00
sb124	1.681E-03	1.749E-03	2.151E-03	2.486E-03	3.261E-03	8.654E-03	1.03E+01	2.00E+01	8.25E-01	5.19E-17	0.00E+00	0.00E+00

Table 34. Major Contributors to Decay Heat Induced in Inner Vertical Target (Zone 82) for SA1 Scenario (in percent)

Time	0	1 m	10 m	1 h	6 h	1 d	1w	1 mo	1 y	10 y	100 y	1000 y
c 14	9.383E-08	1.029E-07	1.711E-07	2.504E-07	3.298E-07	8.815E-07	4.29E-04	6.85E-04	2.06E-03	1.44E-02	3.21E-01	5.60E+01
co 60	2.218E-03	2.432E-03	4.046E-03	5.920E-03	7.796E-03	2.083E-02	1.01E+01	1.60E+01	4.27E+01	9.16E+01	1.48E-02	0.00E+00
ni 63	5.661E-05	6.207E-05	1.033E-04	1.511E-04	1.990E-04	5.318E-04	2.59E-01	4.13E-01	1.24E+00	8.13E+00	9.81E+01	3.79E+01
cu 64	3.941E+01	4.317E+01	7.123E+01	9.957E+01	9.974E+01	9.957E+01	1.84E+01	1.25E-12	0.00E+00	0.00E+00	0.00E+00	0.00E+00
cu 66	5.641E+01	5.397E+01	2.635E+01	4.252E-02	2.053E-10	4.366E-10	3.41E-08	4.28E-11	0.00E+00	0.00E+00	0.00E+00	0.00E+00
ag110m	6.113E-03	6.703E-03	1.115E-02	1.631E-02	2.147E-02	5.727E-02	2.74E+01	4.10E+01	4.88E+01	3.75E-02	2.13E-40	0.00E+00
sb124	6.632E-03	7.272E-03	1.210E-02	1.769E-02	2.324E-02	6.160E-02	2.80E+01	3.41E+01	2.19E+00	6.02E-16	0.00E+00	0.00E+00

Table 35. Major Contributors to Activity Induced in Rails (Zone 104) for SA1 Scenario (in percent)

Time	0	1 m	10 m	1 h	6 h	1 d	1w	1 mo	1 y	10 y	100 y	1000 y
c 14	4.460E-05	4.521E-05	4.945E-05	6.284E-05	1.275E-04	2.191E-04	3.47E-04	5.91E-04	2.86E-03	2.20E-02	3.66E-01	1.06E+01
cr 51	8.907E+00	9.029E+00	9.873E+00	1.254E+01	2.530E+01	4.268E+01	5.81E+01	5.51E+01	6.05E-02	7.84E-37	0.00E+00	0.00E+00
mn 54	3.573E-01	3.622E-01	3.962E-01	5.034E-01	1.021E+00	1.752E+00	2.73E+00	4.43E+00	1.02E+01	5.29E-02	1.77E-32	0.00E+00
mn 56	6.024E+01	6.080E+01	6.386E+01	6.487E+01	3.430E+01	4.659E-01	1.12E-17	0.00E+00	0.00E+00	0.00E+00	0.00E+00	0.00E+00
fe 55	1.362E+00	1.381E+00	1.510E+00	1.919E+00	3.893E+00	6.687E+00	1.05E+01	1.77E+01	6.77E+01	5.31E+01	1.08E-07	0.00E+00
co 58	1.304E+00	1.322E+00	1.446E+00	1.837E+00	3.719E+00	6.345E+00	9.47E+00	1.28E+01	2.36E+00	2.09E-13	0.00E+00	0.00E+00
co 60	2.719E-01	2.756E-01	3.014E-01	3.831E-01	7.772E-01	1.335E+00	2.11E+00	3.57E+00	1.53E+01	3.59E+01	4.35E-03	0.00E+00
ni 59	2.127E-04	2.156E-04	2.358E-04	2.997E-04	6.080E-04	1.045E-03	1.65E-03	2.82E-03	1.36E-02	1.05E-01	1.77E+00	5.67E+01
ni 63	2.325E-02	2.357E-02	2.578E-02	3.276E-02	6.647E-02	1.142E-01	1.81E-01	3.08E-01	1.48E+00	1.07E+01	9.69E+01	6.23E+00
nb 93m	4.330E-05	4.389E-05	4.801E-05	6.101E-05	1.238E-04	2.127E-04	3.37E-04	5.75E-04	2.80E-03	2.30E-02	4.32E-01	1.17E+01
mo 93	6.447E-05	6.535E-05	7.148E-05	9.083E-05	1.843E-04	3.167E-04	5.01E-04	8.55E-04	4.13E-03	3.17E-02	5.26E-01	1.42E+01
mo 99	4.680E+00	4.744E+00	5.180E+00	6.525E+00	1.256E+01	1.787E+01	6.22E+00	2.87E-02	2.85E-38	0.00E+00	0.00E+00	0.00E+00
tc 99m	4.096E+00	4.152E+00	4.542E+00	5.771E+00	1.154E+01	1.716E+01	6.02E+00	2.78E-02	2.76E-38	0.00E+00	0.00E+00	0.00E+00

Table 36. Major Contributors to Decay Heat Induced in Rails (Zone 104) for SA1 Scenario (in percent)

Time	0	1 m	10 m	1 h	6 h	1 d	1w	1 mo	1 y	10 y	100 y	1000 y
c 14	1.223E-06	1.237E-06	1.322E-06	1.665E-06	5.145E-06	2.840E-05	5.80E-05	8.26E-05	2.65E-04	1.16E-03	1.05E+00	2.90E+01
mn 54	1.665E-01	1.683E-01	1.799E-01	2.265E-01	6.996E-01	3.856E+00	7.77E+00	1.05E+01	1.60E+01	4.73E-02	8.59E-31	0.00E+00
mn 56	8.429E+01	8.484E+01	8.710E+01	8.766E+01	7.060E+01	3.080E+00	9.56E-17	0.00E+00	0.00E+00	0.00E+00	0.00E+00	0.00E+00
fe 59	2.800E-01	2.831E-01	3.026E-01	3.808E-01	1.173E+00	6.400E+00	1.19E+01	1.18E+01	2.07E-01	5.64E-23	0.00E+00	0.00E+00
co 58m	5.132E+00	5.182E+00	5.477E+00	6.473E+00	1.368E+01	1.924E+01	6.98E-04	2.75E-22	0.00E+00	0.00E+00	0.00E+00	0.00E+00
co 58	7.305E-01	7.385E-01	7.894E-01	9.937E-01	3.064E+00	1.679E+01	3.23E+01	3.66E+01	4.48E+00	2.24E-13	0.00E+00	0.00E+00
co 60	3.921E-01	3.964E-01	4.237E-01	5.335E-01	1.648E+00	9.098E+00	1.85E+01	2.62E+01	7.45E+01	9.94E+01	6.54E-01	0.00E+00
ni 59	8.681E-07	8.777E-07	9.382E-07	1.181E-06	3.650E-06	2.015E-05	4.11E-05	5.86E-05	1.88E-04	8.21E-04	7.51E-01	2.30E+01
ni 63	2.210E-04	2.235E-04	2.389E-04	3.008E-04	9.294E-04	5.131E-03	1.05E-02	1.49E-02	4.76E-02	1.95E-01	9.59E+01	5.89E+00
nb 93m	6.959E-07	7.036E-07	7.520E-07	9.470E-07	2.926E-06	1.615E-05	3.30E-05	4.70E-05	1.52E-04	7.08E-04	7.23E-01	1.87E+01
nb 94	4.049E-07	4.094E-07	4.376E-07	5.510E-07	1.703E-06	9.400E-06	1.92E-05	2.73E-05	8.78E-05	3.83E-04	3.50E-01	1.05E+01
mo 93	5.720E-07	5.783E-07	6.182E-07	7.785E-07	2.405E-06	1.328E-05	2.71E-05	3.86E-05	1.24E-04	5.40E-04	4.86E-01	1.25E+01
mo 99	1.409E+00	1.424E+00	1.520E+00	1.897E+00	5.563E+00	2.542E+01	1.14E+01	4.40E-02	2.90E-38	0.00E+00	0.00E+00	0.00E+00

Table 37. Major Contributors to Activity Induced in Rails (Zone 105) for SA1 Scenario (in percent)

Time	0	1 m	10 m	1 h	6 h	1 d	1w	1 mo	1 y	10 y	100 y	1000 y
cr 51	9.302E+00	9.442E+00	1.034E+01	1.298E+01	2.485E+01	3.950E+01	5.14E+01	4.52E+01	3.61E-02	5.95E-37	0.00E+00	0.00E+00
mn 54	6.369E-01	6.465E-01	7.079E-01	8.895E-01	1.711E+00	2.767E+00	4.13E+00	6.20E+00	1.04E+01	6.85E-02	3.38E-32	0.00E+00
mn 56	5.730E+01	5.790E+01	6.090E+01	6.115E+01	3.068E+01	3.927E-01	9.03E-18	0.00E+00	0.00E+00	0.00E+00	0.00E+00	0.00E+00
fe 55	2.412E+00	2.448E+00	2.681E+00	3.369E+00	6.482E+00	1.049E+01	1.58E+01	2.46E+01	6.86E+01	6.83E+01	2.05E-07	0.00E+00
co 58	1.406E+00	1.427E+00	1.563E+00	1.963E+00	3.770E+00	6.062E+00	8.64E+00	1.09E+01	1.46E+00	1.64E-13	0.00E+00	0.00E+00
co 60	2.511E-01	2.549E-01	2.791E-01	3.507E-01	6.750E-01	1.093E+00	1.65E+00	2.59E+00	8.07E+00	2.41E+01	4.31E-03	0.00E+00
ni 59	1.944E-04	1.973E-04	2.161E-04	2.715E-04	5.225E-04	8.463E-04	1.28E-03	2.02E-03	7.13E-03	6.96E-02	1.73E+00	5.48E+01
ni 63	2.166E-02	2.198E-02	2.407E-02	3.025E-02	5.821E-02	9.428E-02	1.42E-01	2.25E-01	7.89E-01	7.24E+00	9.66E+01	6.14E+00
nb 93m	4.890E-05	4.963E-05	5.435E-05	6.829E-05	1.314E-04	2.129E-04	3.22E-04	5.09E-04	1.79E-03	1.73E-02	4.13E-01	1.10E+01
mo 93	5.748E-05	5.834E-05	6.389E-05	8.028E-05	1.545E-04	2.502E-04	3.78E-04	5.98E-04	2.11E-03	2.05E-02	5.02E-01	1.34E+01
mo 99	4.785E+00	4.856E+00	5.309E+00	6.613E+00	1.208E+01	1.619E+01	5.39E+00	2.30E-02	1.67E-38	0.00E+00	0.00E+00	0.00E+00
tc 99m	4.188E+00	4.251E+00	4.655E+00	5.849E+00	1.109E+01	1.555E+01	5.21E+00	2.23E-02	1.61E-38	0.00E+00	0.00E+00	0.00E+00

Table 38. Major Contributors to Decay Heat Induced in Rails (Zone 105) for SA1 Scenario (in percent)

Time	0	1 m	10 m	1 h	6 h	1 d	1w	1 mo	1 y	10 y	100 y	1000 y
c 14	1.094E-06	1.109E-06	1.195E-06	1.504E-06	4.515E-06	2.286E-05	4.69E-05	6.57E-05	2.10E-04	1.09E-03	9.85E-01	2.69E+01
mn 54	3.023E-01	3.064E-01	3.302E-01	4.155E-01	1.247E+00	6.302E+00	1.28E+01	1.70E+01	2.58E+01	9.09E-02	1.64E-30	0.00E+00
mn 56	8.166E+01	8.240E+01	8.529E+01	8.579E+01	6.713E+01	2.686E+00	8.39E-17	0.00E+00	0.00E+00	0.00E+00	0.00E+00	0.00E+00
fe 59	2.601E-01	2.637E-01	2.841E-01	3.574E-01	1.069E+00	5.352E+00	1.00E+01	9.73E+00	1.70E-01	5.55E-23	0.00E+00	0.00E+00
co 58m	6.091E+00	6.166E+00	6.570E+00	7.761E+00	1.594E+01	2.056E+01	7.50E-04	2.90E-22	0.00E+00	0.00E+00	0.00E+00	0.00E+00
co 58	8.022E-01	8.131E-01	8.762E-01	1.102E+00	3.303E+00	1.660E+01	3.21E+01	3.58E+01	4.35E+00	2.61E-13	0.00E+00	0.00E+00
co 60	3.689E-01	3.739E-01	4.029E-01	5.071E-01	1.522E+00	7.706E+00	1.58E+01	2.19E+01	6.21E+01	9.91E+01	6.47E-01	0.00E+00
ni 59	8.082E-07	8.192E-07	8.828E-07	1.111E-06	3.336E-06	1.689E-05	3.47E-05	4.85E-05	1.55E-04	8.09E-04	7.36E-01	2.22E+01
ni 63	2.097E-04	2.125E-04	2.290E-04	2.882E-04	8.654E-04	4.382E-03	8.99E-03	1.26E-02	4.00E-02	1.96E-01	9.57E+01	5.80E+00
nb 93m	8.005E-07	8.114E-07	8.744E-07	1.100E-06	3.304E-06	1.673E-05	3.43E-05	4.81E-05	1.53E-04	7.91E-04	6.92E-01	1.76E+01
nb 94	4.152E-07	4.209E-07	4.535E-07	5.708E-07	1.714E-06	8.677E-06	1.78E-05	2.49E-05	7.97E-05	4.16E-04	3.77E-01	1.11E+01
mo 93	5.195E-07	5.266E-07	5.675E-07	7.141E-07	2.144E-06	1.086E-05	2.23E-05	3.12E-05	9.97E-05	5.19E-04	4.64E-01	1.18E+01
mo 99	1.467E+00	1.487E+00	1.600E+00	1.996E+00	5.687E+00	2.383E+01	1.08E+01	4.07E-02	2.68E-38	0.00E+00	0.00E+00	0.00E+00

Table 39. Major Contributors to Activity Induced in Dome PFC (Zone 1) for M5 Scenario (in percent)

Time	0	1 m	10 m	1 h	6 h	1 d	1w	1 mo	1 y	10 y	100 y	1000 y
c 14	2.095E-08	4.021E-08	4.504E-08	4.607E-08	5.153E-08	7.444E-08	2.17E-07	2.74E-07	3.87E-06	2.27E-02	4.91E+00	1.98E+01
ar 39	1.282E-07	2.460E-07	2.755E-07	2.819E-07	3.152E-07	4.554E-07	1.32E-06	1.68E-06	2.36E-05	1.35E-01	2.35E+01	1.04E+01
co 60	9.728E-05	1.867E-04	2.091E-04	2.139E-04	2.392E-04	3.455E-04	1.00E-03	1.26E-03	1.58E-02	2.83E+01	4.45E-02	0.00E+00
ni 63	1.678E-07	3.221E-07	3.608E-07	3.691E-07	4.128E-07	5.963E-07	1.73E-06	2.19E-06	3.08E-05	1.70E-01	2.00E+01	1.78E-01
nb 93m	8.891E-07	1.706E-06	1.911E-06	1.955E-06	2.187E-06	3.159E-06	9.18E-06	1.16E-05	1.58E-04	6.33E-01	6.82E+00	1.50E+01
nb 91	8.359E-08	1.604E-07	1.797E-07	1.838E-07	2.056E-07	2.970E-07	8.64E-07	1.09E-06	1.54E-05	8.96E-02	1.79E+01	3.22E+01
mo 93	2.082E-08	3.995E-08	4.475E-08	4.577E-08	5.120E-08	7.396E-08	2.15E-07	2.72E-07	3.85E-06	2.25E-02	4.84E+00	1.82E+01
ta179	2.600E-03	4.991E-03	5.591E-03	5.721E-03	6.399E-03	9.237E-03	2.67E-02	3.30E-02	3.28E-01	6.19E+01	1.61E-11	0.00E+00
w 181	2.245E+00	4.308E+00	4.826E+00	4.935E+00	5.513E+00	7.931E+00	2.23E+01	2.47E+01	5.14E+01	2.05E-03	0.00E+00	0.00E+00
w 183m	4.503E+01	2.957E-02	2.134E-33	0.000E+00	0.000E+00	0.000E+00	0.00E+00	0.00E+00	0.00E+00	0.00E+00	0.00E+00	0.00E+00
w 185	7.611E+00	1.461E+01	1.636E+01	1.673E+01	1.868E+01	2.679E+01	7.37E+01	7.51E+01	4.80E+01	1.78E-08	0.00E+00	0.00E+00
w 185m	8.352E+00	1.058E+01	2.825E-01	2.785E-10	0.000E+00	0.000E+00	0.00E+00	0.00E+00	0.00E+00	0.00E+00	0.00E+00	0.00E+00
w 187	3.615E+01	6.934E+01	7.733E+01	7.722E+01	7.471E+01	6.407E+01	2.87E+00	3.02E-07	0.00E+00	0.00E+00	0.00E+00	0.00E+00

Table 40. Major Contributors to Decay Heat Induced in Dome PFC (Zone 1) for M5 Scenario (in percent)

Time	0	1 m	10 m	1 h	6 h	1 d	1w	1 mo	1 y	10 y	100 y	1000 y
c 14	2.445E-09	3.634E-09	3.784E-09	3.879E-09	4.456E-09	7.271E-09	8.21E-08	1.24E-07	2.14E-06	1.47E-03	1.07E+00	1.18E+01
ar 39	6.615E-08	9.832E-08	1.024E-07	1.049E-07	1.206E-07	1.967E-07	2.22E-06	3.35E-06	5.77E-05	3.89E-02	2.27E+01	2.75E+01
co 60	5.967E-04	8.869E-04	9.234E-04	9.466E-04	1.088E-03	1.774E-03	2.00E-02	2.99E-02	4.57E-01	9.66E+01	5.09E-01	0.00E+00
nb 94	7.083E-09	1.053E-08	1.096E-08	1.124E-08	1.291E-08	2.107E-08	2.38E-07	3.59E-07	6.19E-06	4.27E-03	3.13E+00	3.74E+01
ag108m	2.606E-07	3.874E-07	4.033E-07	4.135E-07	4.750E-07	7.751E-07	8.75E-06	1.32E-05	2.27E-04	1.49E-01	6.69E+01	6.06E+00
w 181	2.526E-01	3.754E-01	3.909E-01	4.006E-01	4.597E-01	7.469E-01	8.15E+00	1.08E+01	2.73E+01	1.29E-04	0.00E+00	0.00E+00
w 183m	3.139E+01	1.597E-02	1.071E-33	0.000E+00	0.000E+00	0.00E+00	0.00E+00	0.00E+00	0.00E+00	0.00E+00	0.00E+00	0.00E+00
w 185	2.279E+00	3.388E+00	3.527E+00	3.614E+00	4.145E+00	6.716E+00	7.17E+01	8.72E+01	6.81E+01	2.97E-09	0.00E+00	0.00E+00
w 187	6.156E+01	9.146E+01	9.481E+01	9.488E+01	9.430E+01	9.133E+01	1.59E+01	1.99E-06	0.00E+00	0.00E+00	0.00E+00	0.00E+00

Table 41. Major Contributors to Activity Induced in Dome PFC (Zone 2) for M5 Scenario (in percent)

Time	0	1 m	10 m	1 h	6 h	1 d	1w	1 mo	1 y	10 y	100 y	1000 y
ni 63	3.631E-03	3.787E-03	4.722E-03	5.872E-03	7.764E-03	2.080E-02	2.59E+01	6.38E+01	8.56E+01	9.55E+01	9.99E+01	9.94E+01
cu 62	1.547E+01	1.503E+01	9.854E+00	3.450E-01	2.273E-10	1.974E-43	0.00E+00	0.00E+00	0.00E+00	0.00E+00	0.00E+00	0.00E+00
cu 64	6.481E+01	6.754E+01	8.352E+01	9.924E+01	9.981E+01	9.986E+01	4.71E+01	4.96E-12	0.00E+00	0.00E+00	0.00E+00	0.00E+00
cu 66	1.853E+01	1.687E+01	6.173E+00	8.465E-03	3.010E-09	6.416E-09	1.28E-06	2.48E-09	0.00E+00	0.00E+00	0.00E+00	0.00E+00

Table 42. Major Contributors to Decay Heat Induced in Dome PFC (Zone 2) for M5 Scenario (in percent)

Time	0	1 m	10 m	1 h	6 h	1 d	1w	1 mo	1 y	10 y	100 y	1000 y
co 60	4.307E-04	4.816E-04	8.044E-04	1.743E-03	2.373E-03	6.363E-03	3.88E+00	9.24E+00	3.58E+01	6.13E+01	2.15E-03	0.00E+00
ni 63	7.647E-05	8.551E-05	1.428E-04	3.095E-04	4.213E-04	1.130E-03	6.91E-01	1.66E+00	7.19E+00	3.79E+01	9.93E+01	9.41E+01
cu 62	4.343E+01	4.522E+01	3.972E+01	2.424E+00	1.644E-09	1.429E-42	0.00E+00	0.00E+00	0.00E+00	0.00E+00	0.00E+00	0.00E+00
cu 64	2.494E+01	2.786E+01	4.615E+01	9.556E+01	9.894E+01	9.911E+01	2.29E+01	2.35E-12	0.00E+00	0.00E+00	0.00E+00	0.00E+00
cu 66	2.628E+01	2.565E+01	1.257E+01	3.004E-02	1.100E-08	2.347E-08	2.30E-06	4.34E-09	0.00E+00	0.00E+00	0.00E+00	0.00E+00
as 74	2.935E-03	3.282E-03	5.481E-03	1.186E-02	1.602E-02	4.172E-02	2.02E+01	1.94E+01	1.77E-04	0.00E+00	0.00E+00	0.00E+00
ag110m	1.371E-03	1.533E-03	2.561E-03	5.549E-03	7.549E-03	2.021E-02	1.22E+01	2.73E+01	4.72E+01	2.90E-02	3.58E-41	0.00E+00
sb124	1.993E-03	2.229E-03	3.722E-03	8.064E-03	1.095E-02	2.912E-02	1.66E+01	3.05E+01	2.84E+00	6.23E-16	0.00E+00	0.00E+00

Table 43. Major Contributors to Activity Induced in Dome Body (Zone 4) for M5 Scenario (in percent)

Time	0	1 m	10 m	1 h	6 h	1 d	1w	1 mo	1 y	10 y	100 y	1000 y
ni 63	2.200E-03	2.286E-03	2.803E-03	3.330E-03	4.390E-03	1.176E-02	1.64E+01	5.01E+01	7.97E+01	9.53E+01	1.00E+02	9.96E+01
cu 64	6.952E+01	7.214E+01	8.774E+01	9.961E+01	9.988E+01	9.988E+01	5.28E+01	6.89E-12	0.00E+00	0.00E+00	0.00E+00	0.00E+00
cu 66	2.218E+01	2.011E+01	7.236E+00	9.481E-03	1.369E-09	2.917E-09	6.54E-07	1.57E-09	0.00E+00	0.00E+00	0.00E+00	0.00E+00
ag110m	5.667E-04	5.886E-04	7.217E-04	8.575E-04	1.130E-03	3.019E-03	4.15E+00	1.19E+01	7.50E+00	1.05E-03	5.17E-43	0.00E+00
sb124	1.025E-03	1.065E-03	1.305E-03	1.550E-03	2.039E-03	5.413E-03	7.06E+00	1.65E+01	5.62E-01	2.80E-17	0.00E+00	0.00E+00

Table 44. Major Contributors to Decay Heat Induced in Dome Body (Zone 4) for M5 Scenario (in percent)

Time	0	1 m	10 m	1 h	6 h	1 d	1w	1 mo	1 y	10 y	100 y	1000 y
co 60	5.803E-04	6.337E-04	1.042E-03	1.831E-03	2.447E-03	6.549E-03	4.14E+00	9.04E+00	3.26E+01	7.42E+01	3.90E-03	0.00E+00
ni 63	5.670E-05	6.192E-05	1.018E-04	1.789E-04	2.391E-04	6.401E-04	4.05E-01	8.93E-01	3.61E+00	2.52E+01	9.92E+01	9.44E+01
cu 62	2.624E+01	2.668E+01	2.307E+01	1.141E+00	7.601E-10	6.596E-43	0.00E+00	0.00E+00	0.00E+00	0.00E+00	0.00E+00	0.00E+00
cu 64	3.272E+01	3.570E+01	5.822E+01	9.774E+01	9.936E+01	9.935E+01	2.38E+01	2.24E-12	0.00E+00	0.00E+00	0.00E+00	0.00E+00
cu 66	3.848E+01	3.667E+01	1.770E+01	3.429E-02	5.021E-09	1.069E-08	1.09E-06	1.88E-09	0.00E+00	0.00E+00	0.00E+00	0.00E+00
ag110m	2.396E-03	2.617E-03	4.302E-03	7.559E-03	1.010E-02	2.698E-02	1.68E+01	3.47E+01	5.58E+01	4.55E-02	8.42E-41	0.00E+00
sb122	9.492E-03	1.036E-02	1.701E-02	2.962E-02	3.753E-02	8.290E-02	1.13E+01	6.06E-02	1.19E-38	0.00E+00	0.00E+00	0.00E+00
sb124	3.445E-03	3.762E-03	6.185E-03	1.086E-02	1.449E-02	3.845E-02	2.27E+01	3.83E+01	3.32E+00	9.68E-16	0.00E+00	0.00E+00

Table 45. Major Contributors to Activity Induced in Dome Body (Zone 7) for M5 Scenario (in percent)

Time	0	1 m	10 m	1 h	6 h	1 d	1w	1 mo	1 y	10 y	100 y	1000 y
c 14	2.373E-05	2.424E-05	2.619E-05	3.196E-05	6.510E-05	1.110E-04	1.50E-04	2.53E-04	1.75E-03	1.78E-02	2.99E-01	1.15E+01
cr 51	1.438E+01	1.468E+01	1.586E+01	1.934E+01	3.919E+01	6.557E+01	7.62E+01	7.14E+01	1.13E-01	1.93E-36	0.00E+00	0.00E+00
mn 56	6.413E+01	6.520E+01	6.767E+01	6.600E+01	3.504E+01	4.720E-01	9.69E-18	0.00E+00	0.00E+00	0.00E+00	0.00E+00	0.00E+00
fe 55	1.280E+00	1.308E+00	1.413E+00	1.724E+00	3.512E+00	5.984E+00	8.04E+00	1.33E+01	7.34E+01	7.60E+01	1.56E-07	0.00E+00
co 60	6.427E-02	6.564E-02	7.093E-02	8.655E-02	1.763E-01	3.004E-01	4.05E-01	6.77E-01	4.16E+00	1.29E+01	1.58E-03	0.00E+00
ni 59	1.235E-04	1.261E-04	1.363E-04	1.663E-04	3.388E-04	5.775E-04	7.80E-04	1.31E-03	9.12E-03	9.28E-02	1.58E+00	6.69E+01
ni 63	1.526E-02	1.558E-02	1.684E-02	2.055E-02	4.186E-02	7.135E-02	9.63E-02	1.62E-01	1.12E+00	1.07E+01	9.76E+01	8.31E+00

Table 46. Major Contributors to Decay Heat Induced in Dome Body (Zone 7) for M5 Scenario (in percent)

Time	0	1 m	10 m	1 h	6 h	1 d	1w	1 mo	1 y	10 y	100 y	1000 y
c 14	6.009E-07	6.266E-07	6.762E-07	8.443E-07	2.691E-06	2.047E-05	5.12E-05	7.68E-05	3.84E-04	2.56E-03	8.63E-01	3.67E+01
cr 51	2.734E-01	2.851E-01	3.077E-01	3.838E-01	1.217E+00	9.085E+00	1.96E+01	1.63E+01	1.85E-02	2.09E-37	0.00E+00	0.00E+00
mn 54	1.229E-01	1.282E-01	1.383E-01	1.727E-01	5.501E-01	4.178E+00	1.03E+01	1.47E+01	3.49E+01	1.58E-01	1.06E-30	0.00E+00
mn 56	8.281E+01	8.597E+01	8.911E+01	8.892E+01	7.388E+01	4.441E+00	1.69E-16	0.00E+00	0.00E+00	0.00E+00	0.00E+00	0.00E+00
fe 59	1.623E-01	1.693E-01	1.826E-01	2.279E-01	7.242E-01	5.444E+00	1.24E+01	1.29E+01	3.54E-01	1.48E-22	0.00E+00	0.00E+00
co 58m	5.818E+00	6.060E+00	6.465E+00	7.577E+00	1.652E+01	3.202E+01	1.42E-03	5.91E-22	0.00E+00	0.00E+00	0.00E+00	0.00E+00
co 58	4.040E-01	4.213E-01	4.547E-01	5.675E-01	1.805E+00	1.363E+01	3.22E+01	3.84E+01	7.31E+00	5.61E-13	0.00E+00	0.00E+00
co 60	8.554E-02	8.920E-02	9.626E-02	1.202E-01	3.831E-01	2.913E+00	7.27E+00	1.08E+01	4.80E+01	9.80E+01	2.40E-01	0.00E+00
ni 59	4.652E-07	4.851E-07	5.235E-07	6.537E-07	2.084E-06	1.585E-05	3.97E-05	5.95E-05	2.98E-04	1.99E-03	6.76E-01	3.18E+01
ni 63	1.339E-04	1.396E-04	1.506E-04	1.881E-04	5.995E-04	4.560E-03	1.14E-02	1.71E-02	8.51E-02	5.34E-01	9.75E+01	9.20E+00
mo 99	6.509E-01	6.787E-01	7.312E-01	9.050E-01	2.737E+00	1.723E+01	9.49E+00	3.85E-02	3.95E-38	0.00E+00	0.00E+00	0.00E+00

Table 47. Major Contributors to Activity Induced in Central Body (Zone 16) for M5 Scenario (in percent)

Time	0	1 m	10 m	1 h	6 h	1 d	1w	1 mo	1 y	10 y	100 y	1000 y
c 14	2.367E-05	2.401E-05	2.580E-05	3.171E-05	6.647E-05	1.164E-04	1.63E-04	2.86E-04	2.43E-03	2.15E-02	3.00E-01	1.17E+01
cr 51	1.369E+01	1.389E+01	1.492E+01	1.832E+01	3.821E+01	6.566E+01	7.90E+01	7.72E+01	1.49E-01	2.22E-36	0.00E+00	0.00E+00
mn 56	6.659E+01	6.724E+01	6.942E+01	6.818E+01	3.725E+01	5.155E-01	1.10E-17	0.00E+00	0.00E+00	0.00E+00	0.00E+00	0.00E+00
fe 55	9.648E-01	9.786E-01	1.052E+00	1.293E+00	2.709E+00	4.742E+00	6.61E+00	1.14E+01	7.70E+01	6.94E+01	1.18E-07	0.00E+00
co 60	7.121E-02	7.222E-02	7.763E-02	9.540E-02	2.000E-01	3.501E-01	4.89E-01	8.51E-01	6.42E+00	1.74E+01	1.76E-03	0.00E+00
ni 59	1.239E-04	1.257E-04	1.351E-04	1.660E-04	3.480E-04	6.094E-04	8.53E-04	1.50E-03	1.27E-02	1.13E-01	1.59E+00	6.85E+01
ni 63	1.521E-02	1.543E-02	1.658E-02	2.038E-02	4.272E-02	7.480E-02	1.05E-01	1.84E-01	1.55E+00	1.29E+01	9.77E+01	8.46E+00
mo 99	2.790E+00	2.829E+00	3.036E+00	3.699E+00	7.356E+00	1.066E+01	3.28E+00	1.56E-02	2.73E-38	0.00E+00	0.00E+00	0.00E+00
tc 99m	2.451E+00	2.486E+00	2.672E+00	3.282E+00	6.770E+00	1.024E+01	3.18E+00	1.51E-02	2.64E-38	0.00E+00	0.00E+00	0.00E+00

Table 48. Major Contributors to Decay Heat Induced in Central Body (Zone 16) for M5 Scenario (in percent)

Time	0	1 m	10 m	1 h	6 h	1 d	1w	1 mo	1 y	10 y	100 y	1000 y
c 14	6.140E-07	6.270E-07	6.698E-07	8.393E-07	2.800E-06	2.447E-05	5.96E-05	9.60E-05	4.61E-04	2.32E-03	8.65E-01	3.74E+01
cr 51	2.668E-01	2.725E-01	2.910E-01	3.643E-01	1.209E+00	1.037E+01	2.17E+01	1.95E+01	2.12E-02	1.80E-37	0.00E+00	0.00E+00
mn 54	6.598E-02	6.738E-02	7.198E-02	9.018E-02	3.007E-01	2.623E+00	6.31E+00	9.64E+00	2.20E+01	7.50E-02	5.60E-31	0.00E+00
mn 56	8.811E+01	8.958E+01	9.191E+01	9.204E+01	8.002E+01	5.527E+00	2.05E-16	0.00E+00	0.00E+00	0.00E+00	0.00E+00	0.00E+00
fe 59	1.788E-01	1.826E-01	1.951E-01	2.443E-01	8.122E-01	7.016E+00	1.56E+01	1.74E+01	4.58E-01	1.44E-22	0.00E+00	0.00E+00
co 58m	3.641E+00	3.714E+00	3.922E+00	4.613E+00	1.053E+01	2.344E+01	1.02E-03	4.52E-22	0.00E+00	0.00E+00	0.00E+00	0.00E+00
co 58	2.642E-01	2.699E-01	2.883E-01	3.611E-01	1.202E+00	1.043E+01	2.40E+01	3.07E+01	5.60E+00	3.25E-13	0.00E+00	0.00E+00
co 60	9.710E-02	9.917E-02	1.059E-01	1.327E-01	4.427E-01	3.868E+00	9.41E+00	1.50E+01	6.39E+01	9.86E+01	2.66E-01	0.00E+00
ni 59	4.783E-07	4.884E-07	5.218E-07	6.538E-07	2.181E-06	1.906E-05	4.65E-05	7.48E-05	3.59E-04	1.81E-03	6.81E-01	3.26E+01
ni 63	1.367E-04	1.396E-04	1.492E-04	1.869E-04	6.234E-04	5.448E-03	1.33E-02	2.14E-02	1.02E-01	4.83E-01	9.76E+01	9.37E+00
mo 99	7.943E-01	8.110E-01	8.650E-01	1.074E+00	3.400E+00	2.459E+01	1.32E+01	5.74E-02	5.66E-38	0.00E+00	0.00E+00	0.00E+00

Table 49. Major Contributors to Activity Induced in Wings (Zone 24) for M5 Scenario (in percent)

Time	0	1 m	10 m	1 h	6 h	1 d	1w	1 mo	1 y	10 y	100 y	1000 y
ni 63	3.009E-03	3.682E-03	4.437E-03	5.308E-03	6.731E-03	1.465E-02	1.04E-01	1.32E-01	1.93E+00	9.51E+01	9.99E+01	9.90E+01
cu 62	1.286E+01	1.465E+01	9.287E+00	3.128E-01	1.976E-10	1.394E-43	0.00E+00	0.00E+00	0.00E+00	0.00E+00	0.00E+00	0.00E+00
cu 64	4.516E+01	5.523E+01	6.600E+01	7.544E+01	7.277E+01	5.915E+01	1.59E-01	8.61E-15	0.00E+00	0.00E+00	0.00E+00	0.00E+00
cu 66	1.030E+01	1.100E+01	3.890E+00	5.131E-03	2.855E-09	4.944E-09	5.64E-09	5.60E-12	0.00E+00	0.00E+00	0.00E+00	0.00E+00
w 181	5.532E-01	6.771E-01	8.159E-01	9.759E-01	1.236E+00	2.679E+00	1.84E+01	2.04E+01	4.43E+01	1.58E-05	0.00E+00	0.00E+00
w 183m	1.516E+01	6.350E-03	4.928E-34	0.000E+00	0.000E+00	0.000E+00	0.00E+00	0.00E+00	0.00E+00	0.00E+00	0.00E+00	0.00E+00
w 185	2.399E+00	2.936E+00	3.538E+00	4.231E+00	5.355E+00	1.158E+01	7.79E+01	7.93E+01	5.30E+01	1.76E-10	0.00E+00	0.00E+00
w 187	1.083E+01	1.324E+01	1.589E+01	1.855E+01	2.035E+01	2.630E+01	2.88E+00	3.03E-07	0.00E+00	0.00E+00	0.00E+00	0.00E+00

Table 50. Major Contributors to Decay Heat Induced in Wings (Zone 24) for M5 Scenario (in percent)

Time	0	1 m	10 m	1 h	6 h	1 d	1w	1 mo	1 y	10 y	100 y	1000 y
co 60	3.417E-04	3.916E-04	5.949E-04	1.082E-03	1.385E-03	2.952E-03	6.20E-02	9.18E-02	1.44E+00	5.63E+01	1.77E-03	0.00E+00
ni 63	7.374E-05	8.451E-05	1.284E-04	2.334E-04	2.990E-04	6.374E-04	1.34E-02	2.00E-02	3.52E-01	4.23E+01	9.93E+01	9.14E+01
cu 62	4.200E+01	4.482E+01	3.581E+01	1.833E+00	1.170E-09	8.082E-43	0.00E+00	0.00E+00	0.00E+00	0.00E+00	0.00E+00	0.00E+00
cu 64	2.022E+01	2.315E+01	3.489E+01	6.061E+01	5.905E+01	4.700E+01	3.74E-01	2.39E-14	0.00E+00	0.00E+00	0.00E+00	0.00E+00
cu 66	1.699E+01	1.699E+01	7.579E+00	1.519E-02	8.540E-09	1.448E-08	4.89E-08	5.74E-11	0.00E+00	0.00E+00	0.00E+00	0.00E+00
w 181	3.774E-02	4.325E-02	6.571E-02	1.194E-01	1.528E-01	3.243E-01	6.59E+00	8.62E+00	2.24E+01	1.96E-05	0.00E+00	0.00E+00
w 185	4.355E-01	4.992E-01	7.583E-01	1.378E+00	1.762E+00	3.730E+00	7.42E+01	8.93E+01	7.15E+01	5.78E-10	0.00E+00	0.00E+00
w 187	1.118E+01	1.280E+01	1.937E+01	3.437E+01	3.809E+01	4.819E+01	1.56E+01	1.94E-06	0.00E+00	0.00E+00	0.00E+00	0.00E+00

Table 51. Major Contributors to Activity Induced in Wings (Zone 26) for M5 Scenario (in percent)

Time	0	1 m	10 m	1 h	6 h	1 d	1w	1 mo	1 y	10 y	100 y	1000 y
ni 63	3.044E-03	3.729E-03	4.526E-03	5.452E-03	6.904E-03	1.490E-02	9.88E-02	1.25E-01	1.85E+00	9.50E+01	9.99E+01	9.90E+01
cu 62	1.342E+01	1.531E+01	9.771E+00	3.314E-01	2.091E-10	1.462E-43	0.00E+00	0.00E+00	0.00E+00	0.00E+00	0.00E+00	0.00E+00
cu 64	4.407E+01	5.395E+01	6.494E+01	7.473E+01	7.198E+01	5.802E+01	1.46E-01	7.86E-15	0.00E+00	0.00E+00	0.00E+00	0.00E+00
cu 66	1.058E+01	1.132E+01	4.031E+00	5.354E-03	3.015E-09	5.176E-09	5.51E-09	5.46E-12	0.00E+00	0.00E+00	0.00E+00	0.00E+00
w 181	5.719E-01	7.008E-01	8.505E-01	1.024E+00	1.295E+00	2.784E+00	1.78E+01	1.97E+01	4.34E+01	1.61E-05	0.00E+00	0.00E+00
w 183m	1.514E+01	6.348E-03	4.962E-34	0.000E+00	0.000E+00	0.000E+00	0.00E+00	0.00E+00	0.00E+00	0.00E+00	0.00E+00	0.00E+00
w 185	2.586E+00	3.169E+00	3.846E+00	4.631E+00	5.853E+00	1.255E+01	7.87E+01	8.00E+01	5.41E+01	1.87E-10	0.00E+00	0.00E+00
w 187	1.080E+01	1.322E+01	1.598E+01	1.879E+01	2.058E+01	2.636E+01	2.69E+00	2.83E-07	0.00E+00	0.00E+00	0.00E+00	0.00E+00

Table 52. Major Contributors to Decay Heat Induced in Wings (Zone 26) for M5 Scenario (in percent)

Time	0	1 m	10 m	1 h	6 h	1 d	1w	1 mo	1 y	10 y	100 y	1000 y
co 60	3.605E-04	4.131E-04	6.335E-04	1.179E-03	1.510E-03	3.205E-03	6.28E-02	9.20E-02	1.45E+00	5.78E+01	1.88E-03	0.00E+00
ni 63	7.321E-05	8.390E-05	1.287E-04	2.394E-04	3.068E-04	6.511E-04	1.28E-02	1.89E-02	3.33E-01	4.08E+01	9.93E+01	9.12E+01
cu 62	4.301E+01	4.589E+01	3.701E+01	1.939E+00	1.238E-09	8.516E-43	0.00E+00	0.00E+00	0.00E+00	0.00E+00	0.00E+00	0.00E+00
cu 64	1.936E+01	2.217E+01	3.372E+01	5.994E+01	5.843E+01	4.631E+01	3.44E-01	2.17E-14	0.00E+00	0.00E+00	0.00E+00	0.00E+00
cu 66	1.714E+01	1.714E+01	7.714E+00	1.583E-02	9.019E-09	1.523E-08	4.80E-08	5.57E-11	0.00E+00	0.00E+00	0.00E+00	0.00E+00
w 181	3.829E-02	4.387E-02	6.728E-02	1.251E-01	1.602E-01	3.386E-01	6.43E+00	8.30E+00	2.17E+01	1.93E-05	0.00E+00	0.00E+00
w 185	4.608E-01	5.280E-01	8.097E-01	1.506E+00	1.926E+00	4.060E+00	7.55E+01	8.97E+01	7.22E+01	5.94E-10	0.00E+00	0.00E+00
w 187	1.094E+01	1.253E+01	1.913E+01	3.475E+01	3.852E+01	4.853E+01	1.47E+01	1.80E-06	0.00E+00	0.00E+00	0.00E+00	0.00E+00

Table 53. Major Contributors to Activity Induced in Outer Leg (Zone 41) for M5 Scenario (in percent)

Time	0	1 m	10 m	1 h	6 h	1 d	1w	1 mo	1 y	10 y	100 y	1000 y
c 14	2.421E-05	2.448E-05	2.620E-05	3.224E-05	6.821E-05	1.201E-04	1.70E-04	3.06E-04	3.01E-03	2.40E-02	2.99E-01	1.19E+01
cr 51	1.375E+01	1.391E+01	1.488E+01	1.830E+01	3.851E+01	6.653E+01	8.11E+01	8.10E+01	1.81E-01	2.44E-36	0.00E+00	0.00E+00
mn 56	6.778E+01	6.824E+01	7.015E+01	6.899E+01	3.804E+01	5.291E-01	1.14E-17	0.00E+00	0.00E+00	0.00E+00	0.00E+00	0.00E+00
fe 55	8.419E-01	8.514E-01	9.112E-01	1.121E+00	2.372E+00	4.172E+00	5.89E+00	1.04E+01	8.11E+01	6.62E+01	1.01E-07	0.00E+00
co 60	7.160E-02	7.241E-02	7.750E-02	9.536E-02	2.017E-01	3.550E-01	5.02E-01	8.94E-01	7.80E+00	1.91E+01	1.72E-03	0.00E+00
ni 59	1.272E-04	1.287E-04	1.377E-04	1.695E-04	3.585E-04	6.310E-04	8.94E-04	1.61E-03	1.58E-02	1.27E-01	1.59E+00	6.97E+01
ni 63	1.560E-02	1.578E-02	1.689E-02	2.078E-02	4.396E-02	7.738E-02	1.10E-01	1.97E-01	1.92E+00	1.45E+01	9.78E+01	8.59E+00
mo 99	2.984E+00	3.017E+00	3.224E+00	3.933E+00	7.895E+00	1.150E+01	3.59E+00	1.74E-02	3.52E-38	0.00E+00	0.00E+00	0.00E+00
tc 99m	2.622E+00	2.651E+00	2.837E+00	3.490E+00	7.265E+00	1.105E+01	3.47E+00	1.69E-02	3.41E-38	0.00E+00	0.00E+00	0.00E+00

Table 54. Major Contributors to Decay Heat Induced in Outer Leg (Zone 41) for M5 Scenario (in percent)

Time	0	1 m	10 m	1 h	6 h	1 d	1w	1 mo	1 y	10 y	100 y	1000 y
c 14	6.367E-07	6.452E-07	6.854E-07	8.606E-07	2.952E-06	2.847E-05	6.76E-05	1.15E-04	5.47E-04	2.36E-03	8.63E-01	3.82E+01
cr 51	2.717E-01	2.753E-01	2.924E-01	3.669E-01	1.252E+00	1.185E+01	2.42E+01	2.29E+01	2.47E-02	1.80E-37	0.00E+00	0.00E+00
mn 54	3.447E-02	3.493E-02	3.711E-02	4.659E-02	1.597E-01	1.538E+00	3.60E+00	5.82E+00	1.32E+01	3.85E-02	2.82E-31	0.00E+00
mn 56	9.091E+01	9.171E+01	9.357E+01	9.390E+01	8.395E+01	6.399E+00	2.31E-16	0.00E+00	0.00E+00	0.00E+00	0.00E+00	0.00E+00
fe 59	1.888E-01	1.913E-01	2.033E-01	2.551E-01	8.721E-01	8.314E+00	1.80E+01	2.12E+01	5.53E-01	1.50E-22	0.00E+00	0.00E+00
co 58m	2.267E+00	2.294E+00	2.409E+00	2.840E+00	6.662E+00	1.637E+01	6.90E-04	3.25E-22	0.00E+00	0.00E+00	0.00E+00	0.00E+00
co 58	1.788E-01	1.811E-01	1.924E-01	2.415E-01	8.268E-01	7.917E+00	1.77E+01	2.40E+01	4.34E+00	2.16E-13	0.00E+00	0.00E+00
co 60	9.898E-02	1.003E-01	1.065E-01	1.338E-01	4.588E-01	4.425E+00	1.05E+01	1.77E+01	7.46E+01	9.87E+01	2.61E-01	0.00E+00
ni 59	4.978E-07	5.044E-07	5.359E-07	6.728E-07	2.308E-06	2.226E-05	5.28E-05	8.99E-05	4.28E-04	1.85E-03	6.82E-01	3.34E+01
ni 63	1.422E-04	1.441E-04	1.530E-04	1.922E-04	6.591E-04	6.357E-03	1.51E-02	2.57E-02	1.21E-01	4.93E-01	9.77E+01	9.58E+00
mo 99	8.613E-01	8.726E-01	9.255E-01	1.152E+00	3.749E+00	2.993E+01	1.56E+01	7.19E-02	7.03E-38	0.00E+00	0.00E+00	0.00E+00

Table 55. Major Contributors to Activity Induced in Inner Leg (Zone 60) for M5 Scenario (in percent)

Time	0	1 m	10 m	1 h	6 h	1 d	1w	1 mo	1 y	10 y	100 y	1000 y
c 14	2.418E-05	2.442E-05	2.611E-05	3.220E-05	6.864E-05	1.213E-04	1.73E-04	3.14E-04	3.26E-03	2.46E-02	2.98E-01	1.18E+01
cr 51	1.375E+01	1.389E+01	1.485E+01	1.829E+01	3.879E+01	6.727E+01	8.25E+01	8.33E+01	1.97E-01	2.50E-36	0.00E+00	0.00E+00
mn 56	6.844E+01	6.884E+01	7.068E+01	6.966E+01	3.871E+01	5.405E-01	1.17E-17	0.00E+00	0.00E+00	0.00E+00	0.00E+00	0.00E+00
fe 55	8.030E-01	8.112E-01	8.672E-01	1.069E+00	2.279E+00	4.025E+00	5.71E+00	1.02E+01	8.41E+01	6.47E+01	9.56E-08	0.00E+00
co 60	7.390E-02	7.466E-02	7.981E-02	9.841E-02	2.098E-01	3.706E-01	5.27E-01	9.50E-01	8.75E+00	2.02E+01	1.77E-03	0.00E+00
ni 59	1.281E-04	1.294E-04	1.383E-04	1.706E-04	3.637E-04	6.426E-04	9.16E-04	1.66E-03	1.73E-02	1.31E-01	1.59E+00	7.00E+01
ni 63	1.567E-02	1.583E-02	1.693E-02	2.087E-02	4.450E-02	7.863E-02	1.12E-01	2.04E-01	2.10E+00	1.49E+01	9.78E+01	8.61E+00
mo 99	3.058E+00	3.088E+00	3.296E+00	4.029E+00	8.150E+00	1.192E+01	3.74E+00	1.84E-02	3.92E-38	0.00E+00	0.00E+00	0.00E+00
tc 99m	2.686E+00	2.714E+00	2.901E+00	3.575E+00	7.501E+00	1.145E+01	3.62E+00	1.78E-02	3.80E-38	0.00E+00	0.00E+00	0.00E+00

Table 56. Major Contributors to Decay Heat Induced in Inner Leg (Zone 60) for M5 Scenario (in percent)

Time	0	1 m	10 m	1 h	6 h	1 d	1w	1 mo	1 y	10 y	100 y	1000 y
c 14	6.416E-07	6.484E-07	6.872E-07	8.646E-07	3.036E-06	3.230E-05	7.48E-05	1.34E-04	5.94E-04	2.29E-03	8.58E-01	3.81E+01
cr 51	2.741E-01	2.770E-01	2.935E-01	3.690E-01	1.289E+00	1.346E+01	2.68E+01	2.67E+01	2.69E-02	1.75E-37	0.00E+00	0.00E+00
mn 56	9.263E+01	9.320E+01	9.487E+01	9.540E+01	8.730E+01	7.342E+00	2.58E-16	0.00E+00	0.00E+00	0.00E+00	0.00E+00	0.00E+00
fe 59	1.926E-01	1.947E-01	2.063E-01	2.594E-01	9.080E-01	9.550E+00	2.01E+01	2.50E+01	6.09E-01	1.47E-22	0.00E+00	0.00E+00
co 58	9.325E-02	9.423E-02	9.987E-02	1.256E-01	4.401E-01	4.649E+00	1.01E+01	1.44E+01	2.44E+00	1.08E-13	0.00E+00	0.00E+00
co 60	1.031E-01	1.042E-01	1.104E-01	1.389E-01	4.877E+00	5.188E+00	1.20E+01	2.13E+01	8.37E+01	9.88E+01	2.69E-01	0.00E+00
ni 59	5.058E-07	5.111E-07	5.417E-07	6.816E-07	2.393E-06	2.546E-05	5.89E-05	1.05E-04	4.69E-04	1.81E-03	6.84E-01	3.35E+01
ni 63	1.441E-04	1.456E-04	1.544E-04	1.942E-04	6.819E-04	7.256E-03	1.68E-02	3.00E-02	1.33E-01	4.81E-01	9.77E+01	9.61E+00
mo 99	8.905E-01	8.997E-01	9.521E-01	1.187E+00	3.956E+00	3.484E+01	1.77E+01	8.58E-02	7.83E-38	0.00E+00	0.00E+00	0.00E+00

Table 57. Major Contributors to Activity Induced in Outer Vertical Target (Zone 67) for M5 Scenario (in percent)

Time	0	1 m	10 m	1 h	6 h	1 d	1w	1 mo	1 y	10 y	100 y	1000 y
c 14	1.691E-08	3.450E-08	3.816E-08	3.901E-08	4.362E-08	6.291E-08	1.80E-07	2.27E-07	3.36E-06	1.96E-02	4.71E+00	1.87E+01
ar 39	1.087E-07	2.216E-07	2.452E-07	2.507E-07	2.802E-07	4.042E-07	1.16E-06	1.46E-06	2.15E-05	1.23E-01	2.37E+01	1.03E+01
co 60	1.161E-04	2.367E-04	2.619E-04	2.678E-04	2.993E-04	4.316E-04	1.23E-03	1.54E-03	2.02E-02	3.61E+01	6.29E-02	0.00E+00
ni 63	1.375E-07	2.805E-07	3.103E-07	3.173E-07	3.547E-07	5.116E-07	1.47E-06	1.85E-06	2.71E-05	1.49E-01	1.94E+01	1.71E-01
nb 93m	7.423E-07	1.514E-06	1.675E-06	1.713E-06	1.914E-06	2.761E-06	7.91E-06	9.95E-06	1.41E-04	5.66E-01	7.14E+00	1.60E+01
nb 91	6.877E-08	1.403E-07	1.552E-07	1.587E-07	1.774E-07	2.559E-07	7.33E-07	9.25E-07	1.36E-05	7.89E-02	1.75E+01	3.09E+01
mo 93	1.906E-08	3.887E-08	4.300E-08	4.396E-08	4.915E-08	7.089E-08	2.03E-07	2.56E-07	3.79E-06	2.20E-02	5.26E+00	1.95E+01
ta179	2.167E-03	4.420E-03	4.890E-03	5.001E-03	5.591E-03	8.058E-03	2.30E-02	2.82E-02	2.94E-01	5.51E+01	1.59E-11	0.00E+00
w 181	1.920E+00	3.916E+00	4.331E+00	4.427E+00	4.944E+00	7.100E+00	1.97E+01	2.17E+01	4.72E+01	1.88E-03	0.00E+00	0.00E+00
w 183m	4.857E+01	3.391E-02	2.416E-33	0.000E+00	0.000E+00	0.000E+00	0.00E+00	0.00E+00	0.00E+00	0.00E+00	0.00E+00	0.00E+00
w 185	7.700E+00	1.571E+01	1.737E+01	1.776E+01	1.981E+01	2.838E+01	7.70E+01	7.81E+01	5.22E+01	1.93E-08	0.00E+00	0.00E+00
w 187	3.442E+01	7.018E+01	7.729E+01	7.714E+01	7.461E+01	6.387E+01	2.82E+00	2.96E-07	0.00E+00	0.00E+00	0.00E+00	0.00E+00

Table 58. Major Contributors to Decay Heat Induced in Outer Vertical Target (Zone 67) for M5 Scenario (in percent)

Time	0	1 m	10 m	1 h	6 h	1 d	1w	1 mo	1 y	10 y	100 y	1000 y
c 14	2.000E-09	3.098E-09	3.212E-09	3.292E-09	3.782E-09	6.169E-09	6.82E-08	1.01E-07	1.79E-06	1.01E-03	9.91E-01	1.04E+01
ar 39	5.682E-08	8.803E-08	9.128E-08	9.355E-08	1.075E-07	1.753E-07	1.94E-06	2.87E-06	5.07E-05	2.79E-02	2.20E+01	2.53E+01
co 60	7.214E-04	1.118E-03	1.159E-03	1.188E-03	1.364E-03	2.225E-03	2.45E-02	3.60E-02	5.66E-01	9.76E+01	6.96E-01	0.00E+00
nb 94	7.559E-09	1.171E-08	1.214E-08	1.244E-08	1.430E-08	2.332E-08	2.58E-07	3.81E-07	6.76E-06	3.81E-03	3.78E+00	4.27E+01
ag108m	2.303E-07	3.568E-07	3.700E-07	3.792E-07	4.356E-07	7.106E-07	7.85E-06	1.16E-05	2.05E-04	1.10E-01	6.69E+01	5.73E+00
w 181	2.189E-01	3.391E-01	3.515E-01	3.602E-01	4.133E-01	6.713E-01	7.17E+00	9.28E+00	2.42E+01	9.31E-05	0.00E+00	0.00E+00
w 183m	3.432E+01	1.819E-02	1.215E-33	0.000E+00	0.000E+00	0.000E+00	0.00E+00	0.00E+00	0.00E+00	0.00E+00	0.00E+00	0.00E+00
w 185	2.337E+00	3.620E+00	3.753E+00	3.845E+00	4.409E+00	7.142E+00	7.47E+01	8.90E+01	7.14E+01	2.54E-09	0.00E+00	0.00E+00
w 187	5.940E+01	9.198E+01	9.496E+01	9.501E+01	9.442E+01	9.141E+01	1.56E+01	1.91E-06	0.00E+00	0.00E+00	0.00E+00	0.00E+00

Table 59. Major Contributors to Activity Induced in Outer Vertical Target (Zone 68) for M5 Scenario (in percent)

Time	0	1 m	10 m	1 h	6 h	1 d	1w	1 mo	1 y	10 y	100 y	1000 y
c 14	1.925E-08	3.939E-08	4.320E-08	4.415E-08	4.934E-08	7.103E-08	2.02E-07	2.55E-07	3.89E-06	2.32E-02	5.50E+00	2.13E+01
ar 39	1.056E-07	2.161E-07	2.370E-07	2.423E-07	2.707E-07	3.897E-07	1.11E-06	1.40E-06	2.13E-05	1.24E-01	2.36E+01	1.00E+01
co 60	1.209E-04	2.474E-04	2.713E-04	2.773E-04	3.098E-04	4.459E-04	1.27E-03	1.59E-03	2.14E-02	3.91E+01	6.73E-02	0.00E+00
ni 63	1.442E-07	2.950E-07	3.236E-07	3.307E-07	3.696E-07	5.320E-07	1.51E-06	1.91E-06	2.89E-05	1.62E-01	2.09E+01	1.79E-01
nb 93m	8.236E-07	1.685E-06	1.848E-06	1.889E-06	2.111E-06	3.038E-06	8.63E-06	1.09E-05	1.60E-04	6.53E-01	7.76E+00	1.65E+01
nb 91	6.030E-08	1.234E-07	1.353E-07	1.383E-07	1.546E-07	2.225E-07	6.33E-07	8.00E-07	1.22E-05	7.20E-02	1.58E+01	2.72E+01
mo 93	1.955E-08	4.000E-08	4.388E-08	4.484E-08	5.011E-08	7.214E-08	2.05E-07	2.59E-07	3.95E-06	2.35E-02	5.54E+00	2.00E+01
ta179	1.989E-03	4.070E-03	4.464E-03	4.564E-03	5.100E-03	7.337E-03	2.07E-02	2.56E-02	2.75E-01	5.27E+01	1.50E-11	0.00E+00
w 181	1.769E+00	3.620E+00	3.970E+00	4.057E+00	4.528E+00	6.490E+00	1.78E+01	1.97E+01	4.42E+01	1.80E-03	0.00E+00	0.00E+00
w 183m	4.892E+01	3.426E-02	2.420E-33	0.000E+00	0.000E+00	0.000E+00	0.00E+00	0.00E+00	0.00E+00	0.00E+00	0.00E+00	0.00E+00
w 185	8.008E+00	1.638E+01	1.797E+01	1.836E+01	2.048E+01	2.927E+01	7.87E+01	8.01E+01	5.53E+01	2.08E-08	0.00E+00	0.00E+00
w 187	3.451E+01	7.057E+01	7.707E+01	7.689E+01	7.433E+01	6.351E+01	2.78E+00	2.92E-07	0.00E+00	0.00E+00	0.00E+00	0.00E+00

Table 60. Major Contributors to Decay Heat Induced in Outer Vertical Target (Zone 68) for M5 Scenario (in percent)

Time	0	1 m	10 m	1 h	6 h	1 d	1w	1 mo	1 y	10 y	100 y	1000 y
c 14	2.272E-09	3.526E-09	3.646E-09	3.736E-09	4.291E-09	6.990E-09	7.57E-08	1.12E-07	2.03E-06	1.10E-03	1.17E+00	1.11E+01
ar 39	5.515E-08	8.557E-08	8.848E-08	9.067E-08	1.041E-07	1.696E-07	1.84E-06	2.72E-06	4.92E-05	2.61E-02	2.23E+01	2.32E+01
co 60	7.502E-04	1.164E-03	1.204E-03	1.233E-03	1.416E-03	2.307E-03	2.49E-02	3.66E-02	5.88E-01	9.78E+01	7.55E-01	0.00E+00
nb 94	8.652E-09	1.343E-08	1.388E-08	1.422E-08	1.634E-08	2.661E-08	2.88E-07	4.26E-07	7.73E-06	4.21E-03	4.51E+00	4.62E+01
ag108m	2.163E-07	3.357E-07	3.471E-07	3.557E-07	4.085E-07	6.654E-07	7.20E-06	1.07E-05	1.92E-04	9.96E-02	6.56E+01	5.09E+00
w 181	2.014E-01	3.124E-01	3.231E-01	3.310E-01	3.797E-01	6.158E-01	6.44E+00	8.34E+00	2.23E+01	8.27E-05	0.00E+00	0.00E+00
w 183m	3.451E+01	1.832E-02	1.220E-33	0.000E+00	0.000E+00	0.000E+00	0.00E+00	0.00E+00	0.00E+00	0.00E+00	0.00E+00	0.00E+00
w 185	2.426E+00	3.764E+00	3.892E+00	3.987E+00	4.570E+00	7.393E+00	7.57E+01	9.02E+01	7.40E+01	2.55E-09	0.00E+00	0.00E+00
w 187	5.945E+01	9.221E+01	9.493E+01	9.495E+01	9.434E+01	9.122E+01	1.52E+01	1.87E-06	0.00E+00	0.00E+00	0.00E+00	0.00E+00

Table 61. Major Contributors to Activity Induced in Outer Vertical Target (Zone 73) for M5 Scenario (in percent)

Time	0	1 m	10 m	1 h	6 h	1 d	1w	1 mo	1 y	10 y	100 y	1000 y
c 14	3.417E-07	3.566E-07	4.323E-07	5.037E-07	6.633E-07	1.776E-06	2.79E-03	9.80E-03	1.53E-02	2.00E-02	4.10E-02	1.54E+01
ni 63	1.642E-03	1.714E-03	2.077E-03	2.421E-03	3.188E-03	8.535E-03	1.34E+01	4.71E+01	7.32E+01	9.00E+01	9.98E+01	8.32E+01
cu 64	7.148E+01	7.452E+01	8.961E+01	9.975E+01	9.992E+01	9.991E+01	5.93E+01	8.92E-12	0.00E+00	0.00E+00	0.00E+00	0.00E+00
cu 66	2.284E+01	2.080E+01	7.402E+00	9.510E-03	7.591E-10	1.617E-09	4.07E-07	1.12E-09	0.00E+00	0.00E+00	0.00E+00	0.00E+00
ag110m	4.293E-04	4.480E-04	5.432E-04	6.328E-04	8.328E-04	2.225E-03	3.43E+00	1.13E+01	7.00E+00	1.00E-03	5.24E-43	0.00E+00
sb124	7.440E-04	7.763E-04	9.411E-04	1.096E-03	1.440E-03	3.822E-03	5.60E+00	1.50E+01	5.02E-01	2.58E-17	0.00E+00	0.00E+00

Table 62. Major Contributors to Decay Heat Induced in Outer Vertical Target (Zone 73) for M5 Scenario (in percent)

Time	0	1 m	10 m	1 h	6 h	1 d	1w	1 mo	1 y	10 y	100 y	1000 y
be 10	7.731E-09	9.074E-09	1.469E-08	2.341E-08	3.109E-08	8.322E-08	6.67E-05	1.58E-04	5.91E-04	4.04E-03	3.53E-02	1.02E+01
c 14	2.597E-08	3.049E-08	4.934E-08	7.865E-08	1.044E-07	2.796E-07	2.24E-04	5.32E-04	1.99E-03	1.36E-02	1.17E-01	3.04E+01
co 60	5.555E-04	6.520E-04	1.055E-03	1.682E-03	2.233E-03	5.977E-03	4.78E+00	1.12E+01	3.73E+01	7.79E+01	4.89E-03	0.00E+00
ni 63	4.324E-05	5.076E-05	8.215E-05	1.309E-04	1.739E-04	4.655E-04	3.73E-01	8.85E-01	3.29E+00	2.11E+01	9.90E+01	5.68E+01
cu 62	1.595E+01	1.743E+01	1.483E+01	6.658E-01	4.405E-10	3.822E-43	0.00E+00	0.00E+00	0.00E+00	0.00E+00	0.00E+00	0.00E+00
cu 64	3.438E+01	4.032E+01	6.472E+01	9.857E+01	9.956E+01	9.953E+01	3.02E+01	3.06E-12	0.00E+00	0.00E+00	0.00E+00	0.00E+00
cu 66	4.050E+01	4.148E+01	1.971E+01	3.464E-02	2.788E-09	5.937E-09	7.63E-07	1.42E-09	0.00E+00	0.00E+00	0.00E+00	0.00E+00
ag110m	1.856E-03	2.178E-03	3.525E-03	5.618E-03	7.456E-03	1.992E-02	1.57E+01	3.49E+01	5.15E+01	3.87E-02	8.53E-41	0.00E+00
sb122	7.566E-03	8.879E-03	1.435E-02	2.267E-02	2.853E-02	6.301E-02	1.08E+01	6.28E-02	1.13E-38	0.00E+00	0.00E+00	0.00E+00
sb124	2.556E-03	3.000E-03	4.855E-03	7.735E-03	1.025E-02	2.720E-02	2.03E+01	3.69E+01	2.94E+00	7.88E-16	0.00E+00	0.00E+00

Table 63. Major Contributors to Activity Induced in Inner Vertical Target (Zone 76) for M5 Scenario (in percent)

Time	0	1 m	10 m	1 h	6 h	1 d	1w	1 mo	1 y	10 y	100 y	1000 y
c 14	1.909E-08	3.589E-08	3.702E-08	3.781E-08	4.257E-08	6.332E-08	2.21E-07	2.85E-07	5.16E-06	3.89E-02	8.66E+00	3.27E+01
ar 39	6.956E-08	1.307E-07	1.349E-07	1.378E-07	1.551E-07	2.307E-07	8.07E-07	1.04E-06	1.88E-05	1.38E-01	2.47E+01	1.02E+01
co 60	1.188E-04	2.233E-04	2.303E-04	2.352E-04	2.648E-04	3.937E-04	1.37E-03	1.75E-03	2.82E-02	6.50E+01	1.05E-01	0.00E+00
ni 63	1.226E-07	2.304E-07	2.377E-07	2.427E-07	2.732E-07	4.064E-07	1.42E-06	1.83E-06	3.29E-05	2.33E-01	2.82E+01	2.36E-01
nb 93m	7.377E-07	1.387E-06	1.430E-06	1.461E-06	1.644E-06	2.446E-06	8.55E-06	1.10E-05	1.91E-04	9.87E-01	9.32E+00	1.67E+01
nb 91	1.815E-08	3.411E-08	3.519E-08	3.594E-08	4.046E-08	6.018E-08	2.11E-07	2.71E-07	4.90E-06	3.67E-02	7.53E+00	1.27E+01
mo 93	1.280E-08	2.406E-08	2.482E-08	2.535E-08	2.854E-08	4.245E-08	1.48E-07	1.91E-07	3.46E-06	2.61E-02	5.76E+00	2.03E+01
ta179	6.513E-04	1.224E-03	1.263E-03	1.290E-03	1.453E-03	2.159E-03	7.51E-03	9.43E-03	1.20E-01	2.92E+01	7.79E-12	0.00E+00
w 181	7.678E-01	1.443E+00	1.489E+00	1.520E+00	1.709E+00	2.531E+00	8.56E+00	9.63E+00	2.57E+01	1.32E-03	0.00E+00	0.00E+00
w 183m	4.602E+01	2.960E-02	1.967E-33	0.000E+00	0.000E+00	0.000E+00	0.00E+00	0.00E+00	0.00E+00	0.00E+00	0.00E+00	0.00E+00
w 185	8.011E+00	1.506E+01	1.553E+01	1.586E+01	1.782E+01	2.632E+01	8.71E+01	9.03E+01	7.40E+01	3.53E-08	0.00E+00	0.00E+00
w 187	4.268E+01	8.018E+01	8.236E+01	8.210E+01	7.996E+01	7.059E+01	3.80E+00	4.07E-07	0.00E+00	0.00E+00	0.00E+00	0.00E+00

Table 64. Major Contributors to Decay Heat Induced in Inner Vertical Target (Zone 76) for M5 Scenario (in percent)

Time	0	1 m	10 m	1 h	6 h	1 d	1w	1 mo	1 y	10 y	100 y	1000 y
c 14	2.049E-09	2.924E-09	2.961E-09	3.032E-09	3.487E-09	5.723E-09	7.56E-08	1.17E-07	2.33E-06	1.13E-03	1.90E+00	1.24E+01
ar 39	3.302E-08	4.711E-08	4.772E-08	4.886E-08	5.619E-08	9.222E-08	1.22E-06	1.89E-06	3.74E-05	1.78E-02	2.39E+01	1.72E+01
co 60	6.702E-04	9.560E-04	9.683E-04	9.916E-04	1.140E-03	1.871E-03	2.47E-02	3.79E-02	6.68E-01	9.92E+01	1.21E+00	0.00E+00
nb 94	8.891E-09	1.268E-08	1.285E-08	1.316E-08	1.513E-08	2.483E-08	3.28E-07	5.08E-07	1.01E-06	4.90E-03	8.31E+00	5.88E+01
ag108m	1.078E-07	1.538E-07	1.558E-07	1.595E-07	1.834E-07	3.010E-07	3.98E-06	6.16E-06	1.22E-04	5.63E-02	5.86E+01	3.14E+00
w 181	7.946E-02	1.134E-01	1.148E-01	1.175E-01	1.350E-01	2.206E-01	2.82E+00	3.82E+00	1.12E+01	3.70E-05	0.00E+00	0.00E+00
w 183m	2.952E+01	1.441E-02	9.401E-34	0.000E+00	0.000E+00	0.000E+00	0.00E+00	0.00E+00	0.00E+00	0.00E+00	0.00E+00	0.00E+00
w 185	2.207E+00	3.148E+00	3.188E+00	3.264E+00	3.746E+00	6.105E+00	7.63E+01	9.52E+01	8.56E+01	2.63E-09	0.00E+00	0.00E+00
w 187	6.686E+01	9.532E+01	9.613E+01	9.609E+01	9.560E+01	9.313E+01	1.90E+01	2.44E-06	0.00E+00	0.00E+00	0.00E+00	0.00E+00

Table 65. Major Contributors to Activity Induced in Inner Vertical Target (Zone 77) for M5 Scenario (in percent)

Time	0	1 m	10 m	1 h	6 h	1 d	1w	1 mo	1 y	10 y	100 y	1000 y
c 14	2.300E-08	4.147E-08	4.264E-08	4.354E-08	4.896E-08	7.248E-08	2.45E-07	3.15E-07	5.86E-06	3.87E-02	9.96E+00	3.73E+01
ar 39	6.910E-08	1.246E-07	1.281E-07	1.308E-07	1.471E-07	2.178E-07	7.37E-07	9.46E-07	1.76E-05	1.13E-01	2.34E+01	9.63E+00
co 60	1.635E-04	2.948E-04	3.031E-04	3.094E-04	3.479E-04	5.150E-04	1.74E-03	2.21E-03	3.65E-02	7.39E+01	1.38E-01	0.00E+00
ni 63	1.468E-07	2.648E-07	2.722E-07	2.779E-07	3.125E-07	4.627E-07	1.57E-06	2.01E-06	3.72E-05	2.31E-01	3.22E+01	2.68E+01
nb 93m	8.150E-07	1.470E-06	1.511E-06	1.543E-06	1.735E-06	2.568E-06	8.68E-06	1.11E-05	1.99E-04	9.01E-01	9.62E+00	1.68E+01
mo 93	1.356E-08	2.445E-08	2.513E-08	2.566E-08	2.886E-08	4.273E-08	1.45E-07	1.86E-07	3.46E-06	2.28E-02	5.83E+00	2.04E+01
ta179	5.959E-04	1.074E-03	1.105E-03	1.128E-03	1.269E-03	1.877E-03	6.31E-03	7.91E-03	1.04E-01	2.21E+01	6.80E-12	0.00E+00
w 181	7.099E-01	1.280E+00	1.316E+00	1.344E+00	1.509E+00	2.225E+00	7.27E+00	8.17E+00	2.24E+01	1.01E-03	0.00E+00	0.00E+00
w 183m	4.381E+01	2.703E-02	1.790E-33	0.000E+00	0.000E+00	0.00E+00	0.00E+00	0.00E+00	0.00E+00	0.00E+00	0.00E+00	0.00E+00
w 185	8.875E+00	1.600E+01	1.645E+01	1.679E+01	1.885E+01	2.771E+01	8.87E+01	9.18E+01	7.73E+01	3.23E-08	0.00E+00	0.00E+00
w 187	4.429E+01	7.982E+01	8.171E+01	8.144E+01	7.922E+01	6.962E+01	3.63E+00	3.87E-07	0.00E+00	0.00E+00	0.00E+00	0.00E+00

Table 66. Major Contributors to Decay Heat Induced in Inner Vertical Target (Zone 77) for M5 Scenario (in percent)

Time	0	1 m	10 m	1 h	6 h	1 d	1w	1 mo	1 y	10 y	100 y	1000 y
c 14	2.437E-09	3.393E-09	3.433E-09	3.516E-09	4.042E-09	6.624E-09	8.40E-08	1.28E-07	2.59E-06	9.91E-04	2.20E+00	1.35E+01
ar 39	3.239E-08	4.508E-08	4.562E-08	4.671E-08	5.370E-08	8.801E-08	1.12E-06	1.71E-06	3.43E-05	1.29E-02	2.28E+01	1.55E+01
co 60	9.106E-04	1.267E-03	1.283E-03	1.313E-03	1.510E-03	2.474E-03	3.13E-02	4.75E-02	8.47E-01	9.94E+01	1.60E+00	0.00E+00
nb 94	1.003E-08	1.395E-08	1.412E-08	1.446E-08	1.662E-08	2.725E-08	3.46E-07	5.28E-07	1.06E-05	4.08E-03	9.11E+00	6.07E+01
ag108m	1.095E-07	1.524E-07	1.542E-07	1.579E-07	1.815E-07	2.975E-07	3.77E-06	5.77E-06	1.16E-04	4.22E-02	5.78E+01	2.92E+00
w 183m	2.774E+01	1.321E-02	8.614E-34	0.000E+00	0.000E+00	0.00E+00	0.00E+00	0.00E+00	0.00E+00	0.00E+00	0.00E+00	0.00E+00
w 185	2.414E+00	3.360E+00	3.400E+00	3.480E+00	3.993E+00	6.499E+00	7.80E+01	9.60E+01	8.74E+01	2.12E-09	0.00E+00	0.00E+00
w 187	6.850E+01	9.530E+01	9.602E+01	9.597E+01	9.546E+01	9.285E+01	1.81E+01	2.31E-06	0.00E+00	0.00E+00	0.00E+00	0.00E+00

Table 67. Major Contributors to Activity Induced in Inner Vertical Target (Zone 82) for M5 Scenario (in percent)

Time	0	1 m	10 m	1 h	6 h	1 d	1w	1 mo	1 y	10 y	100 y	1000 y
c 14	3.737E-07	3.878E-07	4.711E-07	5.404E-07	7.107E-07	1.903E-06	3.26E-03	1.51E-02	3.49E-02	5.62E-02	1.13E-01	3.36E+01
co 60	1.689E-04	1.753E-04	2.130E-04	2.443E-04	3.213E-04	8.597E-04	1.47E+00	6.75E+00	1.38E+01	6.82E+00	9.96E-05	0.00E+00
ni 63	6.507E-04	6.754E-04	8.204E-04	9.411E-04	1.238E-03	3.313E-03	5.68E+00	2.63E+01	6.03E+01	9.14E+01	9.98E+01	6.57E+01
cu 64	7.297E+01	7.567E+01	9.117E+01	9.992E+01	9.995E+01	9.992E+01	6.49E+01	1.28E-11	0.00E+00	0.00E+00	0.00E+00	0.00E+00
cu 66	2.619E+01	2.373E+01	8.460E+00	1.070E-02	5.664E-11	1.206E-10	3.32E-08	1.21E-10	0.00E+00	0.00E+00	0.00E+00	0.00E+00
ag110m	4.761E-04	4.941E-04	6.003E-04	6.885E-04	9.049E-04	2.417E-03	4.08E+00	1.77E+01	1.61E+01	2.86E-01	1.47E-42	0.00E+00
sb124	1.014E-03	1.052E-03	1.278E-03	1.466E-03	1.923E-03	5.103E-03	8.17E+00	2.89E+01	1.42E+00	9.00E-17	0.00E+00	0.00E+00

Table 68. Major Contributors to Decay Heat Induced in Inner Vertical Target (Zone 82) for M5 Scenario (in percent)

Time	0	1 m	10 m	1 h	6 h	1 d	1w	1 mo	1 y	10 y	100 y	1000 y
c 14	3.348E-08	3.665E-08	5.963E-08	8.514E-08	1.121E-07	2.998E-07	2.39E-04	5.21E-04	1.95E-03	1.44E-02	3.21E-01	5.59E+01
co 60	7.955E-04	8.709E-04	1.417E-03	2.023E-03	2.664E-03	7.121E-03	5.66E+00	1.22E+01	4.05E+01	9.16E+01	1.49E-02	0.00E+00
ni 63	2.020E-05	2.211E-05	3.598E-05	5.137E-05	6.763E-05	1.809E-04	1.44E-01	3.14E-01	1.17E+00	8.09E+00	9.81E+01	3.79E+01
cu 64	4.138E+01	4.526E+01	7.304E+01	9.963E+01	9.978E+01	9.965E+01	3.00E+01	2.80E-12	0.00E+00	0.00E+00	0.00E+00	0.00E+00
cu 66	5.474E+01	5.230E+01	2.498E+01	3.932E-02	2.084E-10	4.434E-10	5.67E-08	9.70E-11	0.00E+00	0.00E+00	0.00E+00	0.00E+00
ag110m	2.425E-03	2.655E-03	4.320E-03	6.167E-03	8.115E-03	2.166E-02	1.70E+01	3.47E+01	5.12E+01	4.15E-02	2.37E-40	0.00E+00
sb122	9.298E-03	1.018E-02	1.653E-02	2.340E-02	2.920E-02	6.443E-02	1.10E+01	5.86E-02	1.06E-38	0.00E+00	0.00E+00	0.00E+00
sb124	4.106E-03	4.495E-03	7.313E-03	1.044E-02	1.371E-02	3.635E-02	2.70E+01	4.50E+01	3.59E+00	1.04E-15	0.00E+00	0.00E+00

Table 69. Major Contributors to Activity Induced in Rails (Zone 104) for M5 Scenario (in percent)

Time	0	1 m	10 m	1 h	6 h	1 d	1w	1 mo	1 y	10 y	100 y	1000 y
c 14	1.702E-05	1.725E-05	1.877E-05	2.366E-05	4.962E-05	9.057E-05	1.61E-04	3.11E-04	2.76E-03	2.18E-02	3.66E-01	1.06E+01
cr 51	8.208E+00	8.317E+00	9.052E+00	1.140E+01	2.378E+01	4.260E+01	6.50E+01	6.99E+01	1.41E-01	1.88E-36	0.00E+00	0.00E+00
mn 54	1.451E-01	1.470E-01	1.601E-01	2.018E-01	4.229E-01	7.706E-01	1.35E+00	2.48E+00	1.05E+01	5.59E-02	1.88E-32	0.00E+00
mn 56	6.311E+01	6.366E+01	6.656E+01	6.706E+01	3.665E+01	5.287E-01	1.43E-17	0.00E+00	0.00E+00	0.00E+00	0.00E+00	0.00E+00
fe 55	5.251E-01	5.321E-01	5.792E-01	7.301E-01	1.531E+00	2.793E+00	4.93E+00	9.39E+00	6.61E+01	5.33E+01	1.09E-07	0.00E+00
co 58	7.985E-01	8.091E-01	8.807E-01	1.110E+00	2.323E+00	4.208E+00	7.04E+00	1.08E+01	3.66E+00	3.33E-13	0.00E+00	0.00E+00
co 60	1.042E-01	1.056E-01	1.149E-01	1.448E-01	3.037E-01	5.542E-01	9.80E-01	1.88E+00	1.48E+01	3.58E+01	4.37E-03	0.00E+00
ni 59	8.117E-05	8.225E-05	8.953E-05	1.129E-04	2.367E-04	4.320E-04	7.66E-04	1.48E-03	1.32E-02	1.04E-01	1.77E+00	5.67E+01
ni 63	8.875E-03	8.993E-03	9.789E-03	1.234E-02	2.588E-02	4.723E-02	8.37E-02	1.62E-01	1.43E+00	1.06E+01	9.69E+01	6.23E+00
nb 93m	1.652E-05	1.674E-05	1.822E-05	2.297E-05	4.817E-05	8.792E-05	1.56E-04	3.02E-04	2.70E-03	2.28E-02	4.32E-01	1.17E+01
mo 93	2.460E-05	2.493E-05	2.714E-05	3.421E-05	7.174E-05	1.309E-04	2.32E-04	4.49E-04	3.99E-03	3.15E-02	5.25E-01	1.42E+01
mo 99	5.336E+00	5.407E+00	5.876E+00	7.343E+00	1.461E+01	2.207E+01	8.61E+00	4.50E-02	8.22E-38	0.00E+00	0.00E+00	0.00E+00
tc 99m	4.688E+00	4.750E+00	5.171E+00	6.516E+00	1.344E+01	2.120E+01	8.33E+00	4.36E-02	7.96E-38	0.00E+00	0.00E+00	0.00E+00

Table 70. Major Contributors to Decay Heat Induced in Rails (Zone 104) for M5 Scenario (in percent)

Time	0	1 m	10 m	1 h	6 h	1 d	1w	1 mo	1 y	10 y	100 y	1000 y
c 14	4.500E-07	4.550E-07	4.862E-07	6.102E-07	1.912E-06	1.219E-05	3.33E-05	5.66E-05	2.52E-04	1.15E-03	1.05E+00	2.90E+01
cr 51	1.630E-01	1.648E-01	1.761E-01	2.208E-01	6.883E-01	4.305E+00	1.01E+01	9.57E+00	9.66E-03	7.45E-38	0.00E+00	0.00E+00
mn 54	6.516E-02	6.589E-02	7.040E-02	8.835E-02	2.767E-01	1.761E+00	4.75E+00	7.67E+00	1.62E+01	5.01E-02	9.14E-31	0.00E+00
mn 56	8.510E+01	8.567E+01	8.791E+01	8.819E+01	7.202E+01	3.628E+00	1.51E-16	0.00E+00	0.00E+00	0.00E+00	0.00E+00	0.00E+00
fe 59	2.054E-01	2.076E-01	2.218E-01	2.783E-01	8.691E-01	5.475E+00	1.36E+01	1.61E+01	3.92E-01	1.12E-22	0.00E+00	0.00E+00
co 58m	5.513E+00	5.568E+00	5.881E+00	6.929E+00	1.485E+01	2.412E+01	1.17E-03	5.51E-22	0.00E+00	0.00E+00	0.00E+00	0.00E+00
co 58	4.311E-01	4.359E-01	4.657E-01	5.843E-01	1.827E+00	1.156E+01	2.98E+01	4.03E+01	6.82E+00	3.59E-13	0.00E+00	0.00E+00
co 60	1.448E-01	1.464E-01	1.564E-01	1.963E-01	6.151E-01	3.919E+00	1.07E+01	1.80E+01	7.10E+01	9.94E+01	6.56E-01	0.00E+00
ni 59	3.193E-07	3.229E-07	3.450E-07	4.329E-07	1.357E-06	8.646E-06	2.36E-05	4.02E-05	1.79E-04	8.17E-04	7.51E-01	2.30E+01
ni 63	8.131E-05	8.222E-05	8.784E-05	1.102E-04	3.454E-04	2.202E-03	6.02E-03	1.02E-02	4.52E-02	1.94E-01	9.59E+01	5.89E+00
nb 93m	2.559E-07	2.588E-07	2.765E-07	3.470E-07	1.087E-06	6.929E-06	1.89E-05	3.22E-05	1.44E-04	7.05E-04	7.23E-01	1.87E+01
nb 94	1.489E-07	1.506E-07	1.609E-07	2.019E-07	6.328E-07	4.033E-06	1.10E-05	1.87E-05	8.33E-05	3.81E-04	3.50E-01	1.05E+01
mo 93	2.104E-07	2.127E-07	2.273E-07	2.853E-07	8.939E-07	5.697E-06	1.56E-05	2.65E-05	1.18E-04	5.38E-04	4.86E-01	1.25E+01
mo 99	1.549E+00	1.566E+00	1.670E+00	2.078E+00	6.177E+00	3.258E+01	1.96E+01	9.01E-02	8.22E-38	0.00E+00	0.00E+00	0.00E+00

Table 71. Major Contributors to Activity Induced in Rails (Zone 105) for M5 Scenario (in percent)

Time	0	1 m	10 m	1 h	6 h	1 d	1w	1 mo	1 y	10 y	100 y	1000 y
cr 51	8.667E+00	8.797E+00	9.607E+00	1.201E+01	2.411E+01	4.133E+01	6.13E+01	6.25E+01	8.44E-02	1.42E-36	0.00E+00	0.00E+00
mn 54	2.615E-01	2.655E-01	2.899E-01	3.628E-01	7.317E-01	1.276E+00	2.17E+00	3.78E+00	1.07E+01	7.23E-02	3.59E-32	0.00E+00
mn 56	6.069E+01	6.132E+01	6.433E+01	6.434E+01	3.384E+01	4.671E-01	1.22E-17	0.00E+00	0.00E+00	0.00E+00	0.00E+00	0.00E+00
fe 55	9.402E-01	9.543E-01	1.042E+00	1.304E+00	2.632E+00	4.594E+00	7.88E+00	1.42E+01	6.71E+01	6.85E+01	2.07E-07	0.00E+00
co 60	9.729E-02	9.875E-02	1.079E-01	1.350E-01	2.723E-01	4.756E-01	8.18E-01	1.49E+00	7.84E+00	2.40E+01	4.32E-03	0.00E+00
ni 59	7.500E-05	7.613E-05	8.315E-05	1.041E-04	2.100E-04	3.668E-04	6.32E-04	1.16E-03	6.90E-03	6.91E-02	1.73E+00	5.48E+01
ni 63	8.357E-03	8.482E-03	9.264E-03	1.159E-02	2.339E-02	4.086E-02	7.04E-02	1.29E-01	7.63E-01	7.18E+00	9.66E+01	6.14E+00
nb 93m	1.887E-05	1.915E-05	2.092E-05	2.618E-05	5.282E-05	9.226E-05	1.59E-04	2.91E-04	1.73E-03	1.71E-02	4.13E-01	1.10E+01
mo 93	2.218E-05	2.251E-05	2.459E-05	3.077E-05	6.208E-05	1.084E-04	1.87E-04	3.43E-04	2.04E-03	2.04E-02	5.02E-01	1.34E+01
mo 99	5.517E+00	5.598E+00	6.105E+00	7.573E+00	1.450E+01	2.096E+01	7.95E+00	3.94E-02	4.82E-38	0.00E+00	0.00E+00	0.00E+00
tc 99m	4.846E+00	4.919E+00	5.372E+00	6.720E+00	1.334E+01	2.014E+01	7.70E+00	3.81E-02	4.66E-38	0.00E+00	0.00E+00	0.00E+00

Table 72. Major Contributors to Decay Heat Induced in Rails (Zone 105) for M5 Scenario (in percent)

Time	0	1 m	10 m	1 h	6 h	1 d	1w	1 mo	1 y	10 y	100 y	1000 y
c 14	4.023E-07	4.079E-07	4.396E-07	5.514E-07	1.682E-06	9.864E-06	2.75E-05	4.59E-05	1.98E-04	1.09E-03	9.85E-01	2.69E+01
mn 54	1.183E-01	1.200E-01	1.293E-01	1.621E-01	4.942E-01	2.894E+00	7.96E+00	1.26E+01	2.59E+01	9.63E-02	1.74E-30	0.00E+00
mn 56	8.244E+01	8.322E+01	8.614E+01	8.636E+01	6.864E+01	3.182E+00	1.35E-16	0.00E+00	0.00E+00	0.00E+00	0.00E+00	0.00E+00
fe 59	1.907E-01	1.934E-01	2.084E-01	2.613E-01	7.943E-01	4.605E+00	1.17E+01	1.36E+01	3.21E-01	1.10E-22	0.00E+00	0.00E+00
co 58m	6.543E+00	6.626E+00	7.060E+00	8.313E+00	1.734E+01	2.592E+01	1.28E-03	5.93E-22	0.00E+00	0.00E+00	0.00E+00	0.00E+00
co 58	4.734E-01	4.800E-01	5.173E-01	6.487E-01	1.974E+00	1.150E+01	3.02E+01	4.02E+01	6.59E+00	4.17E-13	0.00E+00	0.00E+00
co 60	1.362E-01	1.381E-01	1.488E-01	1.867E-01	5.694E-01	3.339E+00	9.29E+00	1.54E+01	5.89E+01	9.91E+01	6.50E-01	0.00E+00
ni 59	2.972E-07	3.014E-07	3.248E-07	4.074E-07	1.242E-06	7.288E-06	2.03E-05	3.39E-05	1.46E-04	8.06E-04	7.36E-01	2.22E+01
ni 63	7.712E-05	7.820E-05	8.428E-05	1.057E-04	3.224E-04	1.891E-03	5.27E-03	8.80E-03	3.77E-02	1.95E-01	9.57E+01	5.80E+00
nb 93m	2.944E-07	2.985E-07	3.217E-07	4.036E-07	1.231E-06	7.219E-06	2.01E-05	3.36E-05	1.45E-04	7.88E-04	6.92E-01	1.76E+01
nb 94	1.527E-07	1.548E-07	1.669E-07	2.093E-07	6.383E-07	3.744E-06	1.04E-05	1.74E-05	7.53E-05	4.14E-04	3.77E-01	1.11E+01
mo 93	1.910E-07	1.937E-07	2.088E-07	2.619E-07	7.986E-07	4.685E-06	1.31E-05	2.18E-05	9.41E-05	5.17E-04	4.64E-01	1.18E+01
mo 99	1.613E+00	1.635E+00	1.759E+00	2.187E+00	6.329E+00	3.073E+01	1.89E+01	8.51E-02	7.55E-38	0.00E+00	0.00E+00	0.00E+00

Table 73. Specific Activities Induced in All Zones for SA1 Scenario ( $\text{Ci}/\text{m}^3$ )

Time	0	1 m	10 m	1 h	6 h	1 d	1w	1 mo	1 y	10 y	100 y	1000 y
Z 1	1.583E+08	9.035E+07	8.239E+07	8.083E+07	7.377E+07	5.542E+07	2.75E+07	2.19E+07	1.63E+06	3.85E+02	1.80E+00	4.05E-01
Z 2	6.128E+07	5.863E+07	4.603E+07	3.593E+07	2.715E+07	1.014E+07	1.42E+04	9.12E+03	7.27E+03	6.07E+03	3.11E+03	6.22E+00
Z 4	4.325E+07	4.155E+07	3.332E+07	2.754E+07	2.088E+07	7.800E+06	8.73E+03	4.82E+03	3.37E+03	2.64E+03	1.35E+03	2.70E+00
Z 7	9.321E+05	9.141E+05	8.469E+05	6.976E+05	3.668E+05	2.358E+05	1.87E+05	1.22E+05	3.16E+04	3.17E+03	1.88E+02	4.39E+00
Z 16	1.216E+05	1.199E+05	1.114E+05	9.078E+04	4.577E+04	2.828E+04	2.16E+04	1.35E+04	3.00E+03	3.45E+02	2.46E+01	5.66E-01
Z 24	7.696E+06	6.376E+06	5.231E+06	4.297E+06	3.428E+06	1.686E+06	4.03E+05	3.23E+05	2.32E+04	6.26E+02	3.20E+02	6.42E-01
Z 26	7.891E+06	6.534E+06	5.324E+06	4.342E+06	3.472E+06	1.728E+06	4.39E+05	3.53E+05	2.50E+04	6.48E+02	3.31E+02	6.64E-01
Z 41	1.794E+05	1.774E+05	1.654E+05	1.344E+05	6.670E+04	4.065E+04	3.05E+04	1.85E+04	3.70E+03	4.68E+02	3.75E+01	8.48E-01
Z 60	1.536E+05	1.520E+05	1.419E+05	1.149E+05	5.640E+04	3.411E+04	2.54E+04	1.52E+04	2.93E+03	3.92E+02	3.23E+01	7.29E-01
Z 67	1.209E+08	6.522E+07	6.005E+07	5.894E+07	5.380E+07	4.045E+07	2.03E+07	1.63E+07	1.16E+06	2.78E+02	1.17E+00	2.66E-01
Z 68	8.454E+07	4.554E+07	4.223E+07	4.147E+07	3.788E+07	2.854E+07	1.444E+07	1.15E+07	7.94E+05	1.87E+02	7.93E-01	1.85E-01
Z 73	1.939E+06	1.855E+06	1.508E+06	1.277E+06	9.694E+05	3.621E+05	3.46E+02	1.76E+02	1.24E+02	9.44E+01	4.57E+01	1.09E-01
Z 76	7.292E+07	4.178E+07	4.068E+07	3.994E+07	3.609E+07	2.606E+07	1.11E+07	8.75E+06	4.99E+05	9.70E+01	4.36E-01	1.04E-01
Z 77	5.118E+07	3.049E+07	2.977E+07	2.924E+07	2.646E+07	1.921E+07	8.38E+06	6.63E+06	3.67E+05	8.20E+01	3.18E-01	7.64E-02
Z 82	1.190E+06	1.144E+06	9.301E+05	8.046E+05	6.118E+05	2.286E+05	1.79E+02	7.06E+01	3.65E+01	2.27E+01	1.12E+01	3.38E-02
Z 104	1.167E+02	1.151E+02	1.052E+02	8.281E+01	4.082E+01	2.375E+01	1.50E+01	8.80E+00	1.82E+00	2.37E-01	1.40E-02	4.34E-04
Z 105	1.108E+04	1.092E+04	9.972E+03	7.936E+03	4.123E+03	2.546E+03	1.68E+03	1.06E+03	3.02E+02	3.09E+01	1.24E+00	3.89E-02

Table 74. Specific Decay Heat Induced in All Zones for SA1 Scenario ( $\text{MW}/\text{m}^3$ )

Time	0	1 m	10 m	1 h	6 h	1 d	1w	1 mo	1 y	10 y	100 y	1000 y
Z 1	3.728E-01	2.562E-01	2.466E-01	2.408E-01	2.108E-01	1.331E-01	2.00E-02	1.41E-02	8.66E-04	1.76E-06	2.38E-09	2.00E-10
Z 2	3.181E-01	2.858E-01	1.674E-01	6.973E-02	5.085E-02	1.896E-02	4.66E-05	2.67E-05	8.43E-06	1.55E-06	3.18E-07	6.68E-10
Z 4	1.808E-01	1.656E-01	9.849E-02	5.228E-02	3.897E-02	1.456E-02	3.65E-05	2.24E-05	7.09E-06	1.01E-06	1.39E-07	2.89E-10
Z 7	1.015E-02	9.765E-03	9.060E-03	7.253E-03	2.313E-03	3.661E-04	1.95E-04	1.46E-04	4.07E-05	6.48E-06	1.91E-08	4.03E-10
Z 16	1.308E-03	1.282E-03	1.201E-03	9.573E-04	2.908E-04	3.946E-05	2.10E-05	1.51E-05	4.52E-06	9.40E-07	2.51E-09	5.19E-11
Z 24	3.372E-02	2.968E-02	1.905E-02	9.627E-03	7.503E-03	3.592E-03	2.94E-04	2.13E-04	1.27E-05	1.43E-07	3.27E-08	7.07E-11
Z 26	3.521E-02	3.099E-02	1.971E-02	9.718E-03	7.571E-03	3.645E-03	3.19E-04	2.33E-04	1.38E-05	1.53E-07	3.38E-08	7.32E-11
Z 41	1.915E-03	1.891E-03	1.780E-03	1.416E-03	4.173E-04	5.063E-05	2.71E-05	1.87E-05	5.83E-06	1.40E-06	3.81E-09	7.73E-11
Z 60	1.629E-03	1.612E-03	1.521E-03	1.207E-03	3.471E-04	3.780E-05	2.04E-05	1.36E-05	4.64E-06	1.24E-06	3.28E-09	6.64E-11
Z 67	2.819E-01	1.859E-01	1.796E-01	1.753E-01	1.535E-01	9.676E-02	1.47E-02	1.07E-02	6.35E-04	1.61E-06	1.61E-09	1.41E-10
Z 68	1.972E-01	1.299E-01	1.258E-01	1.229E-01	1.076E-01	6.801E-02	1.05E-02	7.60E-03	4.38E-04	1.16E-06	1.08E-09	1.04E-10
Z 73	7.798E-03	6.683E-03	4.036E-03	2.403E-03	1.806E-03	6.749E-04	1.33E-06	7.87E-07	2.67E-07	4.07E-08	4.68E-09	1.62E-11
Z 76	1.886E-01	1.342E-01	1.326E-01	1.296E-01	1.132E-01	7.052E-02	8.82E-03	6.20E-03	3.21E-04	9.86E-07	5.80E-10	8.02E-11
Z 77	1.334E-01	9.718E-02	9.607E-02	9.389E-02	8.205E-02	5.123E-02	6.66E-03	4.73E-03	2.41E-04	9.44E-07	4.21E-10	6.17E-11
Z 82	3.999E-03	3.647E-03	2.193E-03	1.499E-03	1.138E-03	4.257E-04	8.74E-07	5.48E-07	1.82E-07	2.60E-08	1.16E-09	5.94E-12
Z 104	1.247E-06	1.234E-06	1.154E-06	9.165E-07	2.966E-07	5.373E-08	2.63E-08	1.85E-08	5.75E-09	1.32E-09	1.44E-12	4.67E-14
Z 105	1.163E-04	1.148E-04	1.065E-04	8.461E-05	2.818E-05	5.566E-06	2.71E-06	1.94E-06	6.06E-07	1.16E-07	1.28E-10	4.19E-12

Table 75. Specific Activities Induced in All Zones for M5 Scenario ( $\text{Ci}/\text{m}^3$ )

Time	0	1 m	10 m	1 h	6 h	1 d	1w	1 mo	1 y	10 y	100 y	1000 y
Z 1	1.421E+08	7.405E+07	6.611E+07	6.463E+07	5.778E+07	4.000E+07	1.37E+07	1.09E+07	7.69E+05	1.31E+02	5.99E-01	1.33E-01
Z 2	5.694E+07	5.459E+07	4.378E+07	3.521E+07	2.663E+07	9.939E+06	7.98E+03	3.24E+03	2.40E+03	2.02E+03	1.04E+03	2.07E+00
Z 4	4.087E+07	3.934E+07	3.208E+07	2.700E+07	2.048E+07	7.649E+06	5.48E+03	1.79E+03	1.12E+03	8.81E+02	4.51E+02	9.00E-01
Z 7	8.005E+05	7.838E+05	7.254E+05	5.944E+05	2.918E+05	1.712E+05	1.27E+05	7.52E+04	1.08E+04	1.07E+03	6.27E+01	1.46E+00
Z 16	1.054E+05	1.039E+05	9.668E+04	7.866E+04	3.753E+04	2.143E+04	1.53E+04	8.72E+03	1.02E+03	1.16E+02	8.22E+00	1.89E-01
Z 24	7.072E+06	5.778E+06	4.795E+06	4.008E+06	3.161E+06	1.452E+06	2.04E+05	1.61E+05	1.09E+04	2.09E+02	1.07E+02	2.14E-01
Z 26	7.222E+06	5.898E+06	4.860E+06	4.035E+06	3.186E+06	1.476E+06	2.23E+05	1.76E+05	1.18E+04	2.16E+02	1.10E+02	2.21E-01
Z 41	1.563E+05	1.545E+05	1.444E+05	1.173E+05	5.547E+04	3.151E+04	2.22E+04	1.24E+04	1.26E+03	1.57E+02	1.25E+01	2.83E-01
Z 60	1.341E+05	1.327E+05	1.241E+05	1.007E+05	4.722E+04	2.673E+04	1.88E+04	1.03E+04	9.93E+02	1.32E+02	1.08E+01	2.43E-01
Z 67	1.095E+08	5.366E+07	4.851E+07	4.745E+07	4.244E+07	2.942E+07	1.03E+07	8.14E+06	5.51E+05	9.45E+01	3.89E-01	8.79E-02
Z 68	7.642E+07	3.735E+07	3.406E+07	3.332E+07	2.982E+07	2.071E+07	7.29E+06	5.76E+06	3.78E+05	6.34E+01	2.64E-01	6.12E-02
Z 73	1.846E+06	1.769E+06	1.459E+06	1.252E+06	9.509E+05	3.551E+05	2.26E+02	6.44E+01	4.11E+01	3.14E+01	1.52E+01	3.63E-02
Z 76	6.671E+07	3.549E+07	3.440E+07	3.369E+07	2.992E+07	2.012E+07	5.75E+06	4.47E+06	2.47E+05	3.27E+01	1.45E-01	3.45E-02
Z 77	4.653E+07	2.580E+07	2.509E+07	2.458E+07	2.186E+07	1.476E+07	4.36E+06	3.40E+06	1.82E+05	2.76E+01	1.06E-01	2.54E-02
Z 82	1.141E+06	1.100E+06	9.053E+05	7.892E+05	6.001E+05	2.242E+05	1.31E+02	2.83E+01	1.22E+01	7.58E+00	3.73E+00	1.13E-02
Z 104	1.019E+02	1.006E+02	9.240E+01	7.330E+01	3.495E+01	1.915E+01	1.08E+01	5.58E+00	6.28E-01	7.95E-02	4.68E-03	1.45E-04
Z 105	9.575E+03	9.434E+03	8.637E+03	6.902E+03	3.421E+03	1.958E+03	1.14E+03	6.20E+02	1.04E+02	1.04E+01	4.15E-01	1.30E-02

Table 76. Specific Decay Heat Induced in All Zones for M5 Scenario ( $\text{MW}/\text{m}^3$ )

Time	0	1 m	10 m	1 h	6 h	1 d	1w	1 mo	1 y	10 y	100 y	1000 y
Z 1	3.572E-01	2.403E-01	2.308E-01	2.251E-01	1.960E-01	1.201E-01	1.06E-02	7.04E-03	4.08E-04	5.92E-07	8.06E-10	6.54E-11
Z 2	2.747E-01	2.457E-01	1.471E-01	6.787E-02	4.986E-02	1.859E-02	3.04E-05	1.27E-05	5.18E-07	1.06E-07	2.22E-10	
Z 4	1.611E-01	1.476E-01	8.976E-02	5.108E-02	3.822E-02	1.427E-02	2.25E-05	1.02E-05	2.51E-06	3.38E-07	4.62E-08	9.64E-11
Z 7	9.272E-03	8.891E-03	8.239E-03	6.599E-03	2.070E-03	2.722E-04	1.09E-04	7.25E-05	1.45E-05	2.17E-06	6.37E-09	1.34E-10
Z 16	1.191E-03	1.167E-03	1.092E-03	8.716E-04	2.613E-04	2.990E-05	1.23E-05	7.62E-06	1.59E-06	3.15E-07	8.36E-10	1.73E-11
Z 24	2.932E-02	2.558E-02	1.684E-02	9.260E-03	7.229E-03	3.392E-03	1.61E-04	1.08E-04	6.10E-06	4.77E-08	1.09E-08	2.36E-11
Z 26	3.052E-02	2.664E-02	1.737E-02	9.336E-03	7.285E-03	3.432E-03	1.75E-04	1.18E-04	6.66E-06	5.11E-08	1.13E-08	2.44E-11
Z 41	1.743E-03	1.720E-03	1.619E-03	1.289E-03	3.759E-04	3.897E-05	1.64E-05	9.65E-06	2.03E-06	4.69E-07	1.27E-09	2.58E-11
Z 60	1.482E-03	1.466E-03	1.383E-03	1.099E-03	3.131E-04	2.943E-05	1.27E-05	7.11E-06	1.60E-06	4.15E-07	1.09E-09	2.21E-11
Z 67	2.715E-01	1.752E-01	1.690E-01	1.649E-01	1.435E-01	8.800E-02	7.96E-03	5.38E-03	3.03E-04	5.38E-07	5.41E-10	4.64E-11
Z 68	1.899E-01	1.224E-01	1.183E-01	1.155E-01	1.006E-01	6.173E-02	5.70E-03	3.85E-03	2.12E-04	3.90E-07	3.63E-10	3.43E-11
Z 73	7.122E-03	6.068E-03	3.749E-03	2.352E-03	1.771E-03	6.617E-04	8.26E-07	3.48E-07	9.31E-08	1.36E-08	1.56E-09	5.40E-12
Z 76	1.823E-01	1.278E-01	1.261E-01	1.232E-01	1.071E-01	6.527E-02	4.94E-03	3.19E-03	1.60E-04	3.30E-07	1.94E-10	2.66E-11
Z 77	1.288E-01	9.250E-02	9.140E-02	8.926E-02	7.764E-02	4.738E-02	3.73E-03	2.44E-03	1.21E-04	3.16E-07	1.41E-10	2.05E-11
Z 82	3.736E-03	3.413E-03	2.098E-03	1.469E-03	1.116E-03	4.172E-04	5.24E-07	2.40E-07	6.43E-08	8.70E-09	3.85E-10	1.98E-12
Z 104	1.130E-06	1.118E-06	1.046E-06	8.337E-07	2.661E-07	4.174E-08	1.53E-08	8.98E-09	2.02E-09	4.41E-10	4.80E-13	1.56E-14
Z 105	1.054E-04	1.040E-04	9.648E-05	7.691E-05	2.522E-05	4.299E-06	1.54E-06	9.23E-07	2.14E-07	3.89E-08	4.26E-11	1.40E-12

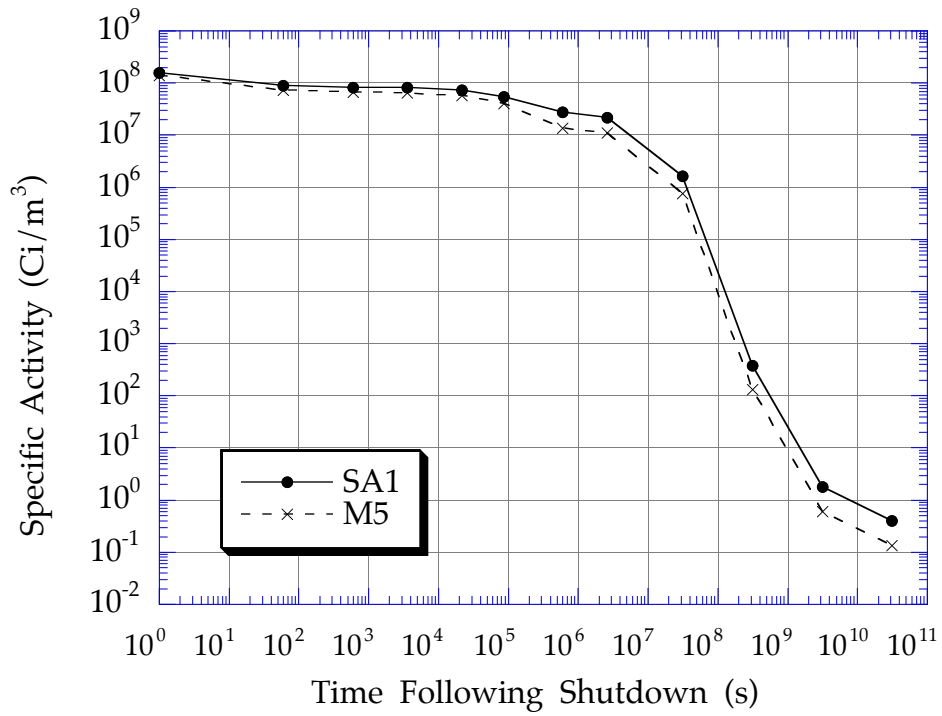


Fig. 16. Activity induced in dome PFC (zone 1).

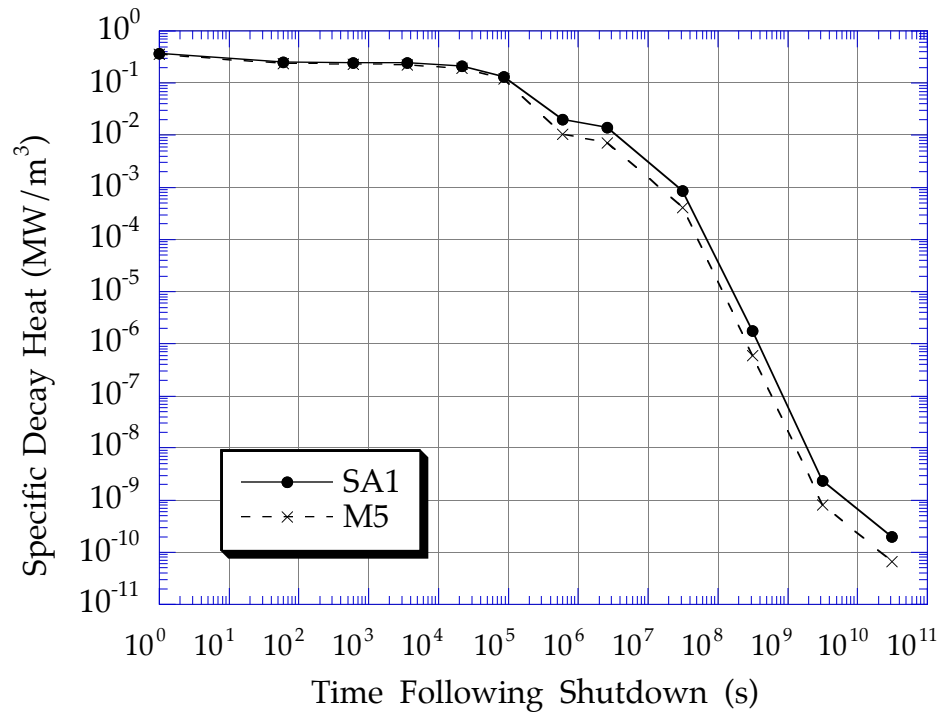


Fig. 17. Decay heat induced in dome PFC (zone 1).

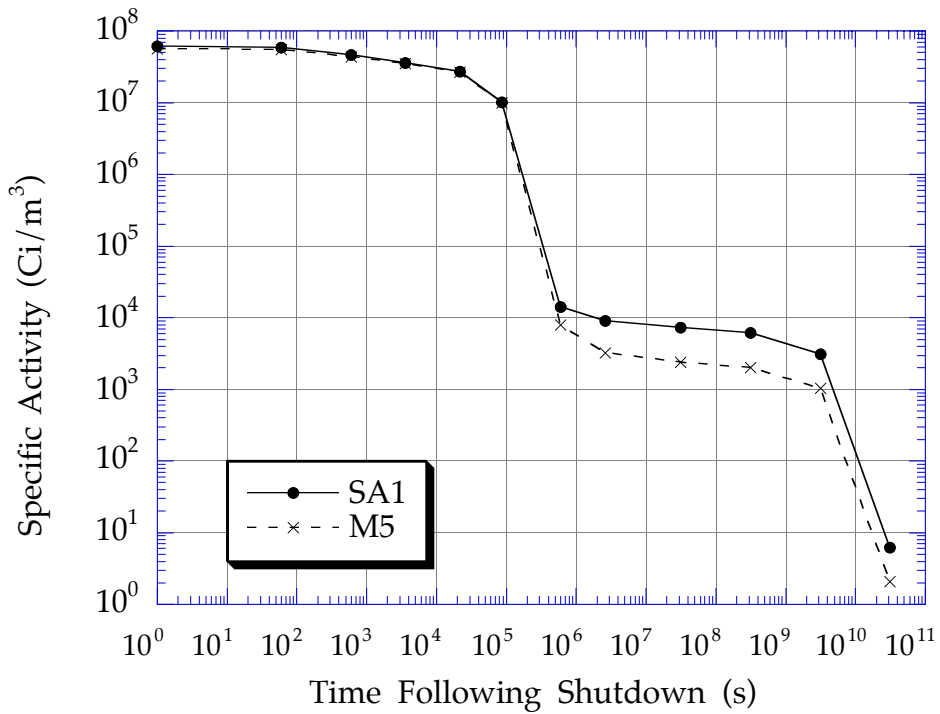


Fig. 18. Activity induced in dome PFC (zone 2).

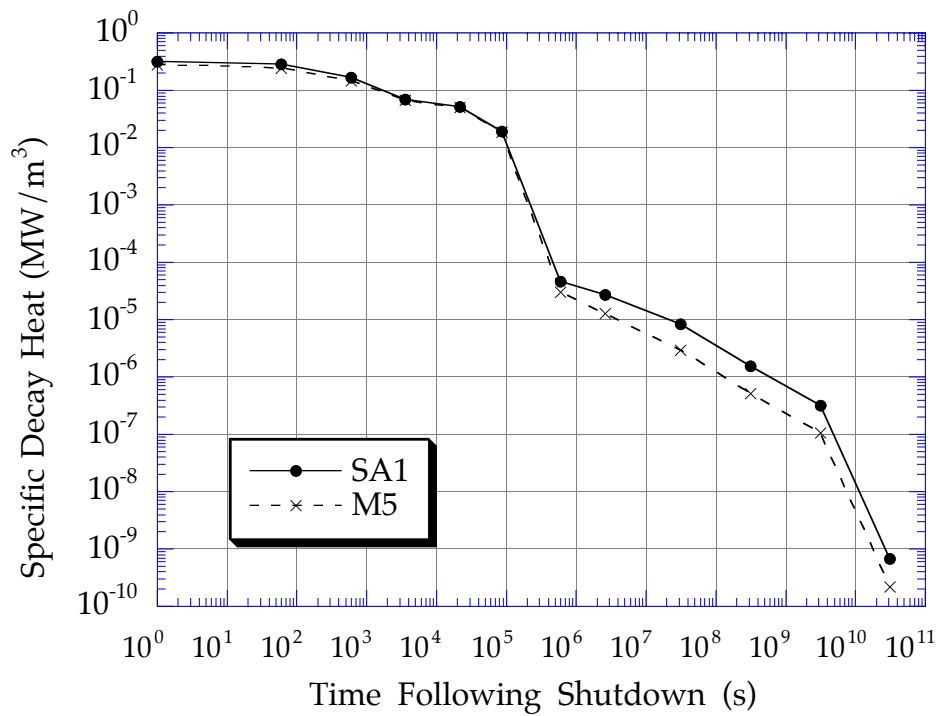


Fig. 19. Decay heat induced in dome PFC (zone 2).

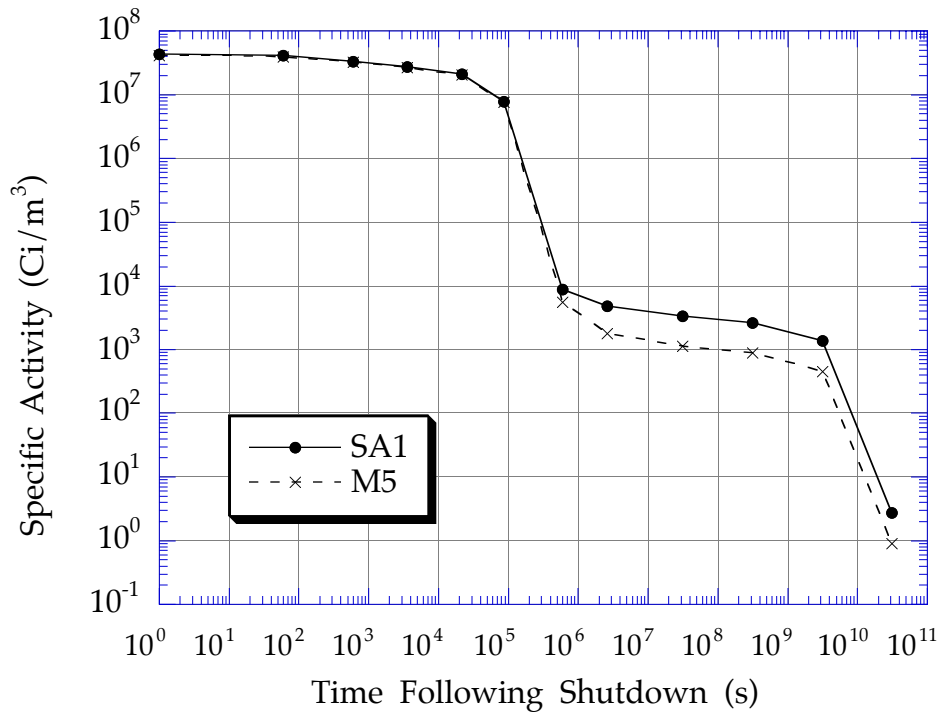


Fig. 20. Activity induced in dome body (zone 4).

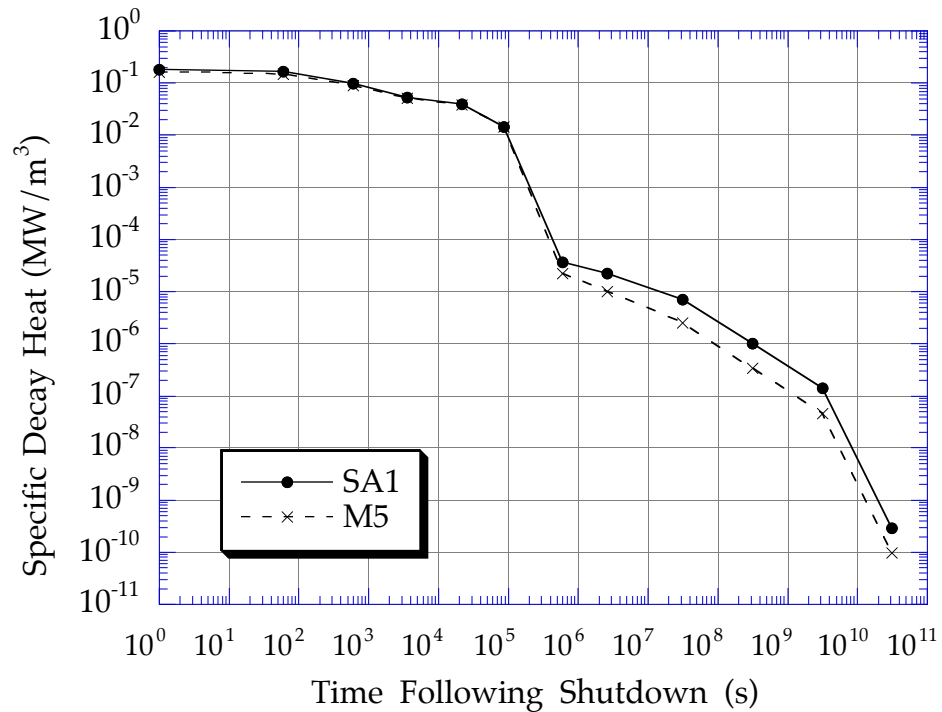


Fig. 21. Decay heat induced in dome body (zone 4).

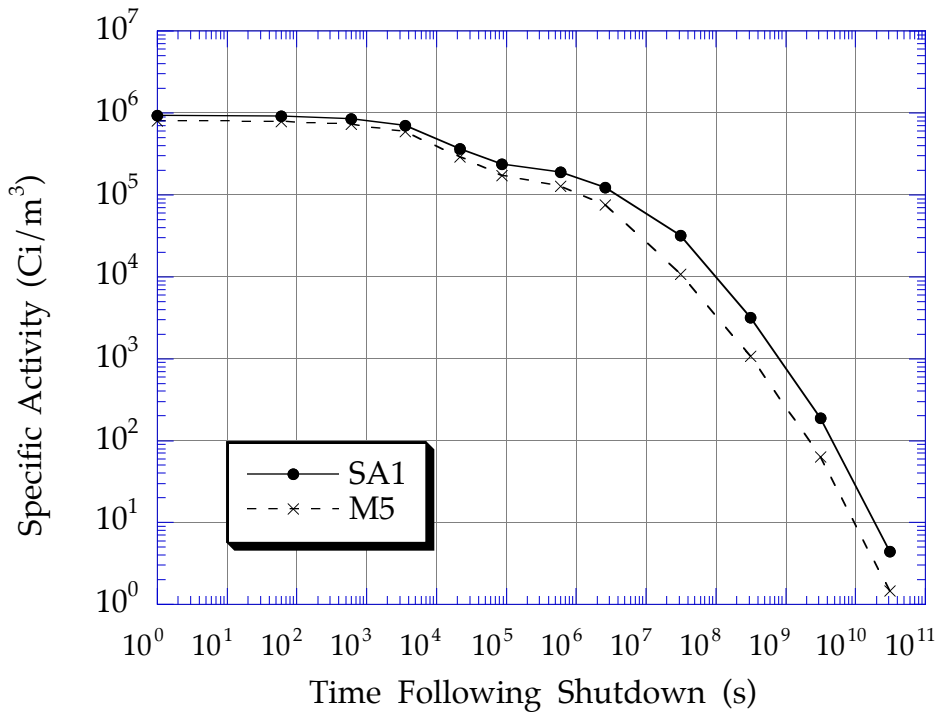


Fig. 22. Activity induced in dome body (zone 7).

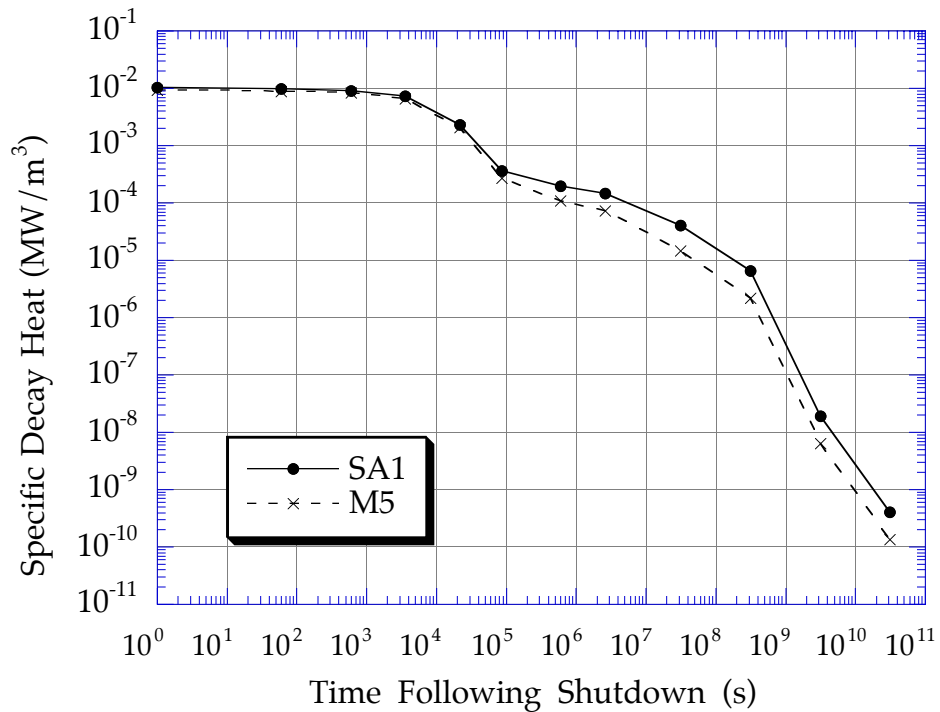


Fig. 23. Decay heat induced in dome body (zone 7).

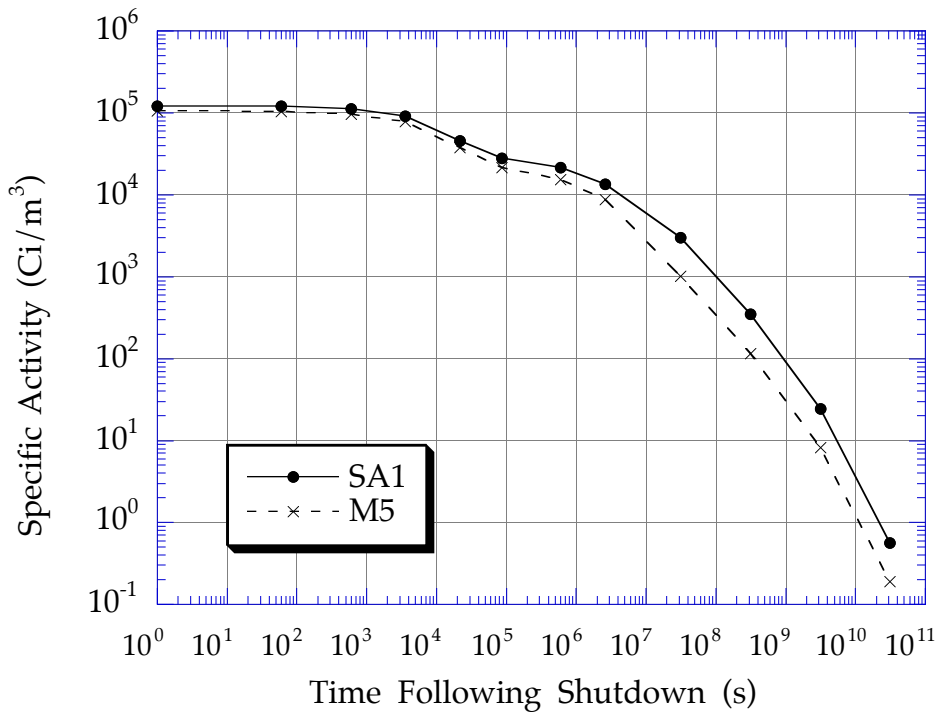


Fig. 24. Activity induced in central body (zone 16).

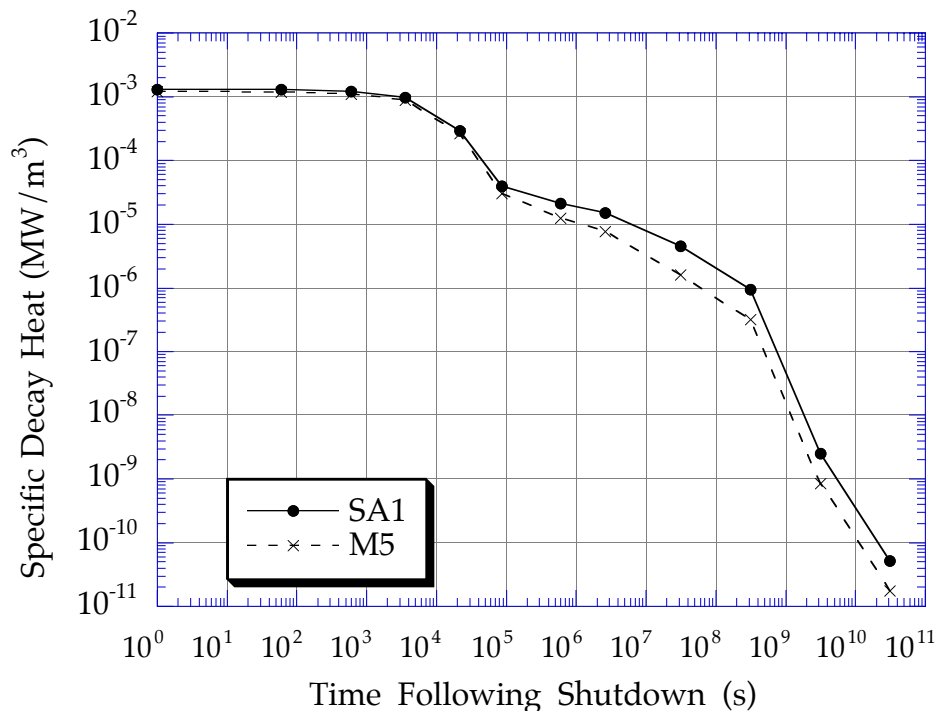


Fig. 25. Decay heat induced in central body (zone 16).

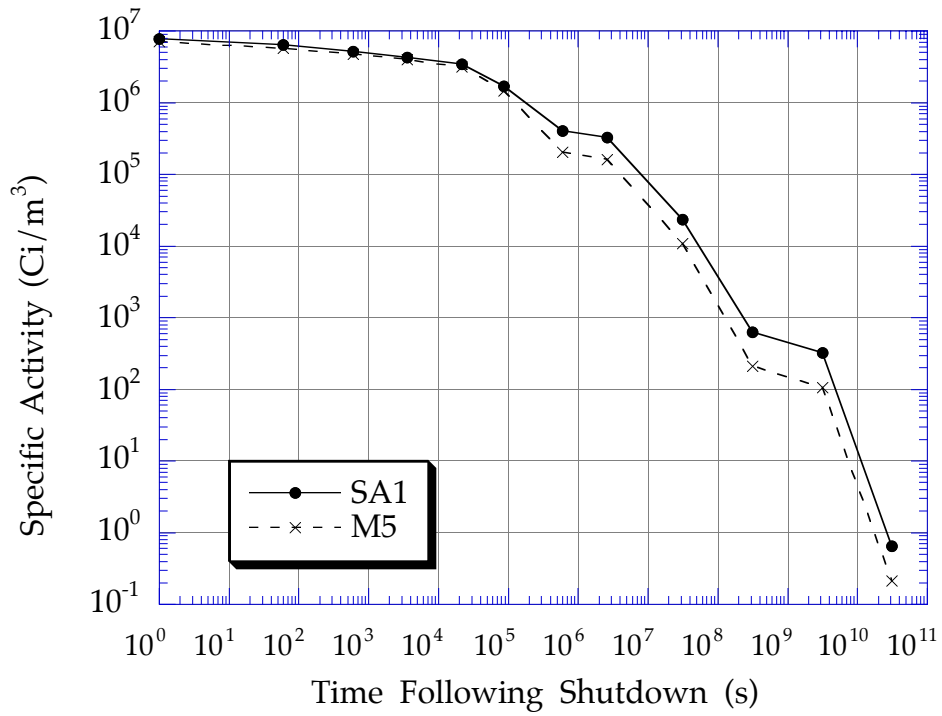


Fig. 26. Activity induced in wings (zone 24).

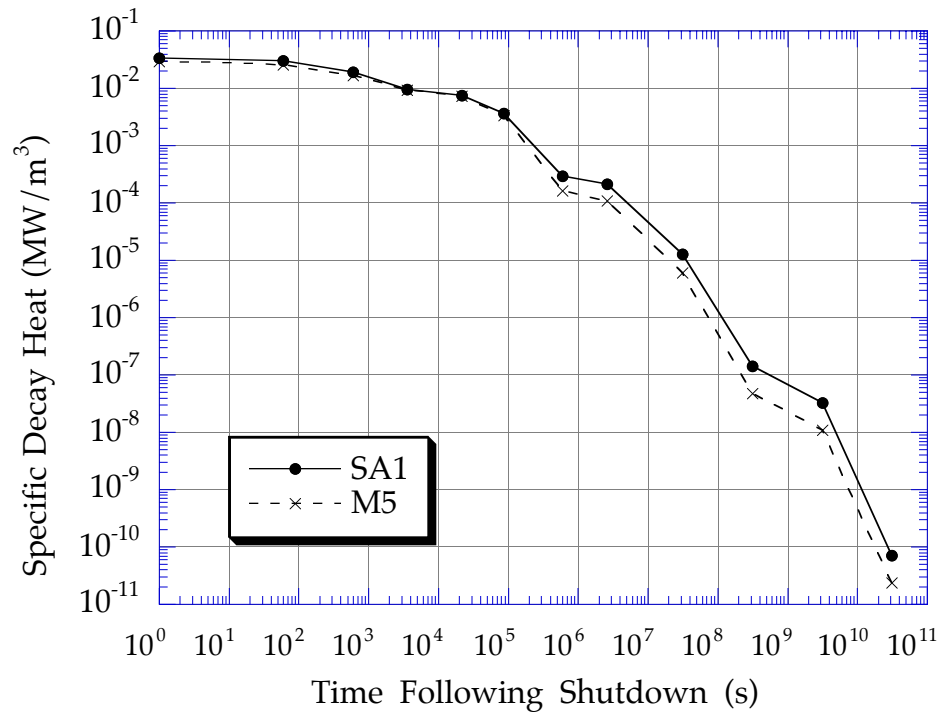


Fig. 27. Decay heat induced in wings (zone 24).

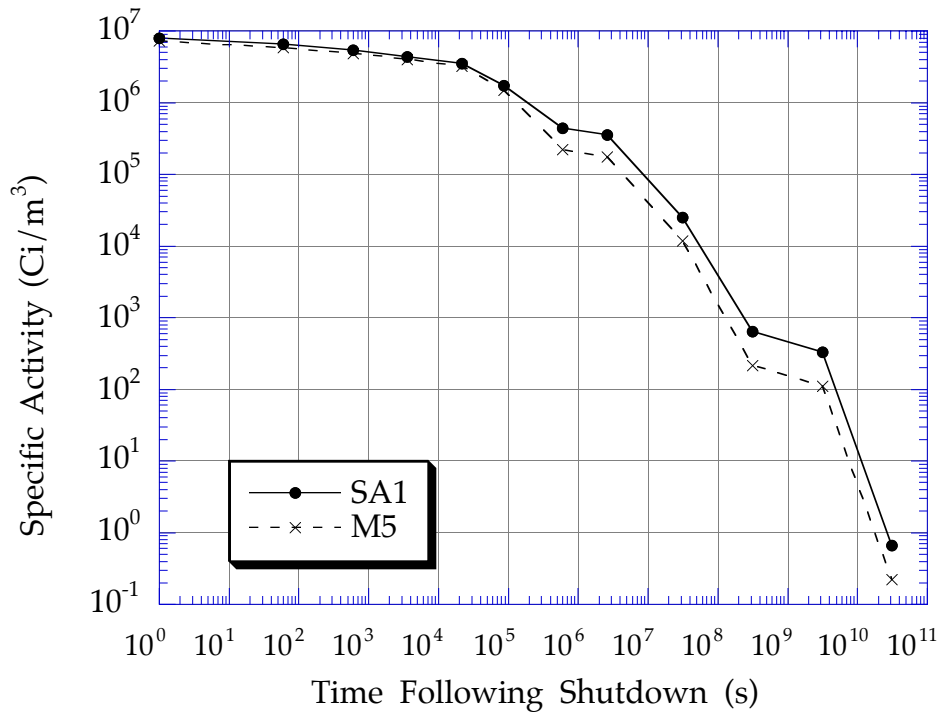


Fig. 28. Activity induced in wings (zone 26).

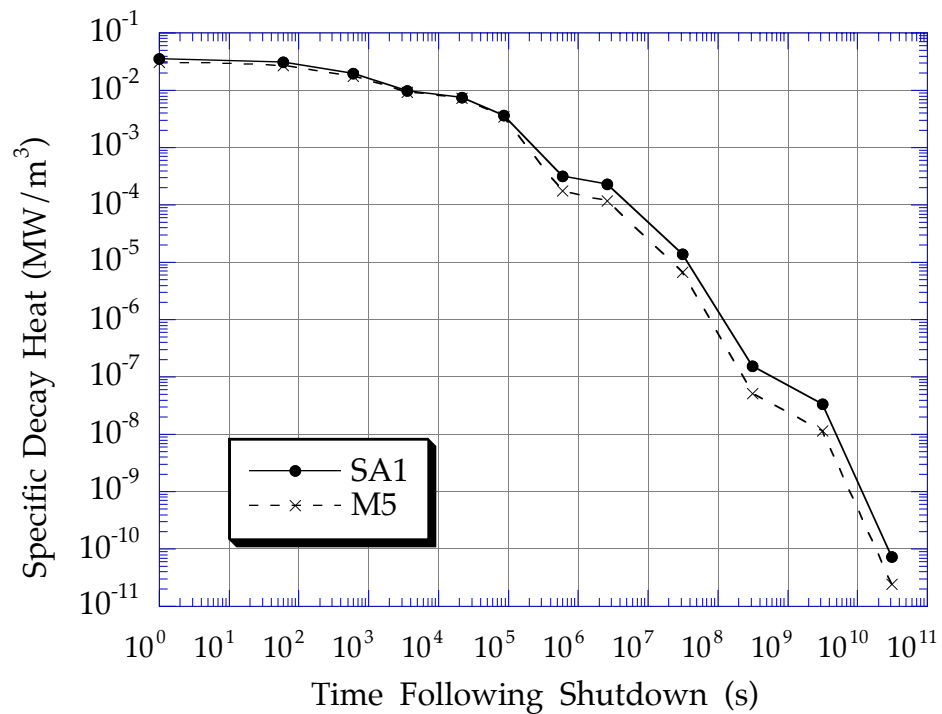


Fig. 29. Decay heat induced in wings (zone 26).

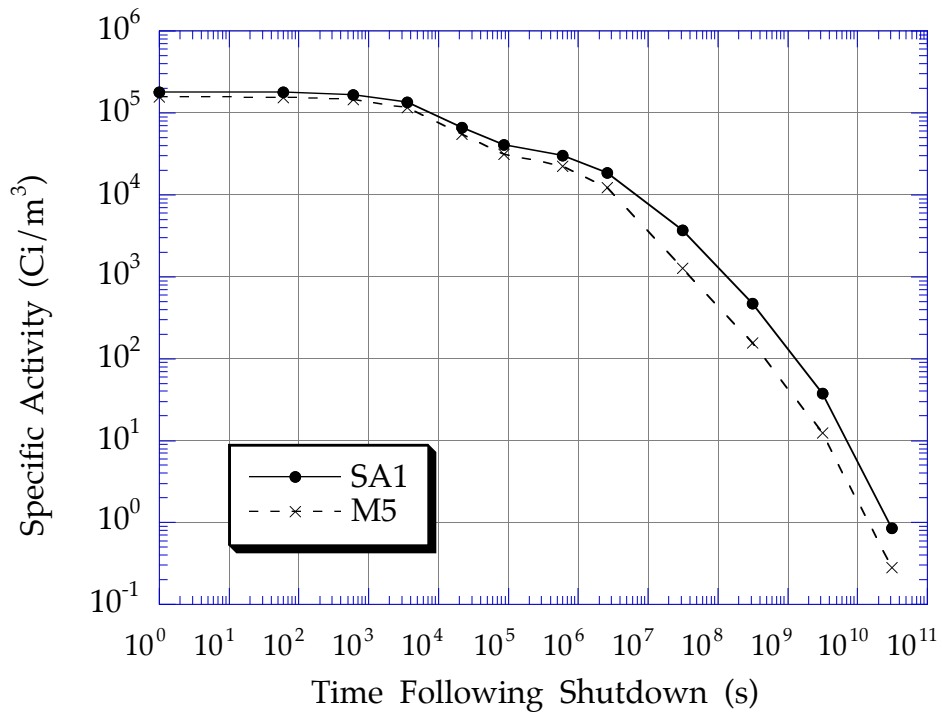


Fig. 30. Activity induced in outer leg (zone 41).

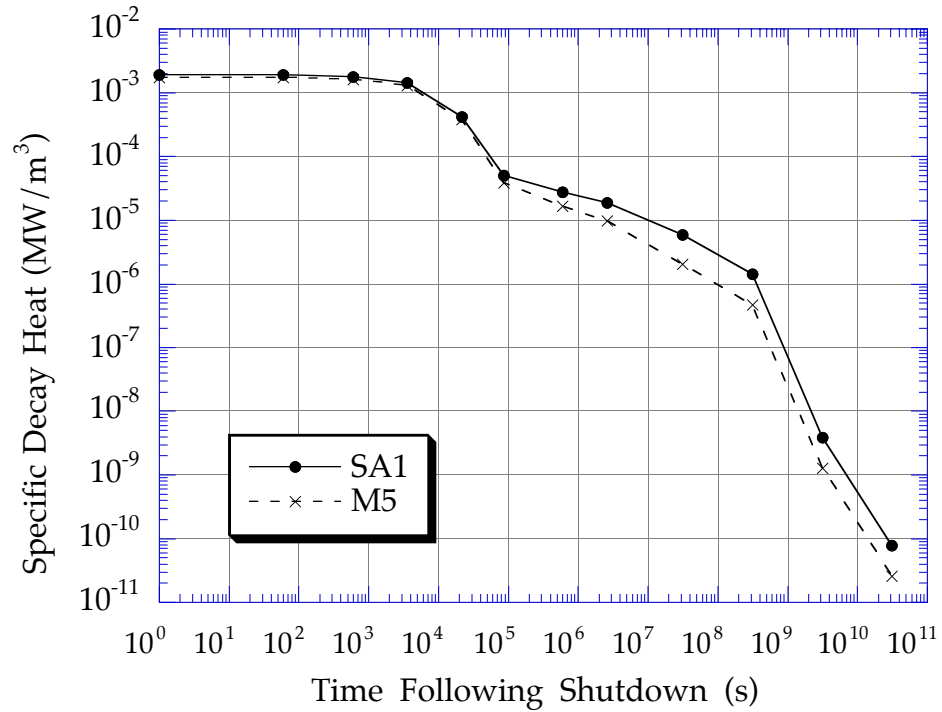


Fig. 31. Decay heat induced in outer leg (zone 41).

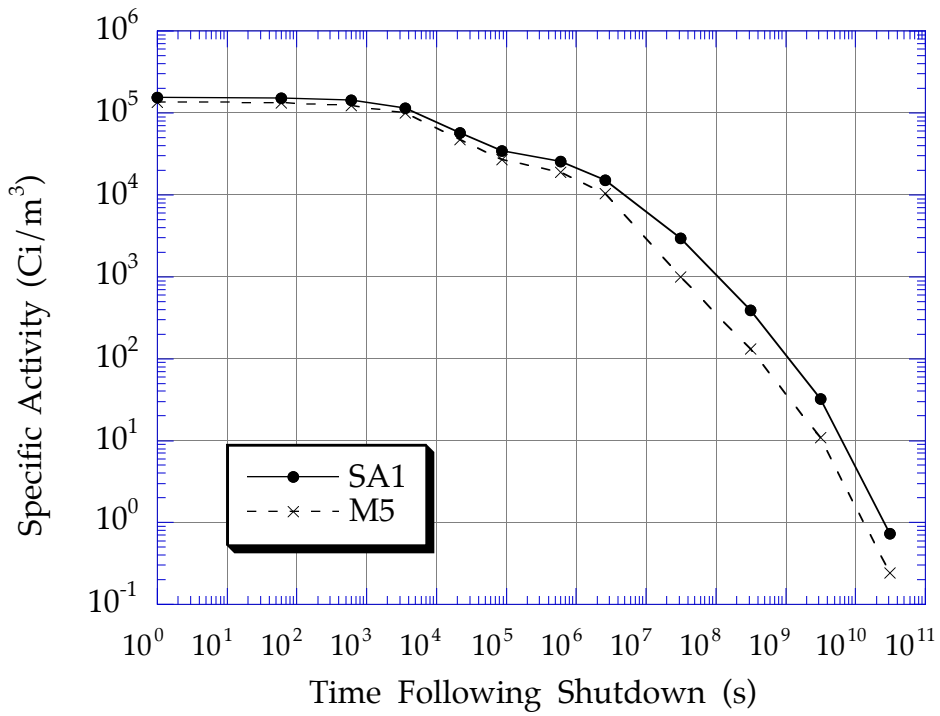


Fig. 32. Activity induced in inner leg (zone 60).

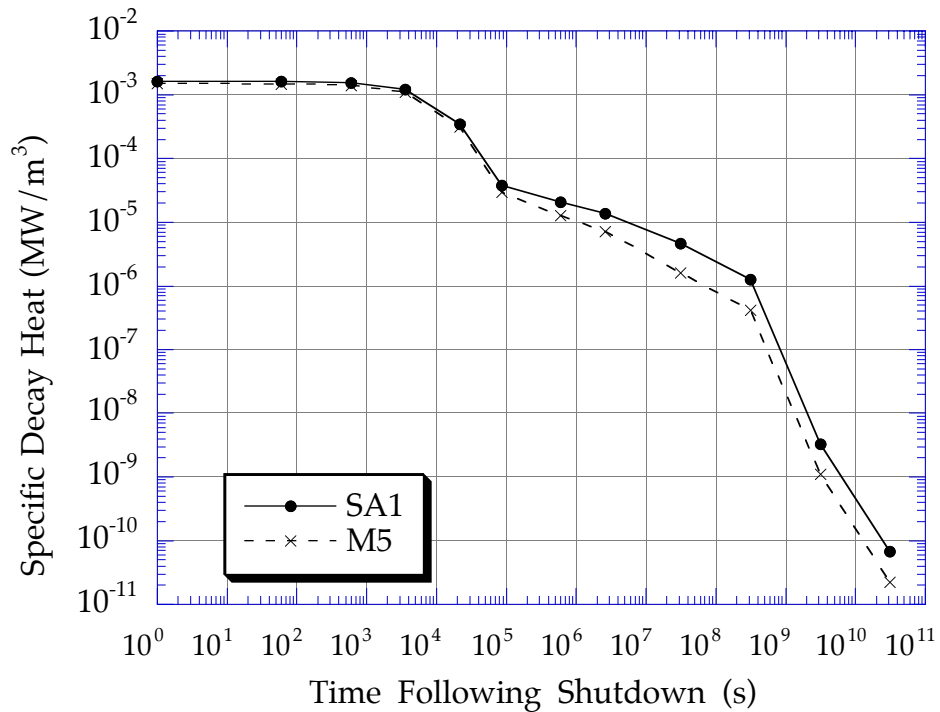


Fig. 33. Decay heat induced in inner leg (zone 60).

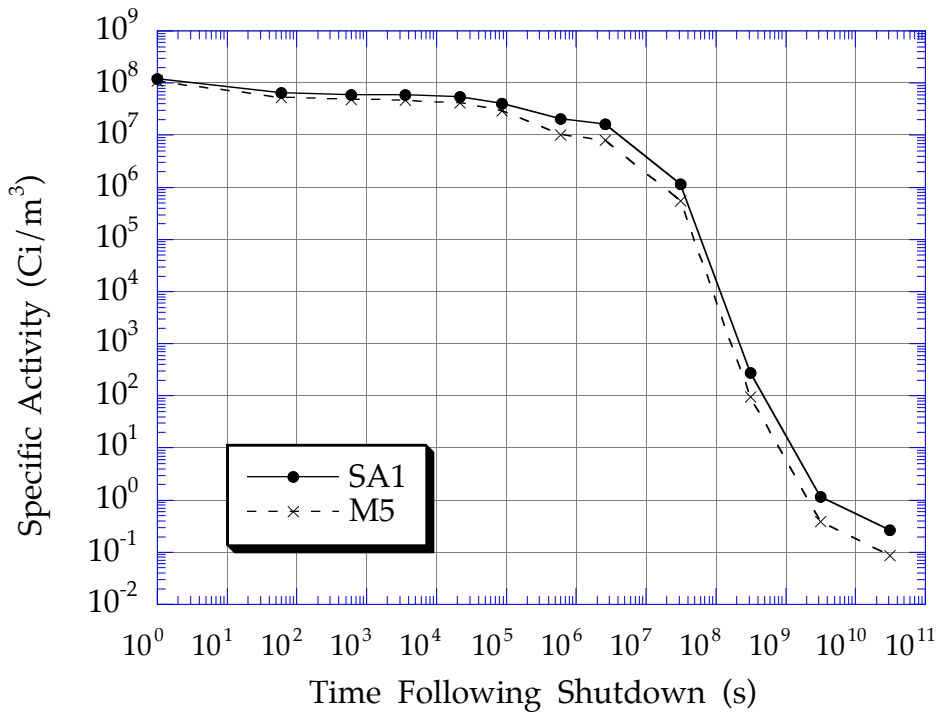


Fig. 34. Activity induced in outer vertical target (zone 67).

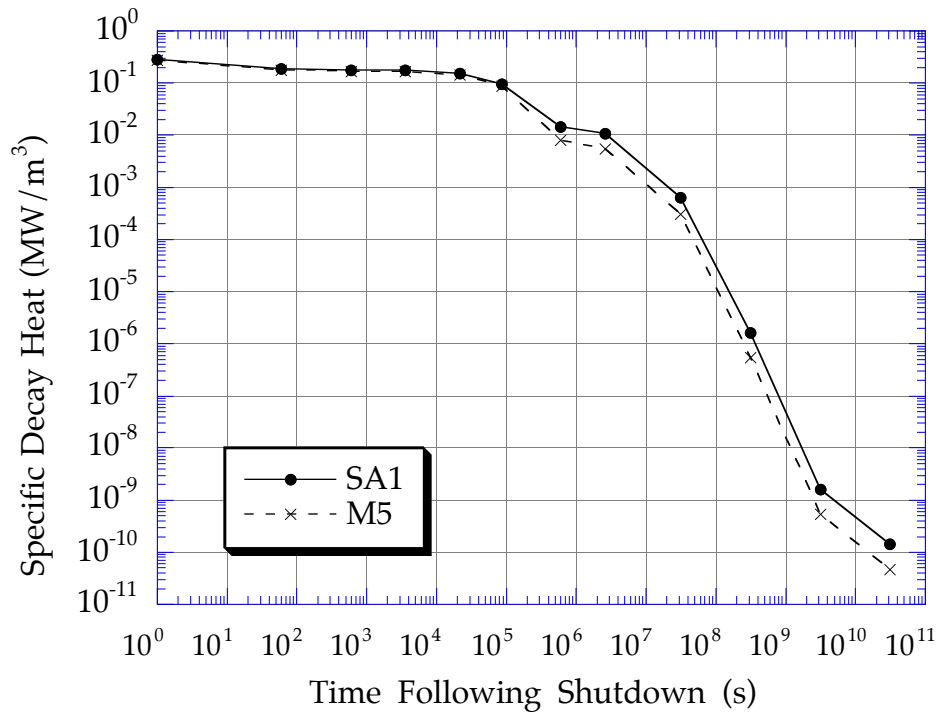


Fig. 35. Decay heat induced in outer vertical target (zone 67).

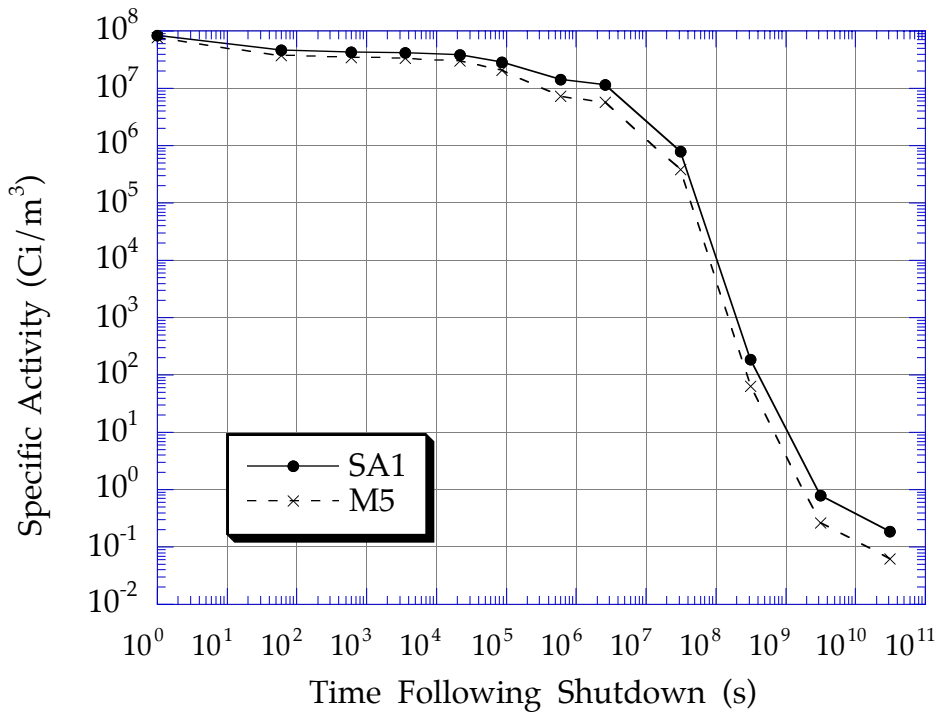


Fig. 36. Activity induced in outer vertical target (zone 68).

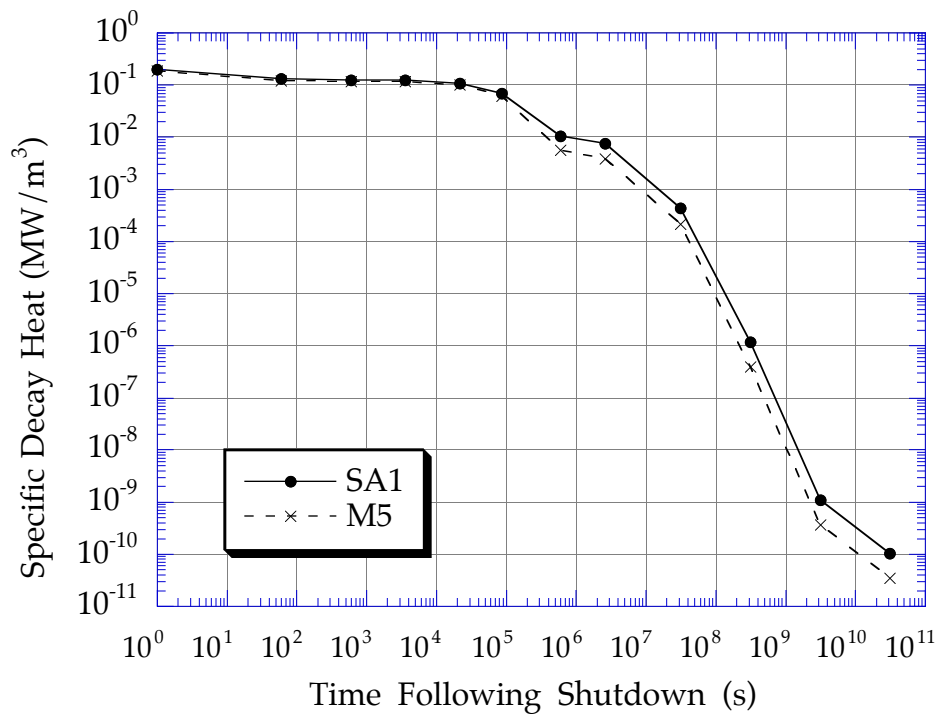


Fig. 37. Decay heat induced in outer vertical target (zone 68).

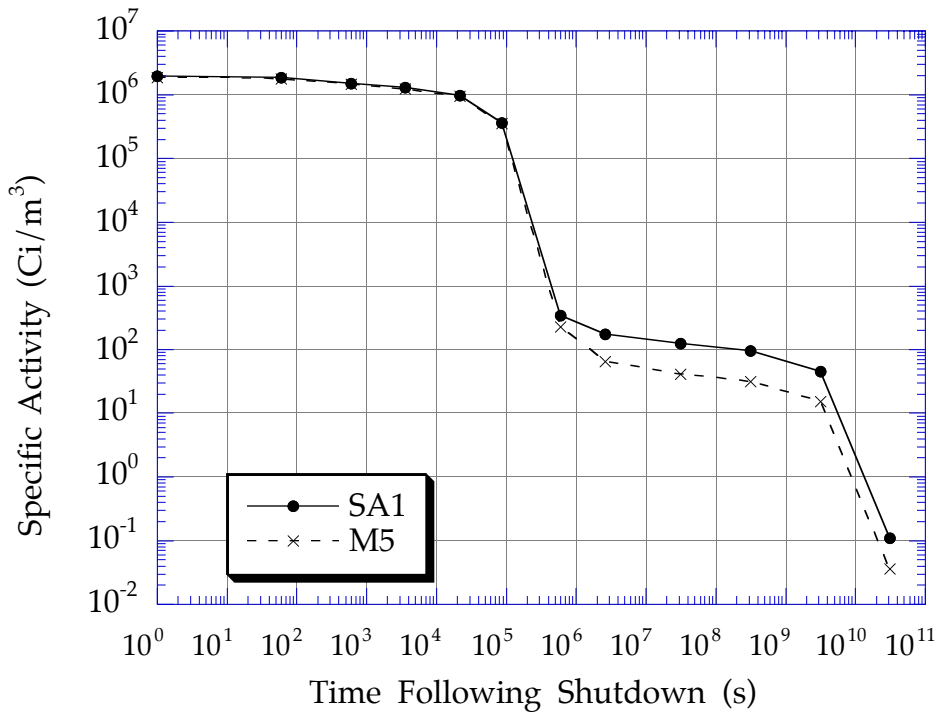


Fig. 38. Activity induced in outer vertical target (zone 73).

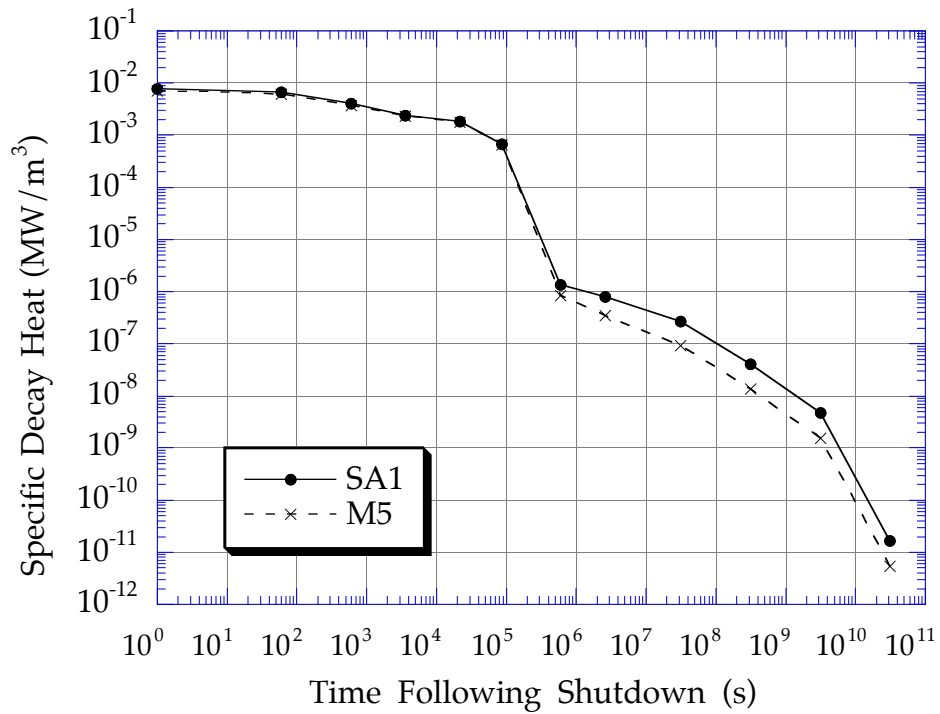


Fig. 39. Decay heat induced in outer vertical target (zone 73).

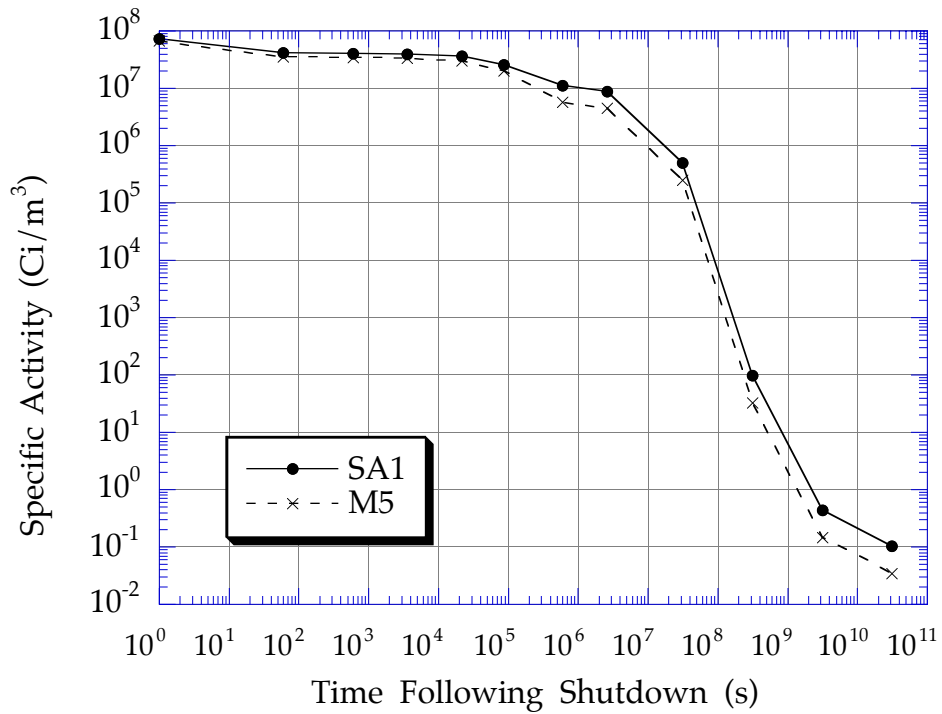


Fig. 40. Activity induced in inner vertical target (zone 76).

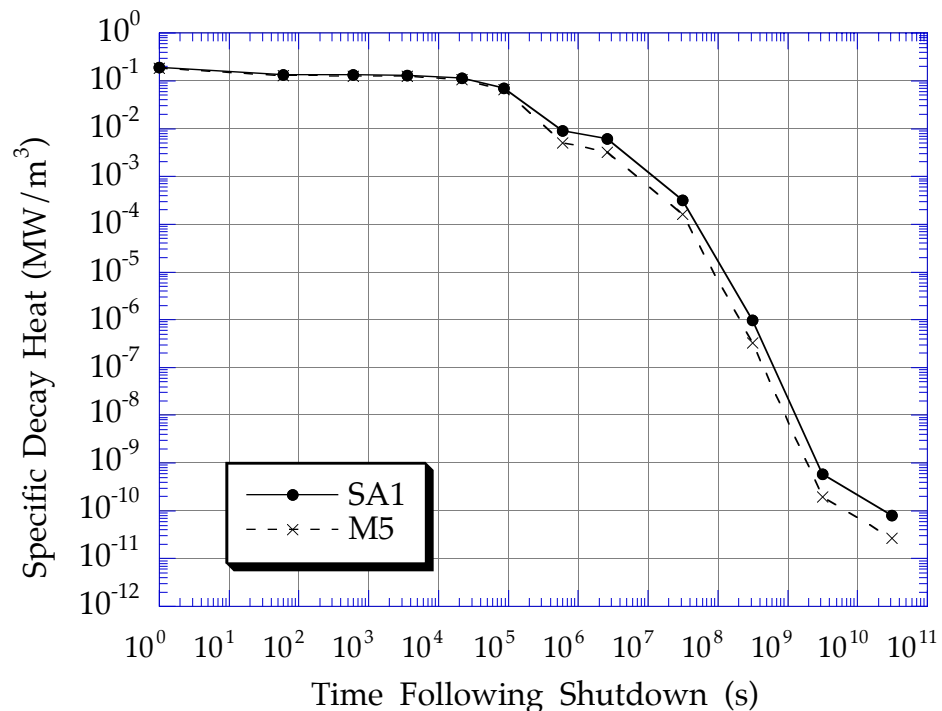


Fig. 41. Decay heat induced in inner vertical target (zone 76).

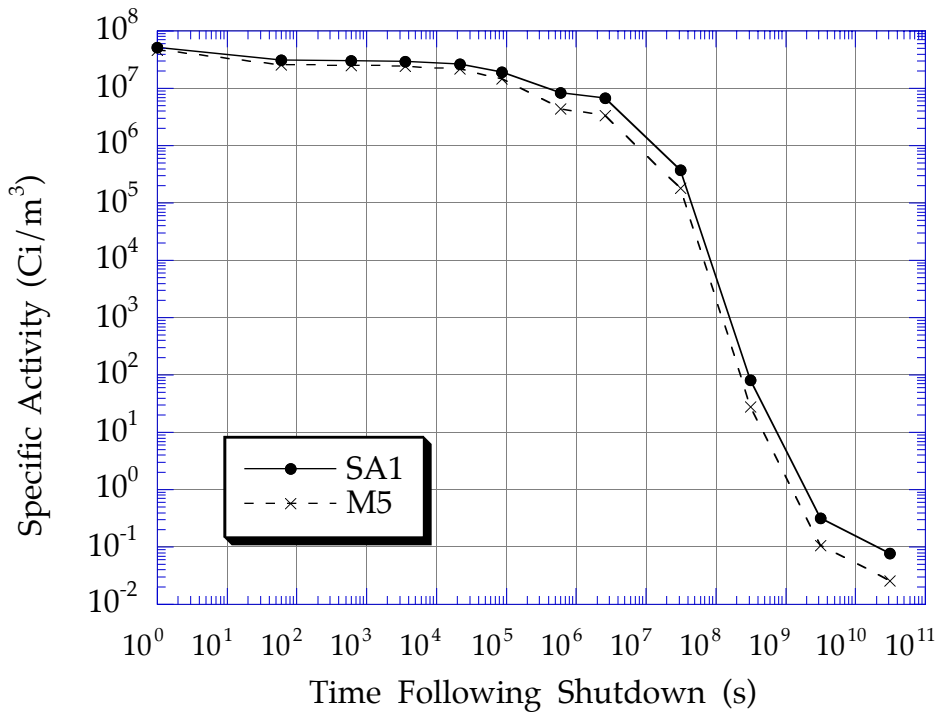


Fig. 42. Activity induced in inner vertical target (zone 77).

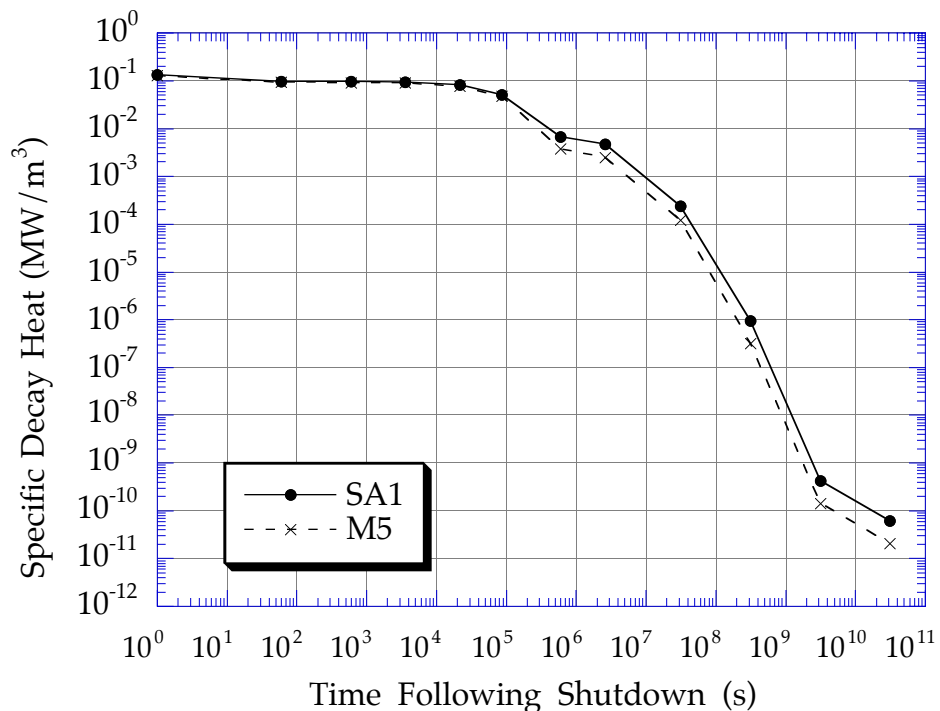


Fig. 43. Decay heat induced in inner vertical target (zone 77).

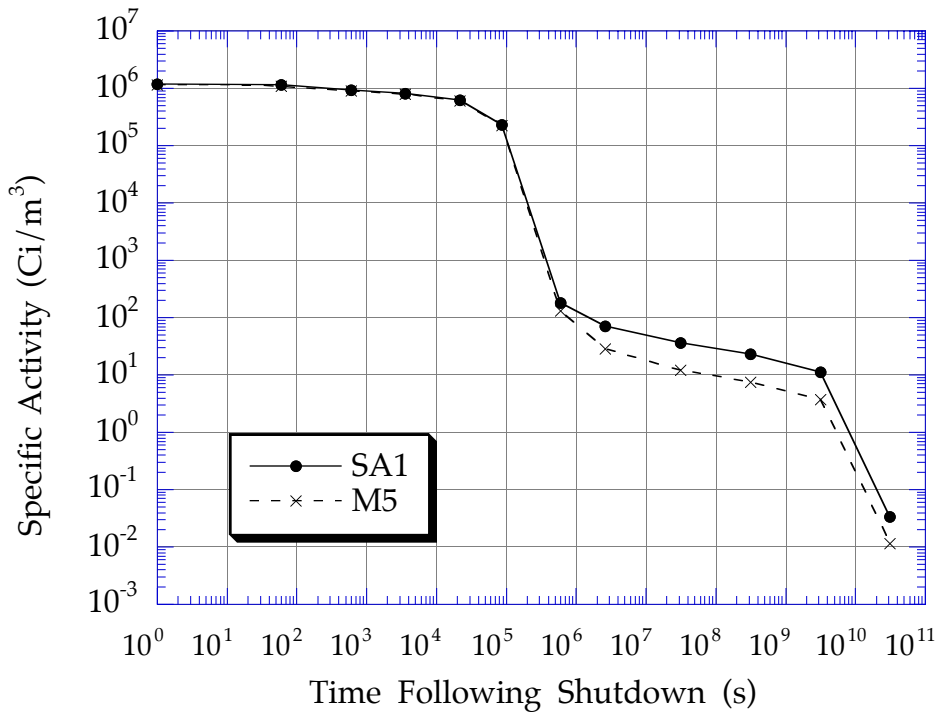


Fig. 44. Activity induced in inner vertical target (zone 82).

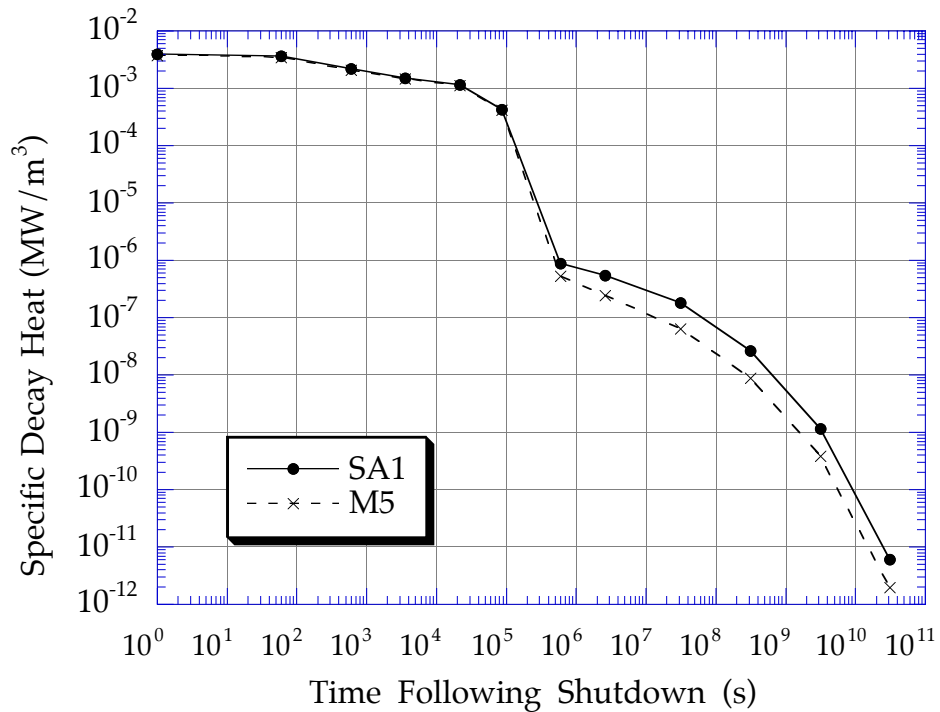


Fig. 45. Decay heat induced in inner vertical target (zone 82).

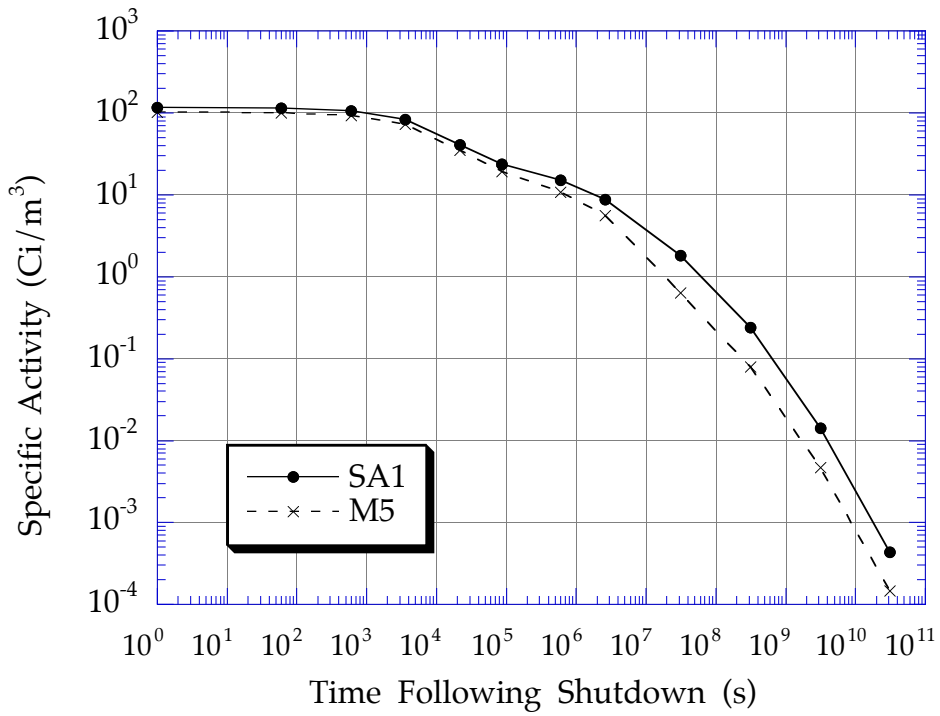


Fig. 46. Activity induced in rails (zone 104).

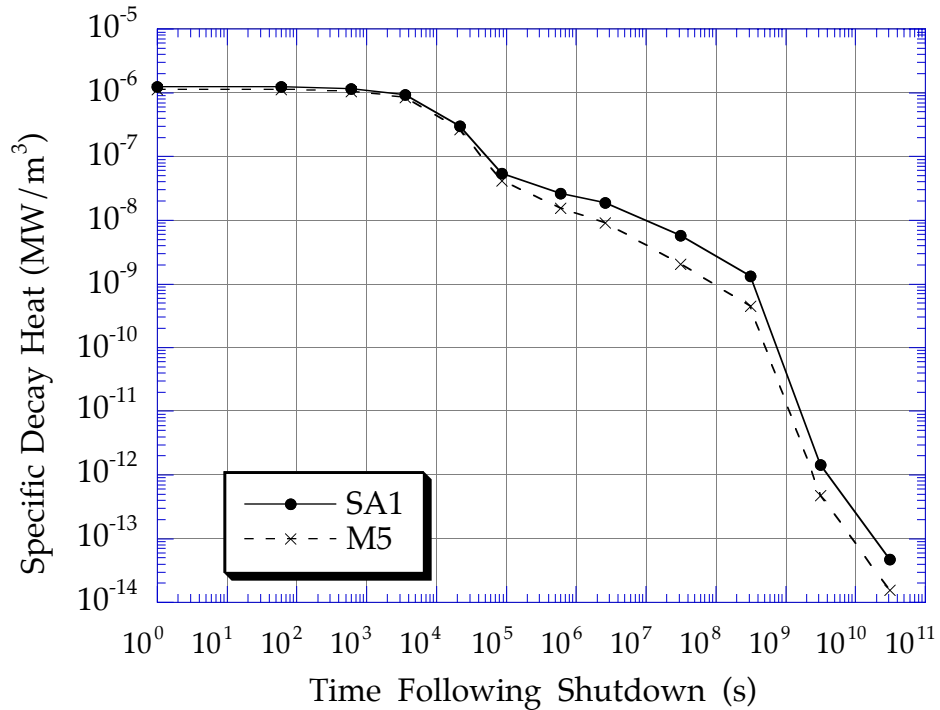


Fig. 47. Decay heat induced in rails target (zone 104).

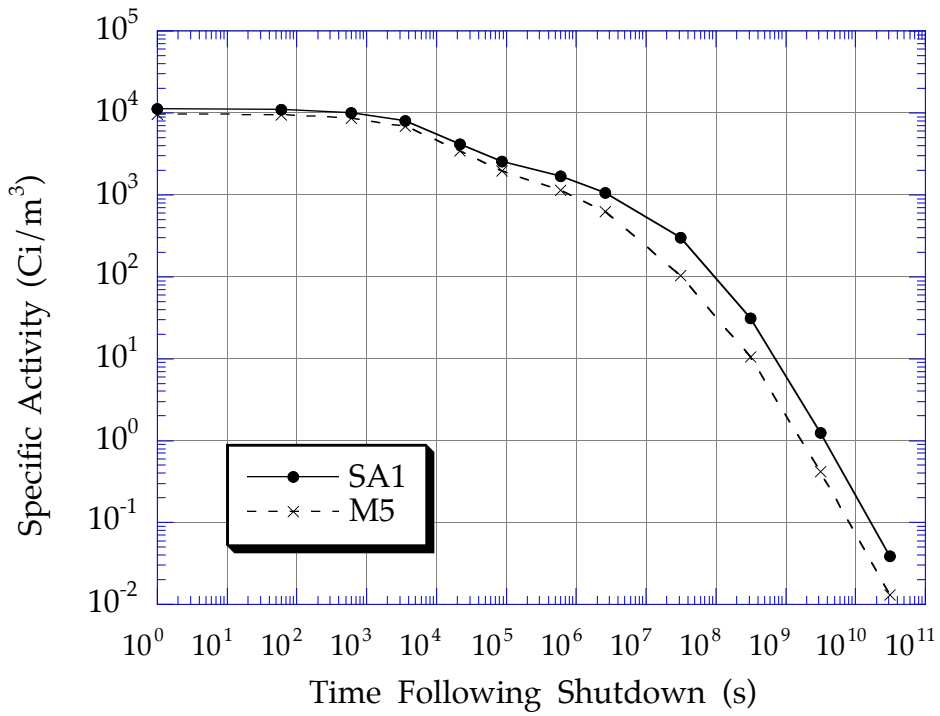


Fig. 48. Activity induced in rails (zone 105).

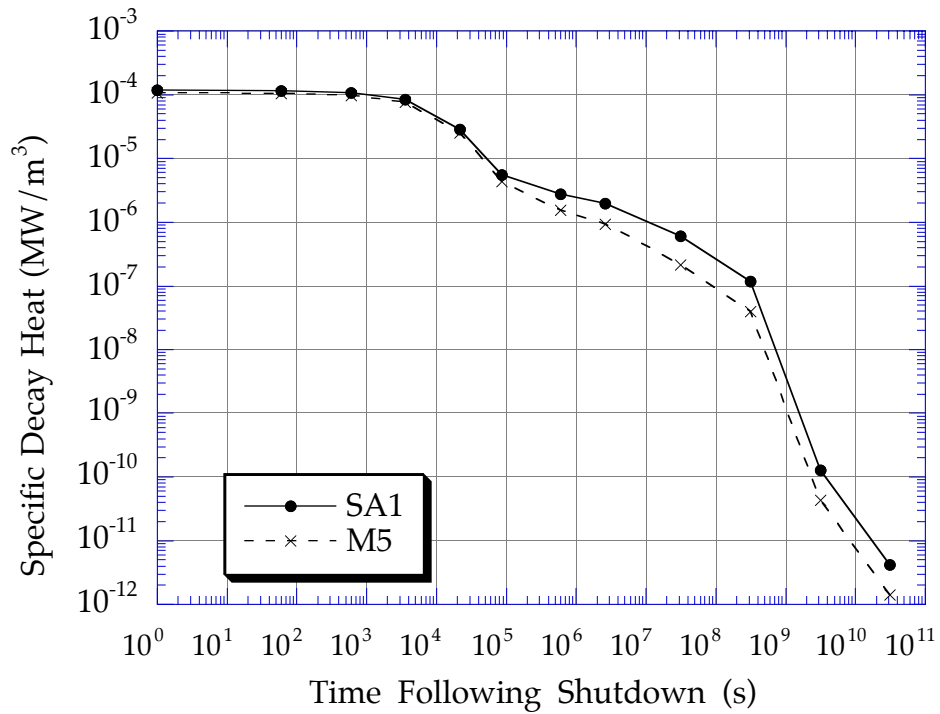


Fig. 49. Decay heat induced in rails target (zone 105).

## 7. SUMMARY AND CONCLUSIONS

3-D neutronics and shielding analyses have been performed for the divertor region. A detailed 3-D model has been developed for the divertor region of the ITER Detailed Design. The model includes in detail the PFC, the vertical targets, the wings with associated plates, the gas boxes, as well as the central dome and cassette bodies. Each divertor cassette in the model was divided into 103 regions to provide detailed spatial distribution of nuclear heating and radiation damage. The layered configurations of the dome PFC and vertical targets were modeled accurately with the front tungsten layer modeled separately. Separate regions are included in the model to represent the mechanical attachments and coolant pipe connections for the dome, vertical targets, and wings. The divertor cassette model was integrated with the general ITER model based on the Interim ITER Design.

3-D neutronics calculations have been performed using the continuous energy MCNP-4A code with cross section data from FENDL-1 to determine the detailed spatial distribution of the neutron flux in the divertor cassette. The neutron flux values were provided at the 103 cassette regions used in the model. A detailed activation analysis has been performed for zones representing the different critical components of the divertor cassette. The activation calculations have been performed using the latest version of the activation code DKR-PULSAR2.0. The DKR-PULSAR2.0 code combined the 175-group neutron flux calculated by the MCNP-4A code with the the FENDL/A-2.0 and FENDL/D-2.0 data libraries to calculate the radioactive inventories.

To examine the effect of pulsing sequences on the activity and decay heat generation, the calculations have been performed for two different operational scenarios. The first scenario (SA1) corresponds to a machine total fluence of  $0.3 \text{ MW}\cdot\text{a}/\text{m}^2$  with a long term availability of 25% and a final month availability of 50%. A burn pulse length of one hour has been used in this scenario. The second scenario (M5) corresponds to a total fluence of  $0.1 \text{ MW}\cdot\text{a}/\text{m}^2$ . The M5 scenario has a long term availability of only 4% and a last month availability of 50%. A 1000 second burn pulse length is used for the M5 scenario. The short term activity and decay heat results are nearly identical since the availability is the same during the last month of operation in both operation scenarios. On the other hand, the long term activity and decay heat determined by the total fluence are lower by about a factor of 3 for the M5 scenario.

Special attention has been given to the top 1 cm tungsten layer of the divertor dome. The radioactivity generated in the tungsten layers of the divertor are mostly dominated by  $^{187}\text{W}$  during the first day after shutdown. Accurate calculation of the  $^{187}\text{W}$  inventory that takes into account the self-shielding effect, also yielded accurate results for other radioisotopes produced by multi-step reactions with  $^{187}\text{W}$ . The GlidCop copper and 316 SS-LN parts of the divertor also generated a considerable level of activity and decay heat. Nevertheless, the analysis showed that the tungsten PFC is clearly the most critical part of the divertor from a decay heat generation point of view.

## REFERENCES

- [1] Technical Basis for the ITER Detailed Design Report, Cost Review and Safety Analysis, ITER EDA Documentation Series, International Atomic Energy Agency, Vienna, December 1996.
- [2] M.E. Sawan, "Three-Dimensional Neutronics Analysis for the ITER Divertor Cassette," ITER U.S. Home Team Report ITER/US/97-IV-10 and University of Wisconsin Fusion Technology Institute Report UWFDM-1056, November 1997.
- [3] J. Briesmeister, Ed., "MCNP, A General Monte Carlo N-Particle Transport Code, Version 4A," LA-12625-M, (1993).
- [4] R. MacFarlane, "FENDL/MC-1.0, Library of Continuous Energy Cross Sections in ACE Format for MCNP-4A," Summary Documentation by A. Pashchenko, H. Wienke and S. Ganesan, Report IAEA-NDS-169, Rev. 3, International Atomic Energy Agency (Nov. 1995).
- [5] Technical Basis for the ITER Interim Design Report, Cost Review and Safety Analysis, ITER EDA Documentation Series, No. 7, International Atomic Energy Agency, Vienna, April 1996.
- [6] M. Sawan, L. Petrizzi, R. Santoro, and D. Valenza, "Three-Dimensional Neutronics and Shielding Analyses for the ITER Divertor," Fusion Technology, 30, 601 (1996).

- [7] J-Ch. Sublet, “Three-Dimensional Neutronic, Activation and Residual Decay Heat Analysis for the ITER Design,” UKAEA FUS 340, UKAEA/Euratom Fusion Association, Culham, United Kingdom (July 1996).
- [8] H. Iida, R. Plenteda, R. T. Santoro, and V. Khripunov, “Effect of Homogenisation of Armour and Substrates on Estimating Decay Heat Density in Tungsten,” Memo No. NA:NAG-14-12-12-96-ReV, Nuclear Analysis Group ITER JCT, Garching, 17 March 1997.
- [9] E.T. Cheng, TSI Research, Inc., Solana Beach, CA, Private Communications, April 1997.
- [10] J-Ch. Sublet, UKAEA, Culham, United Kingdom, Private Communications, April 1997.
- [11] A. Pashchenko and P. McLaughlin, “FENDL/A-1.0: Neutron Activation Cross-Section Data Library for Fusion Applications,” Report INDC(NDS)-148, IAEA Nuclear Data Section, February 1995.
- [12] A. Pashchenko et al., “FENDL/A-2.0: Neutron Activation Cross-Section Data Library for Fusion Applications,” Report INDC(NDS)-173, IAEA Nuclear Data Section, March 1997.
- [13] D. Henderson et al., “DKR-Pulsar: A Radioactivity Calculation Code that Includes Pulsed/Intermittent Operation,” to be published.
- [14] G. Saji and E.T. Cheng, “Initial Activation Data for NSSR-2: Data for Dose-Release Calculation,” Revision 1a, Document No. D71-07-SEHD-005, Safety, Environmental and Health Division, ITER JCT, San Diego, June 1997.
- [15] H. Iida, Nuclear Analysis Group, ITER JCT, Garching, Private Communications, March 1997.
- [16] J. E. Sisolak, S. E. Spangler and D. L. Henderson, “Pulsed/Intermittent Activation in Fusion Energy Reactor Systems,” *Fusion Technology*, 21, 2145 (1992).
- [17] S.E. Spangler, J.E. Sisolak, and D.L. Henderson, “Calculational Models for the Treatment of Pulsed/Intermittent Activation Within Fusion Energy Devices,” *Fusion Engineering and Design*, 22, 349 (1993).

- [18] V. Barabash, Materials Group, ITER JCT, Garching, Private Communications, March 1997.
- [19] J-Ch. Sublet, “Three-Dimensional Heterogeneous Monte Carlo Neutronic and Activation Analysis for the ITER Divertor,” UKAEA FUS 368, UKAEA/Euratom Fusion Association, Culham, United Kingdom (June 1997).